

Declaration

I, Martine Bernard, born in Ottawa, Canada, hereby declare, that the dissertation “Role of the Co-Inhibitory Molecule PD-1 (CD279) and its Ligand PD-L1 (CD274) in a Mouse (*Mus musculus*; Linnaeus, 1758) Model of Malaria” by Ángeles Jurado Jiménez is written in correct English.

Martine Bernard

Hamburg, March 24th, 2009

**Role of the Co-Inhibitory Molecule PD-1 (CD279)
and its Ligand PD-L1 (CD274)
in a Mouse (*Mus musculus*; Linnaeus, 1758)
Model of Malaria**

A dissertation submitted

by

Ángeles Jurado Jiménez

to

the Faculty of Mathematics, Informatics and Science

Department of Biology, University of Hamburg

in partial fulfilment of the requirements

for the degree

Dr. rer. nat.

Hamburg, Germany

2009

Genehmigt vom Department Biologie
der Fakultät für Mathematik, Informatik und Naturwissenschaften
an der Universität Hamburg
auf Antrag von Professor Dr. B. FLEISCHER
Weiterer Gutachterin der Dissertation:
Frau Professor Dr. I. BRUCHHAUS
Tag der Disputation: 06. Mai 2009

Hamburg, den 22. April 2009




Professor Dr. Jörg Ganzhorn
Leiter des Departments Biologie

*“If A is success in life, then A equals x plus y plus z.
Work is x; y is play; and z is keeping your mouth shut.”*

Albert Einstein

ACKNOWLEDGEMENTS

I would like to thank Professor Dr. Fleischer who gave me the opportunity to do my Ph. thesis in his department.

Thanks to Dr. Thomas Jacobs for his support and supervision.

My gratitude to “Fundació La Caixa” (Barcelona) and “Deutscher Akademischer Austausch Dienst” (DAAD) for the financial support.

To all members of the “*Immunologie Abteilung*” who always assisted me with friendly patience, not only in scientific matters but also in my almost daily problems with the German language “*Wir haben Spaß gehabt*”.

My special thanks to Dr. Thomas Bickert and Dr. Susanne Tartz for their advisements about this thesis.

Thanks a lot to all my family and friends, both Spanish and German sides.

Thanks to my parents for their support in almost all my decisions in life (almost all...), and my brother, who always makes me laugh.

Thank you very much to my German family, for their affection and their help.

And last but not least, thanks to my husband Sven and my son Paul, “*meine Männer*”.

ABSTRACT

Role of the Co-Inhibitory Molecule PD-1 (CD279) and its Ligand PD-L1 (CD274) in a Mouse (*Mus musculus*; Linnaeus, 1758) Model of Malaria

Ángeles Jurado Jiménez

Several mechanisms are involved in the regulation of the immune system allowing the necessary balance between an effective defense against pathogens and tolerance. The control over this immune response is necessary to prevent self damage. The newly described co-inhibitory molecules of the B7/CD28 family, PD-1 and its ligand PD-L1 are involved in the control of the immune response in target organs. PD-1 expression has been found on activated T cells, whereas the endothelial expression of its ligand PD-L1 assures its presence in a high variety of tissues, including the liver. The importance of the PD-1/PD-L1 pathway in controlling autoimmunity during immune responses has been demonstrated using several infection models.

Regulatory T cells (Tregs) are also involved in this control by their capacity of inhibiting T cell responses through the production of inhibitory cytokines and by a cell-cell contact mechanism. The implicated molecules are currently under investigation.

In this study the PD-1 and PD-L1 expression was analyzed on several cell types under different stimulation conditions. Hence, PD-1 was found on activated T cells whereas PD-L1 was constitutively expressed on bone marrow-derived dendritic cells and induced after stimulation. Tregs showed constitutive expression of PD-1 and PD-L1. Both molecules were induced after stimulation. *In vitro* experiments using anti-PD-1 and a new generated anti-PD-L1 antibody showed a co-inhibitory function for the PD-1/PD-L1 pathway regulating T cell responses. Nevertheless the suppressive capacity of Tregs was not affected by a PD-1 blockade.

The role of the interaction between PD-1 and PD-L1 during infection was analyzed using a mouse model of malaria. The disease transmitted by *Plasmodium* is characterized by two different stages known as liver and blood stage. During the liver stage, which is asymptomatic, the sporozoites replicate inside the hepatocytes inducing only a low specific CD8⁺ T cell response against the pathogen. Despite the continuous contact with the parasite, people living in endemic areas are not protected against re-infections. The reasons for that phenomenon are unclear. The parasite's life cycle follows with the invasion of the erythrocytes, known as the blood stage and provokes their posterior destruction. This results

in bouts of fever and anaemia. Only the immunization with γ -irradiated sporozoitic forms, which are unable to proceed with the blood stage, induces effective and protective CD8⁺ T cells suggesting that the blood stage negatively regulates liver stage-specific responses.

The results obtained in this study showed that the PD-L1 expression is induced in the liver during the blood stage in the mouse model of malaria and that it regulates the liver stage-specific CD8⁺ T cells which express PD-1. The immunization with an experimental vaccine, that induces liver stage-specific CD8⁺ T cells without conferring protection, together with the blockade of the PD-1/PD-L1 pathway using an antibody against PD-1 during the sporozoite infection, results in an increased number of liver-stage specific IFN- γ producing CD8⁺ T cells. Additionally, this enhanced T cell response coincided with a lower parasitemia in antibody-treated mice.

In conclusion, the control of the immune response during infection is of major importance in order to avoid cell mediated tissue damage. Along the evolution, *Plasmodium* as well as other pathogens appears to have been taken advantage of the PD-1/PD-L1 pathway as an escape mechanism to evade the host's immune system.

First referee: Prof. Dr. Bernhard Fleischer

Second referee: Prof. Dr. Iris Bruchhaus

TABLE OF CONTENTS

1. INTRODUCTION	1
1.1 The immune system and its regulation	1
1.1.1 The immune system	1
1.1.2 Innate immunity	1
1.1.3 Adaptive immunity	2
1.1.4 The B7/CD28 family	4
1.1.5 PD-1	7
1.1.6 Regulatory T cells	10
1.1.7 Liver tolerance	11
1.2 Malaria disease and host defense	12
1.2.1 Malaria	12
1.2.2 <i>Plasmodium</i> life cycle	13
1.2.3 Immunity against malaria	14
1.2.4 Pathogenesis of malaria disease	16
1.2.5 Co-stimulation and pathology	17
1.2.6 Co-stimulation and protection	18
1.2.7 Animal models of malaria	19
1.3 Aims of this study	21
2. MATERIALS	22
2.1 Instruments	22
2.2 Plastic and glass material	23
2.3 Mouse, rat and <i>Plasmodium berghei</i> strains	23
2.3.1 Mouse strains	23
2.3.2 Rat strain	24
2.3.3 <i>Plasmodium</i> strain	24
2.4 Antibodies and fusion molecules	24
2.5 Chemicals	25
2.6 Materials for cell culture, animal immunization and histology	25
2.6.1 Reagents	25
2.6.2 Culture media and buffers	26

3. METHODS	30
3.1 Blockade of the binding of the fusion molecules PD-L1Ig and PD-L2Ig to endogenous PD-1 by anti-PD-1 8A7 antibody_____	30
3.2 Labelling of anti-PD-1 8A7 with Alexa Fluor®488_____	30
3.3 Generation of a monoclonal antibody anti-PD-L1 6H6_____	30
3.3.1 Immunization_____	30
3.3.2 Selection of hybridomas and fusion_____	31
3.3.3 Screening of positive clones_____	32
3.3.4 Cloning by limiting dilution_____	32
3.3.5 Obtaining a stable monoclonal antibody producing hybridoma_____	33
3.3.6 Purification of anti-PD-L1 6H6 and anti-PD-L1 16B8 antibodies_____	33
3.3.7 LPS contamination test_____	33
3.3.8 Determination of isotypes for anti-PD-1 8A7, anti-PD-L1 6H6 and anti-PD-L1 16B8 antibodies_____	34
3.3.9 Blockade of the binding of the fusion molecule PD-1Ig to endogenous PD-1 by anti-PD-L1 6H6_____	34
3.4 Methods in cell biology_____	34
3.4.1 General culture conditions_____	34
3.4.2 Count of viable cells_____	34
3.4.3 Staining of blood smears to determine parasitemia_____	34
3.4.4 Determination of cell proliferation _____	35
3.4.5 Preparation of spleen cells_____	35
3.4.6 Preparation of bone marrow-derived dendritic cells (BMDCs)_____	35
3.4.7 Isolation of infiltrated lymphocytes in the liver_____	36
3.4.8 Isolation of non-parenchymal liver cells _____	36
3.4.9 Isolation of hepatocytes_____	37
3.4.10 Isolation of T cells by magnetic sorting (MACS)_____	37
3.4.11 Isolation of CD4 ⁺ /CD25 ⁺ T cells by magnetic sorting_____	38
3.4.12 Flow cytometry_____	39
3.4.13 Histology_____	40
3.4.14 ELISA (Enzyme linked immunosorbent assay)_____	41
3.4.15 IFN- γ -ELISPOT (Enzyme linked immunospot assay)_____	42

3.5	<i>In vivo</i> experiments_____	42
3.5.1	Induction of malaria disease with <i>P. berghei</i> ANKA_____	42
3.5.2	Immunization with ACT-CSP_____	43
3.5.3	Administration of anti-PD-1 8A7 antibody _____	43
3.6	Statistical analysis_____	43
4.	RESULTS	44
4.1	Antibody evaluation_____	44
4.1.1	Comparison of anti-PD-1 8A7 antibody with the commercially available anti-PD-1 J43 _____	44
4.1.2	Evaluation of the blocking capacity of anti-PD-1 8A7 antibody_____	45
4.1.3	Evaluation of the blocking capacity of anti-PD-L1 6H6 antibody_____	46
4.1.4	Determination of isotypes of anti-PD-1 8A7, anti-PD-L1 6H6 and anti-PD-L1 16B8 antibodies_____	47
4.2	PD-1 and PD-L1 expression on different cell types_____	47
4.2.1	Induction of PD-1 expression on T cells upon <i>in vitro</i> stimulation of spleen cells with anti-CD3_____	47
4.2.2	Induction of PD-1 and PD-L1 expression on BMDCs upon <i>in vitro</i> stimulation with LPS and CpG ODN1826_____	49
4.2.3	Induction of PD-1 and PD-L1 expression on Tregs upon <i>in vitro</i> stimulation with anti-CD3_____	51
4.3	<i>In vitro</i> effects of the blockade between PD-1 and its ligands_____	52
4.3.1	<i>In vitro</i> effect of anti-PD-1 8A7 on spleen cells stimulated with anti-CD3_____	52
4.3.2	<i>In vitro</i> effect of anti-PD-1 8A7 on antigen specific stimulation_____	53
4.3.3	<i>In vitro</i> effect of anti-PD-1 8A7 concerning the suppressive capacity of Tregs_____	54
4.3.4	<i>In vitro</i> effect of anti-PD-L1 6H6 antibody on spleen cells_____	55

4.4	Analysis of the interaction between PD-1 and its ligands during <i>P. berghei</i> ANKA infection	56
4.4.1	Regulation of the CSP-specific CD8 ⁺ T cell response during <i>P. berghei</i> ANKA infection	56
4.4.2	Regulation of Tregs during infection with γ -irradiated <i>P. berghei</i> ANKA sporozoites	59
4.4.3	PD-1 expression on CSP-specific CD8 ⁺ T cells	60
4.4.4	PD-L1 expression on non-parenchymal liver cells during liver stage of <i>P. berghei</i> ANKA malaria	61
4.4.5	PD-1 and PD-L1 expression on CD4 ⁺ and CD8 ⁺ T cells during blood stage of <i>P. berghei</i> ANKA malaria	62
4.4.6	PD-L1 is induced on non-parenchymal liver cells and hepatocytes during the blood stage of <i>P. berghei</i> ANKA malaria	64
4.4.7	<i>In vivo</i> blockade of the interaction between PD-1 and PD-L1 with anti-PD-1 8A7 during <i>P. berghei</i> ANKA infection	65
5.	DISCUSSION	70
5.1	<i>In vitro</i> PD-1 and PD-L1 expression on T cells and BMDCs	70
5.2	<i>In vitro</i> effect of the blockade of PD-1 on spleen cells by anti-PD-1 8A7 antibody	71
5.3	<i>In vitro</i> effect of the blockade of PD-L1 on spleen cells by anti-PD-1 6H6 antibody	72
5.4	<i>In vivo</i> PD-1 and PD-L1 expression during <i>P. berghei</i> ANKA infection	73
5.5	<i>In vivo</i> effect of PD-1 blockade during <i>P. berghei</i> ANKA infection	76
5.6	Control of peripheral T cell tolerance and autoimmunity via PD-1 pathway	77
5.7	Role of PD-1 pathway on Tregs	79
6.	REFERENCES	82

LIST OF FIGURES

- Fig. 1.1:** B7/CD28 family and their ligands.
- Fig. 1.2:** Signalling through PD-1.
- Fig. 1.3:** The organization of hepatic anatomy.
- Fig. 1.4:** *Plasmodium* life cycle in humans.
- Fig. 4.1.1:** Comparison between anti-PD-1 8A7 antibody and the commercially available anti-PD-1 J43.
- Fig. 4.1.2:** Blockade of the binding of the fusion molecules PD-L1Ig and PD-L2 to endogenous PD-1 by anti-PD-1 8A7 antibody.
- Fig. 4.1.3:** Blockade of the binding of the fusion molecule PD-L1Ig to endogenous PD-1 by anti-PD-L1 6H6 antibody.
- Fig. 4.2.1:** PD-1 expression on naïve CD4⁺ and CD8⁺ T cells.
- Fig. 4.2.2:** PD-1 expression on CD11c⁺ BMDCs upon stimulation with LPS or CpG ODN1826.
- Fig. 4.2.3:** PD-L1 expression on CD11c⁺ BMDCs upon stimulation with LPS or CpG ODN1826.
- Fig. 4.2.4:** PD-1 and PD-L1 expression on T effs and Tregs upon stimulation with anti-CD3.
- Fig. 4.3.1:** *In vitro* effect of anti-PD-1 8A7 antibody on spleen cells in the presence or absence of anti-CD3.
- Fig. 4.3.2:** *In vitro* effect of anti-PD-1 8A7 antibody on antigen specific stimulation.
- Fig. 4.3.3:** *In vitro* effect of anti-PD-1 8A7 antibody concerning the suppressive capacity of Tregs.
- Fig. 4.3.4:** *In vitro* effect of anti-PD-L1 6H6 antibody on spleen cells.
- Fig. 4.4.1:** Regulation of the CSP-specific CD8⁺ T cell response during *P. berghei* ANKA infection.
- Fig. 4.4.2:** Analysis of the Treg population in mice during *P. berghei* ANKA malaria.
- Fig. 4.4.3:** PD-1 expression on CSP-specific CD8⁺ T cells in the liver.
- Fig. 4.4.4:** PD-L1 expression on non-parenchymal liver cells during liver stage *P. berghei* ANKA malaria.
- Fig. 4.4.5:** PD-1 and PD-L1 expression on CD4⁺ and CD8⁺ T cells during blood stage *P. berghei* ANKA malaria.
- Fig. 4.4.6:** PD-L1 expression on non-parenchymal liver cells during blood stage *P. berghei* ANKA malaria.

Fig. 4.4.7: PD-L1 expression during the blood stage malaria analyzed by immunohistology and flow cytometry.

Fig. 4.4.8: *In vivo* blockade of PD-1 during *P. berghei* ANKA infection.

Fig. 4.4.9: *In vivo* blockade of PD-1 during *P. berghei* ANKA infection after immunization with ACT-CSP.

LIST OF ABBREVIATIONS

aa	Aminoacids
ACT	Adenylate cyclase toxoid
ANKA	ANtwerpKatango
APC	Allophycocyanin
APC	Antigen presenting cell
BMDCs	Bone marrow–derived dendritic cells
BSA	Bovine serum albumin
BTLA	B and T lymphocyte attenuator
CpG	Unmethylated guanosine–cytosine sequences
cpm	Counts per minute
CSP	Circumsporozoite protein
CTLA–4	Cytotoxic T lymphocyte–associated antigen–4
DC	Dendritic cell
DNA	Deoxyribonucleic acid
EAE	Experimental autoimmune encephalomyelitis
ELISA	Enzyme linked immunosorbent assay
ELISPOT	Enzyme linked immunospot
FACS	Fluorescence–activated sorter
FITC	Fluorescein–isothiocyanat
FoxP3	Forkhead box protein P3
GM–CSF	Granulocyte–macrophage colony–stimulating factor
GPI	Glycosylphosphatidylinositol
HBV	Hepatitis B virus
HCV	Hepatitis C virus
HIV	Human immunodeficiency virus
HVEM	herpes virus entry mediator
ICOS	Inducible co–stimulatory molecule
IFN	Interferon
Ig	Immunoglobulin
IL	Interleukin
ITIM	Immunoreceptor tyrosine–based inhibitory motif
iTregs	Inducible regulatory T cells
ITSM	Immunoreceptor tyrosine–based switch motif

K.O.	Knock-out
KCs	Kupffer cells
LCMV	Lymphocytic choriomeningitis virus
LPS	Lipopolysaccharide
LSECs	Liver sinusoidal endothelial cells
LT- α	Lymphotoxin alpha
MACS	Magnetic cell sorting
MHC	Major histocompatibility complex
mRNA	Messenger RNA
NK cells	Natural killer cells
NO	Nitric oxide
NOD	Nonobese diabetic
nTregs	Naturally occurring regulatory T cells
OVA	Ovalbumin
p.i.	post-infection
PC	Lymphocytes Pit cells
PD-1	Programmed cell death-1
PD-L	Programmed cell death ligand
PE	Phycoerythrin
PEG	Polyethylene glycol
PfEMP1	<i>Plasmodium falciparum</i> erythrocyte membrane protein 1
PI3K	Phosphoinositol 3 kinase
pO ₂	partial pressure of oxygen
pRBCs	Parasitized red blood cells
PRRs	Pattern recognition receptors
RBCs	Red blood cells
RNA	Ribonucleic acid
rpm	rounds per minute
sfu	spot forming units
SHP-2	Src homology region 2 domain-containing tyrosine phosphase-2
TCR	T cell receptor
Teffs	T effector cells
TLR	Toll-like receptor
TNF	Tumor necrosis factor

Tregs

Regulatory T cells

1. INTRODUCTION

1.1 The immune system and its regulation

1.1.1 The immune system

The immune system of an organism consists of a group of mechanisms involved in the protection and defense against other organisms considered pathogens. It is found in nearly all forms of life in a different degree of complexity. Already bacteria possess enzymes able to neutralize viruses.

The first line of defense is provided by physical and biochemical barriers and it is present in almost all organisms. Membranes, cuticles, shells and skin are examples of mechanical barriers that avoid the adherence and entrance of pathogens. These structures are usually covered by fluids containing antimicrobial molecules like lysozyme and other enzymes. These secretions can be eliminated mechanically by ciliary action (mucus) or just flushed like in the case of tears, saliva or urine.

Another important mechanism of defense is provided by the commensal flora that not only competes with pathogens for the space and nutrients, but also changes the conditions of the environment, such as pH or available iron. These actions prevent the replication of the pathogen and thus reduce the possibility of invasion (Janeway C. *et al.*, 2001).

1.1.2 Innate immunity

However in some cases these barriers are not sufficient. The innate immunity is the next step of defense, more complex and found in all plants and animals (Janeway C. *et al.*, 2001). Innate immunity is triggered by the recognition of repeated molecular patterns that are conserved among broad groups of microorganisms and therefore a non-specific mechanism recognizing pathogens only in a generic way. Some of these structures are recognized by toll-like receptors (TLR) and can be extracellular patterns like lipopolysaccharide (LPS) on bacteria, mannans on the yeast cell wall or mycobacterial glycolipids. Examples of intracellular repeated molecular patterns are the unmethylated guanosine-cytosine (CpG) sequences of bacterial deoxyribonucleic acid (DNA) and double-stranded ribonucleic acid (RNA) from RNA viruses. The recognition of these repetitive patterns is done by specialized cells called phagocytes which are also able to engulf and kill those microorganisms. Neutrophils and macrophages are the most abundant phagocytes. Neutrophils are mainly found in the bloodstream and they are the first cells arriving at the infection site. Macrophages

reside within tissues. Both cell types secrete important factors like cytokines or interleukins involved in the recruitment of other immune cells and in the activation of the adaptive immune response.

Natural killer cells (NK cells) represent a very important cellular component of the innate immunity. NK cells can detect cells that have been infected by virus and eliminate them by a cytotoxic mechanism that consists of the release of cytoplasmic granules. These granules contain perforin and granzymes that lyse infected cells by creating pores in their membranes and subsequently inducing apoptosis.

Besides the cellular component of the innate immunity, the humoral component is very important in the destruction of pathogens. After their coating (opsonization), bacteria can be recognized and destroyed. The mechanism is called complement system and is characterized by the enzymatic cascade of activation of its components. Many organisms have complement systems including non-mammals (Janeway C. *et al.*, 2001).

In humans, the activation of the complement system is mediated either by the binding of the complement proteins directly to the carbohydrates on the bacterial surface (alternative pathway) or by the binding of specific antibodies to such bacteria (classical pathway). The activation of these complement factors initiates a cascade of proteolytic enzymes that need to be activated and in turn activate other factors, thereby leading to an enormously amplification of the initial signal and thus providing a rapid and effective response.

Opsonization with antibodies can directly kill bacteria by disruption of their membrane. Additionally, it acts as a mark for destruction that attracts other immune cells stimulating them to engulf these pathogens (Janeway C. *et al.*, 2001).

1.1.3 Adaptive immunity

Due to generic pathogen recognition, the innate immunity can not specifically recognize a pathogen in case of a second infection. The innate immunity lacks a memory. Vertebrates have developed sophisticated specific mechanisms, known as adaptive immunity, that include specialized cells, tissues and organs. All together cooperate in order not only to eliminate the pathogen, but also to prime the system, which is able to respond faster and better against a second encounter with the same pathogen.

INTRODUCTION

T and B cells are the major cellular components of the adaptive immunity. Both cell types derive from hematopoietic stem cells in the bone marrow. B lymphocytes mature in the bone marrow and their main characteristic is the ability to produce immunoglobulins. Immunoglobulins, also known as antibodies, are plasma proteins able to bind to pathogenic structures either directly neutralizing them or mediating the recruitment of cells and molecules that activate other effector mechanisms. This leads to the elimination of the opsonized pathogen. During their development, B cells undergo several differentiation steps in which their immunoglobulin genes result from different DNA arrangements. This specialized and unique mechanism together with the phenomenon of the somatic hypermutation, allow a single individual to recognize almost all structures. T and B cells have receptors that bind specifically foreign antigens. T cells, which migrate to the thymus very early during the embryonic development, have a specialized T cell receptor (TCR) that is the result of the rearrangement of the germline genes coding for it. T cells are only able to recognize peptides if they are “presented” by specific peptide binding glycoproteins known as major histocompatibility complex (MHC) on so called antigen presenting cells (APCs). During their development in the thymus, T cells become positively selected for their ability to bind these self MHC molecules ensuring the selection of a functional TCR. Later on T cells undergo a negative selection, leading to the elimination of T cells recognizing self antigens, bound to self MHC molecules. The immune system will then not react against self structures. There are two classes of MHC molecules known as MHC I and II. MHC I molecules are expressed by almost all cell types (except erythrocytes) and bind short peptides generated from viruses and bacteria that replicate in the cytosol of infected cells. In contrast MHC II molecules bind longer peptides derived from phagocytosed and digested pathogens in lysosomes and endosomes of APCs. The way of peptide presentation by determined class MHC molecules is important because it defines the kind of immune response to be activated. MHC I molecules are specifically recognized by a T cell subset defined by the presence of the CD8 molecule on their surface. CD8⁺ T cells recognize cells harbouring intracellular pathogens such as virus and degenerated tumor cells and exhibit cytotoxic activity. In contrast, peptides derived from digested pathogens in lysosomes are presented by MHC II molecules expressed on APCs such as dendritic cells (DCs), B cells and macrophages. Peptides on MHC II molecules are recognized by CD4⁺ T cells. These cells are also known as “helpers” (Th cells)

because they are able to activate other cells with different functions. CD4⁺ Th1 effector cells can activate macrophages whereas Th2 effector cells stimulate B cells to produce specific antibodies. Hence the consequence of inducing Th1 or Th2 cells is very important for the success of the immune response against a specific pathogen. A Th1 dominated response leads to cell-mediated immunity, very important in the defense against intracellular pathogens such as most bacteria and protozoa whereas Th2 cells induce a humoral response most required in infections with extracellular pathogens as helminths.

But definitely one of the most important characteristics of the adaptive immunity is the establishment of an immunological memory. After a primary infection, naïve T and B cells start a clonal expansion of pathogen-specific cells which is accompanied by a different gene-expression profile and the acquisition of special characteristics required to combat the infection. Once effector cells have eliminated the pathogen, populations of long-living memory T and B cells become established. Main characteristics of these cells are their fast mobilization and efficiency. Memory T cells can rapidly act as effector cells that secrete inflammatory cytokines and mediate the killing of pathogens. In the case of memory B cells, they develop into plasma cells that constitutively produce high-affinity neutralizing antibodies as a result of changes in their immunoglobulin genes through isotype switching and somatic hypermutation. Their development and requirements in terms of abundance of antigen and duration of antigen exposure are still under investigation. A better knowledge in this area will allow the design of new vaccination therapies (Kaech S. *et al.*, 2002; Harty J. *et al.*, 2008).

1.1.4 The B7/CD28 family

The activation of naive T cells to T effector cells (Teffs) requires not only a TCR signal by which foreign structures are recognised on MHC molecules but also a co-stimulatory signal that is delivered by APCs. The B7/CD28 family of cell surface glycoproteins plays an important role in this context (Chen L., 2004). Although the members of this family share high structural similarity as most of them belong to the immunoglobulin or tumor-necrosis factor (TNF) superfamily, they exhibit functional differences. Hence, there are molecules that can be classified as co-stimulators (enhancing TCR-mediated signalling) or co-inhibitors (abrogating TCR-mediated responses).

INTRODUCTION

Both responses are TCR dependent in a way that the absence of a proper TCR signal leads to loss of function of these co–signalling molecules. This characteristic is very important regarding induction and maintenance of tolerance characterised by the lack of immune response against self structures or foreign harmless proteins as in the case of dietary components. Although T cells undergo a negative selection during their development in the thymus that eliminates those cells that react to self structures, it is plausible that some of these autoreactive T cells escape of that control. Self proteins present in specialized cells of peripheral tissues as well as foreign innocuous proteins might be not present in the thymus during negative selection of T cell development. These potentially autoreactive T cells travel to the periphery where they can recognize self antigens provoking an autoimmune response. The dependence of both antigen recognition and co–stimulatory signals simultaneously in T cell activation guarantees the control of these cells and avoids the destruction of self structures. Members of the B7/CD28 family are shown in Fig. 1.1.

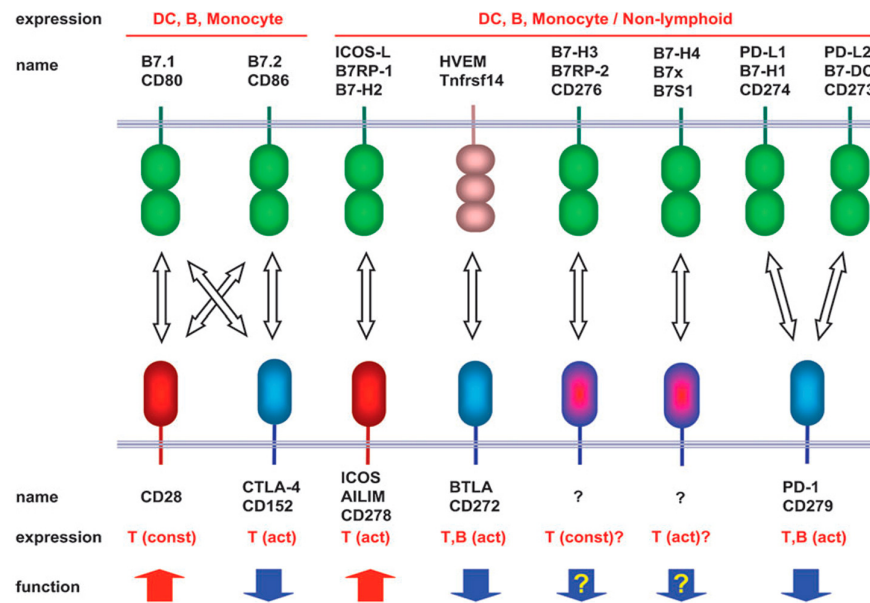


Fig. 1.1: B7/CD28 family and its ligands. Act: expression upon activation; const: constitutive expression; red arrows: co–stimulation function; blue arrows: co–inhibitory function; ?: unknown ligand or unknown function (Okazaki T. *et al.*, 2007).

The most studied co–signalling molecules are CD28, CD80 (B7–1), CD86 (B7–2) and cytotoxic T lymphocyte–associated antigen 4 (CTLA–4, also CD152). The expression of CD28 and CTLA–4 is found on T cells whereas CD80 and CD86 are expressed typically on APCs. The engagement of CD28 by CD80 and CD86

stimulates and sustains T cell responses by increasing their proliferation, cytokine production, mainly interleukin-2 (IL-2) and survival.

The inducible co-stimulatory molecule (ICOS) is also a member of the B7/CD28 family. ICOS is up-regulated on T cells following activation. Both Th1 and Th2 express ICOS but in Th2, ICOS persists at a higher level (Greenwald R. *et al.*, 2005). The ligand of ICOS (ICOSL) has been found on B cells, macrophages, DCs, some endothelial and epithelial cells. The interaction of ICOS with its ligand (ICOS-L) enhances Th2 effector T cell responses with a high production of IL-10 and IL-4 (Chen L., 2004; Khoury S. *et al.*, 2004). ICOS/ICOS-L pathway seems to have an important role in B cell differentiation, immunoglobulin class switching, germinal center formation and memory B cell development (Khoury S. *et al.*, 2004; Greenwald R. *et al.*, 2005).

A negative regulatory mechanism is also needed not only to sharpen an effective T cell response by avoiding the activation of T cells having low affinity TCRs but also to avoid the development of autoimmunity. Thus, the binding of CTLA-4, expressed rapidly on T cells after their activation, to CD80 and CD86 inhibits T cell responses, proliferation and cytokine production and induces cell cycle arrest. CTLA-4 binds B7 molecules with a higher affinity than CD28 does (Janeway C. *et al.*, 2001). Other studies have demonstrated the direct inhibition of the TCR signalling by binding of CTLA-4 with the ζ chain in the TCR (Lee K.M. *et al.*, 1998; Chikuma S. *et al.*, 2003). Recent investigations propose an additional role for CTLA-4 inducing signalling through CD80 and CD86 into DC to produce indoleamine 2,3-dyoxigenase (IDO), which is known to inhibit T cell responses (Chen L., 2004). The importance of CTLA-4 is demonstrated by the observation that CTLA-4 knock-out (K.O.) mice develop massive lymphoproliferation and lethal autoimmunity (Tivol E. *et al.*, 1995; Waterhouse P. *et al.*, 1995). CTLA-4 plays an important role in the maintenance of the T cell tolerance (Chen L., 2004; Khoury S. *et al.*, 2004; Greenwald R. *et al.*, 2005).

Another recently discovered co-inhibitory member of the B7/CD28 family is B and T lymphocyte attenuator (BTLA, also CD272). BTLA is found constitutively on naïve T cells and induced after activation (Watanabe N. *et al.*, 2003). B cells, macrophages and bone marrow-derived dendritic cells (BMDCs) also express BTLA. Functionally, BTLA is similar to CTLA-4 and exerts inhibitory effects on T and B lymphocytes.

1.1.5 PD-1

Programmed cell death-1 (PD-1) was originally identified from a T cell hybridoma undergoing programmed cell death (Ishida Y. *et al.*, 1992). PD-1 is a 288 aa type I transmembrane protein with a 20 aa Ig-superfamily domain and a 95 aa intracellular domain. The cytoplasmatic tail contains two tyrosine molecules (Zhang S. *et al.*, 2004). One is located in an immunoreceptor tyrosine-based inhibitory motif (ITIM) and the second one in an immunoreceptor tyrosine-based switch motif (ITSM). Mutagenesis studies have shown that the ITSM is responsible for the inhibitory effect of PD-1 (Okazaki T. *et al.*, 2001). When ITSM is mutated the function of PD-1 is lost. PD-1 is a monomeric protein but it is still unclear if dimerization is necessary to transduce signals.

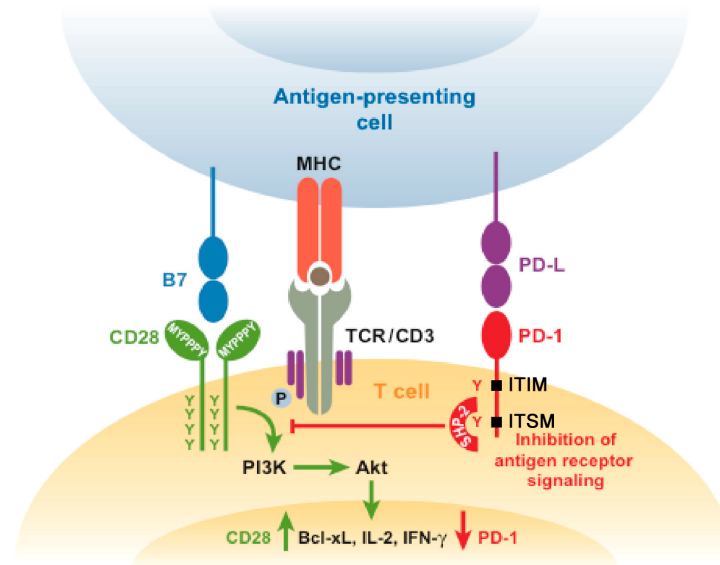


Fig. 1.2: Signalling through PD-1. The engagement of PD-1 with its ligands leads to phosphorylation of the cytoplasmatic tyrosines and the subsequent sequestration of Src homology region 2 domain-containing phosphatase-2 (SHP-2). The T-cell receptor (TCR) signalling cascade through phosphoinositol 3 kinase (PI3K) is impaired resulting in a decrease in IFN- γ production and cell proliferation. Akt: thymoma viral proto-oncogene; Bcl-xL: B-cell leukaemia/lymphoma x ITIM: Immunoreceptor tyrosine-based inhibitory motif; ITSM: Immunoreceptor tyrosine-based switch motif; P: phosphorylation. (Keir M. *et al.*, 2007).

PD-1 acts inhibiting the co-stimulatory signal through B7-CD28 by sequestration of Src homology region 2 domain-containing tyrosine phosphatase-2 (SHP-2). After the engagement of PD-1 with its ligand, the phosphorylation of the cytoplasmatic tyrosines increases the association of SHP-2 with the ITSM of PD-1 (Fig. 1.2).

The recruitment of SHP-2 diminishes the signalling through phosphoinositol 3 kinase (PI3K) that leads to an impaired TCR signalling, inhibiting cell proliferation and cytokine production. The PD-1 gene is located in chromosome 1 in mice and chromosome 2 in humans. In mice as well as in humans, PD-1 is expressed on activated T cells, B cells, NK T cells, activated monocytes and DCs (Yamazaki T. *et al.*, 2002; Liang S. *et al.*, 2003; Keir *et al.*, 2007).

The absence of PD-1 in K.O. mice produces different organ-specific disorders depending on their genetic background. PD-1 K.O. in C57BL/6 mice develop a lupus-like disease at 14 months of age with glomerulonephritis while BALB/c mice show a severe dilated cardiomyopathy at 5 months of age (Liang S. *et al.*, 2003). PD-1 has two ligands known as PD-L1 (CD274; B7-H1) and PD-L2 (CD273; B7-DC), both members of the B7-family (Freeman G. *et al.*, 2000; Latchman Y. *et al.*, 2001). PD-L1 is a 290 aa type I transmembrane protein with a very conserved intracellular short domain of about 30 aa. The function of this intracellular domain is still unknown. PD-L1 gene is found in chromosome 19 in mice and in chromosome 9 in humans (Keir *et al.*, 2007).

The mRNA of both mouse and human PD-L1 are constitutively expressed in the vascular endothelium of several tissues such as heart, liver, kidney, lung, thymus and placenta (Iwai Y. *et al.*, 2003). PD-L1 is furthermore expressed on DCs, macrophages, B cells and T cells and is up-regulated after activation.

PD-L2 is also a type I transmembrane protein. The length of its cytoplasmic domain varies in accordance with the species. In mice the PD-L2 cytoplasmic tail has only 4 aa whereas the longer form, about 30 aa is found in humans, macaques, dogs, pigs and horses. The cytoplasmic domain does not have any signalling motifs and its function is unknown. PD-L2 shares about 38 % homology with PD-L1. Murine PD-L2 expression is more restricted than its human counterpart. Human PD-L2 mRNA is found in non-lymphoid organs as well as lymphoid organs while murine PD-L2 is only expressed on DCs and macrophages (Iwai Y. *et al.*, 2003).

Several studies have demonstrated the important role of the PD-1/PD-L1 interaction in central and peripheral tolerance (Ansari M. *et al.*, 2003; Zhu B. *et al.*, 2006).

In the Nonobese Diabetic (NOD) mouse model of autoimmune T-cell mediated diabetes, Ansari found an up-regulation of PD-L1 on the islet β -cells in the pancreas. The blockade of PD-1/PD-L1 interaction led to a high production of

pro-inflammatory cytokines by T cells that caused a rapid and exacerbated insulinitis resulting in diabetes (Ansari M. *et al.*, 2003).

The role of PD-1/PD-L1 interaction has been also analyzed in experimental autoimmune encephalomyelitis (EAE), the mouse model of the human multiple sclerosis (Zhu B. *et al.*, 2006). The administration of monoclonal antibodies against PD-1 or PD-L1 during the induction of the disease accelerates its severity and onset (Zhu B. *et al.*, 2006).

These results are consistent with the idea that blocking the ligation of PD-1 with its ligand PD-L1 leads to an enhancement of the immune response.

Indeed, the interaction between PD-1 and PD-L1 plays an important role in immune responses against virus and bacteria that produce chronic infections. Iway found that liver sinusoidal endothelial cells (LSECs) and Kupffer cells (KCs) express PD-L1 constitutively and inhibit proliferation of virus-specific activated T cells expressing PD-1 (Iway Y. *et al.*, 2003). PD-1 K.O. mice show a rapid clearance of adenovirus in the liver (Ansari M. *et al.*, 2003).

Some authors have proposed an exhausted phenotype for virus-specific CD8⁺ T cells (Barber DL. *et al.*, 2006). These cells seem to be dysregulated after persistent viral antigen stimulation. They do not proliferate or show cytotoxic activity and neither can produce cytokines (Barber DL. *et al.*, 2006). It has been shown that these cells express PD-1. The blockade of the interaction between PD-1 and PD-L1 recuperates the normal activated phenotype by these cells, being able to eliminate the virus responsible for the chronic infection (Barber DL. *et al.*, 2006). In humans, PD-1 expression has been found on LCMV-, HIV-, HBV- and HCV-specific T cells and therefore PD-1 has been proposed as a marker for chronic infections (Golden-Mason L. *et al.*, 2007; Elrefaei M. *et al.*, 2008; D'Souza M. *et al.*, 2008).

In contrast with all these publications, some other *in vitro* and *in vivo* studies have demonstrated a co-stimulatory role for the interaction of PD-1 with PD-L1 (Dong H., *et al.*, 1999; Tamura H. *et al.*, 2001; Subudhi S. *et al.*, 2004). Subudhi and his collaborators constructed a transgenic mouse expressing PD-L1 on pancreatic islet β -cells. This expression induced the proliferation of CD8⁺ T cells that led to the rejection of transplanted allogenic PD-L1-expressing islet β -cells (Subudhi S. *et al.*, 2004).

Supporting this idea, Shin *et al.* showed that mutants of PD-L1 and PD-L2 that lost their capacity to bind PD-1 remained co-stimulatory for T cells (Shin T. *et al.*,

2003). It has been postulated that these molecules could also have another receptor in addition to PD-1 that would mediate these positive stimulatory signals. Recently it has been described that PD-L1 also specifically interacts with CD80 but thereby inhibiting T cell responses, too (Butte M. *et al.*, 2007).

Additionally, the co-stimulatory role of PD-L1 has been also described in an infection mouse model with *Listeria monocytogenes* (Seo S. *et al.*, 2007, Rowe J. *et al.*, 2008). The blockade of PD-L1 through a monoclonal antibody during the priming with an attenuated *L. monocytogenes* reduced the magnitude of the T cell expansion to the subsequent challenge with a virulent *L. monocytogenes* (Seo S. *et al.*, 2007, Rowe J. *et al.*, 2008).

Maybe these contradictory results are consequence of different roles of PD-L1 depending on the activation state of T cells. Hence, PD-L1 could modulate T cell responses, stimulating priming and cytokine production by naïve T cells (through an unknown receptor) and inhibiting effector responses in activated T cells through PD-1.

1.1.6 Regulatory T cells

Intracellular and extracellular pathogens induce different immune responses. These pathways are characterized by a typical cytokine secretion pattern and cellular activation in order to eliminate the pathogen. Hence a Th1 response with interferon gamma (IFN- γ) and IL-2 production has been described to be essential for the eradication of intracellular pathogens whereas a Th2 response with production of IL-4, IL-5 and IL-13 is important in the response against extracellular pathogens as in the case of helminths (O'Garra A. *et al.*, 2004).

Although effective, these responses must be controlled in order to avoid tissue damage that can occur as a consequence of high pro-inflammatory reactions mainly related to Th1-type immune response. In the case of the Th2 responses, to avoid allergic reactions that can occur as a secondary effect due to overwhelming Th2 responses. Therefore the anti-inflammatory reactions are necessary.

It has been described that regulatory T cells (Tregs) are implicated in these control since they are able to inhibit pathology and autoimmune diseases *in vivo* (O'Garra A. *et al.*, 2004; Zozulya A. *et al.*, 2008). Tregs also play a role in the suppression of immune responses to viral, bacterial and protozoal infections (Sakaguchi S. *et al.*, 2003). Indeed it has been observed that a population of Tregs that develop in the

thymus, known as naturally occurring CD4⁺/CD25⁺ Tregs (nTregs) that express the transcription factor forkhead box protein P3 (foxp3) can inhibit the stimulation of naïve CD4⁺ T cells *in vitro* (O'Garra A. *et al.*, 2004). Tregs also produce IL-10, an important suppressive cytokine. IL-10 can modulate both Th1 and Th2 pathways and it is discussed whether the suppressive role mediated by these Tregs would be exerted by the action of this cytokine, by cell-cell contact or by both in combination. Since IL-10 can also be produced by dendritic cells, macrophages and B cells, it is likely that different cells others than Tregs contribute to those regulatory mechanisms (O'Garra A. *et al.*, 2004).

1.1.7 Liver tolerance

The liver is an important organ that induces tolerance rather than immunity (Crispe N., 2003). It receives blood directly from the gut with a high concentration of harmless antigenic material from food and therefore a level of tolerance is necessary to avoid a constant activation of the immune system. Nevertheless, the existence of rapid mechanisms that allow the breakdown of this tolerance is important whenever the body is invaded by pathogens that trespass the intestinal mucosa and reach the blood stream.

Some pathogens are detected when they invade the liver. In the case of viral infections there is a T cell activation that leads to the destruction of the pathogen. However several other infections, e.g. malaria, persist in the liver despite an ongoing immune response. Additionally, it has been observed that tumour cells expressing well-defined antigens can reach the liver and thus evade the immune system (Crispe N., 2003).

The tolerance status of the liver partially depends on its special anatomic organization (Fig. 1.3). The blood from the portal vein flows between plates of hepatocytes in a structure called sinusoid. These structures allow the transport of different substances such as nutrients between the blood stream and the hepatocytes. This transport is mediated and controlled by a special cell type, the liver sinusoidal endothelial cells (LSECs) which line the sinusoid.

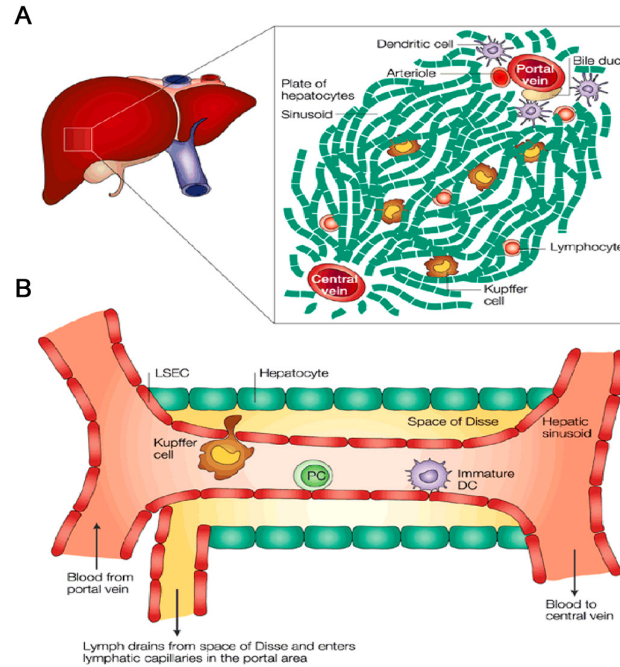


Fig. 1.3: Organization of the hepatic anatomy. A. Structure of a liver lobule. Blood flows from the portal vein through sinusoids that are present between cords of hepatocytes. B. Sinusoid organization. Kupffer cells, lymphocytes Pit cells (PC) and immature dendritic cells (DCs) are found in the sinusoids. Liver sinusoidal endothelial cells (LSECs) allow the trespassing of cells from blood stream to hepatic tissue. (Crispe N. *et al.*, 2003).

The sinusoidal endothelium is fenestrated and LSECs control the trespassing of T cells to the hepatic parenchyma reaching this way the tissue if it is necessary. The sinusoids also contain a special population of macrophages known as Kupffer cells. LSECs and Kupffer cells constitutively express molecules necessary for the establishment of the interaction with leucocytes as well as molecules involved in antigen presentation like MHC class I and II, ICAM-1 (CD54), CD80 and CD86. They also secrete anti-inflammatory mediators. It has been found that these cells are involved in the induction of hepatic tolerance (Crispe N., 2003). Beside these cells, hepatocytes have been shown to be important in the modulation of the T cell response. *In vitro* hepatocytes can prime specific activation and proliferation of naïve CD8⁺ T cells (Wahl C. *et al.*, 2008) as efficient as they were professional APCs (Wahl C. *et al.*, 2008).

1.2 Malaria disease and host defense

1.2.1 Malaria

According to the World Health Organization in its last report, malaria affected 247 million people among 3.3 billion people at risk in 2006 and caused nearly

a million deaths, mostly of children under 5 years of age. Malaria is one of the most severe health problems in Africa, India, the Far West and South America (World Malaria report 2008; World Health Organization). It is caused by the infection with a protozoan parasite belonging to the genus *Plasmodium*. The parasite is transmitted by the bite of an infected female *Anopheles* mosquito. Four members of the genus *Plasmodium* can cause the disease in humans in a different degree of severity. *P. malariae* and *P. ovale* rarely cause clinical malaria whereas *P. falciparum*, endemic in most of sub-Saharan regions in Africa and other tropical areas, causes the highest mortality. *P. vivax* causes severe and acute febrile illness but is rarely fatal.

1.2.2 *Plasmodium* life cycle

Plasmodium has a complex life cycle, which alternates between extracellular and intracellular forms including sexual reproduction in the mosquito and asexual division in liver cells and erythrocytes in humans (Fig. 1.4).

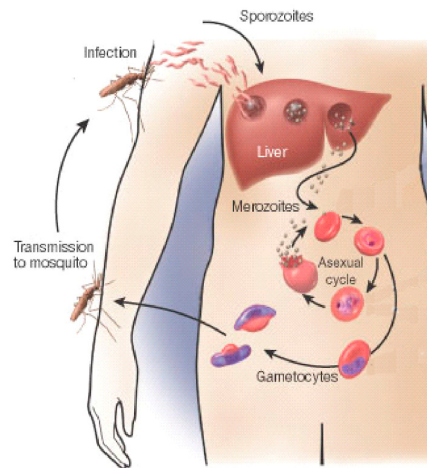


Fig. 1.4: *Plasmodium* life cycle in humans. The sporozoitic form of the parasite is transmitted by the bite of the female *Anopheles* mosquito. Sporozoites invade hepatocytes, divide rapidly and develop into merozoites. After their release into the blood stream, merozoites invade erythrocytes (RBC, red blood cells) initiating the symptomatic stage of the disease. Some merozoites develop into trophozoites and these to gametocytes that pass to the mosquito when it bites. The sexual stage of the parasite occurs in the mosquito's mid gut where gametes fuse and form the zygote that after maturation produces sporozoites, closing the cycle. (Miller L. *et al.*, 2002).

The parasite enters the human host during the bite of an infected female mosquito *Anopheles*. Thereby, sporozoites are injected from the salivary glands of the mosquito into the blood stream of the host. They travel to the liver where they invade parenchymal cells. In these cells they develop into schizonts. Over the next

5–10 days these schizonts divide rapidly and produce merozoites. Each schizont can generate around 30,000 merozoites. Up to this point the infection is silent, asymptomatic and is known as the liver stage. The parasite induces apoptosis in the hepatocytes and form vesicles filled with parasites known as merosomes (Sturm A. *et al.*, 2006). These structures not only ensure the migration of the parasite into the bloodstream but also evade the recognition of the parasite by phagocytes. Once in the bloodstream merozoites invade erythrocytes. Inside the erythrocytes merozoites develop into trophozoites and finally into schizonts which then produce more merozoites. After 2–3 days the erythrocytes explode releasing the merozoites back into the blood stream. Consequently, these merozoites invade new erythrocytes and the cycle continues.

In the case of *P. falciparum* infection these erythrocytic cycles occur every 48 hours and correspond to the appearance of bouts of chills, fever and sweats in the host. This phase is known as the blood stage. Some of the trophozoites develop into male and female gametocytes, the sexual stage of the parasites. These gametocytes are taken up by the female mosquito during the blood meal. Inside the mosquito's mid gut the gametocytes develop into gametes, fuse and the zygote forms. Within 24 hours the zygotes transform into motile ookinetes that are burrowed into the stomach wall. After encysting, they become oocysts that divide and produce approximately 1,000 sporozoites each. After 7 days the oocysts rupture releasing the sporozoites, which travel to the salivary glands and become transmitted into a new host (Miller L. *et al.*, 2002; Stevenson M. *et al.*, 2004).

1.2.3 Immunity against malaria

In the life cycle of *P. falciparum* in humans there is only a short window where T cells can be directly activated by infected cells. Immediately after infection, during the liver stage when the parasites develop and replicate in hepatocytes, for some days these parasitized cells are able to present *Plasmodium*-derived peptides on MHC I molecules to CD8⁺ T cells. Later during the blood stage, the parasites inside the erythrocytes do not promote a direct T cell activation since erythrocytes lack MHC molecules.

The role of CD8⁺ T cells is very important during the liver stage of malaria infection (Hafalla J. *et al.*, 2003; Ocaña-Mogner C. *et al.*, 2003). After infection of mice with irradiated *P. berghei*, an expansion of a MHC I-restricted CD8⁺ T cell population

specific for a peptide present in the C-terminal portion of the malaria circumsporozoite protein (CSP) was found (Morrot A. *et al.*, 2004). These cells produce large amounts of IFN- γ and TNF- α when stimulated *in vitro* with the antigen. CD8⁺ T cells strongly inhibit the parasite development during the liver stage but are also stage specific since they fail to eliminate the parasite during the blood stage of the infection where the sporozoites are longer not present. Similar results have been obtained with humans using irradiated *P. falciparum* sporozoites (Clyde D.F. *et al.*, 1973; Hoffman S. *et al.*, 2002). Moreover the natural infections only generate low cytotoxic CD8⁺ T cell responses during the liver stage. In this context it has been described that the blood stage of malaria infection would induce DCs to suppress CD8⁺ T cell responses (Ocaña-Mogner C. *et al.*, 2003). This mechanism could explain in part the immune suppression observed in malaria patients.

During the blood stage of malaria infection, the parasitized red blood cells (pRBCs) and several parasite molecules can activate DCs and macrophages.

TLRs and other surface receptors present in the host such as CD36 on macrophages seem to play an important role in triggering cellular immune responses (Stevenson M. *et al.*, 2004).

Glycosylphosphatidylinositol (GPI) is present on the membrane of the parasite and it has been shown *in vitro* to be recognised by TLR 2 and 4, inducing macrophages to secrete TNF- α , nitric oxide (NO) and IL-1 (Schofield *et al.*, 2000). These mediators are directed to kill the parasite but are also implicated in the pathogenesis of the cerebral malaria, a complication derived from *P. falciparum* malaria (Maneerat Y. *et al.*, 2000). Recent contradictory results using *P. berghei* infected TLR 2 /4 /9 K.O. mice have demonstrated that the myeloid differentiation factor 88 (Myd88), an essential intracellular adaptor molecule of TLR pathway, rather than TLR 2, 4 and 9 is responsible for the parasite clearance (Cramer J. *et al.*, 2008).

The *P. falciparum* erythrocyte membrane protein 1 (PfEMP1) is encoded by the large and diverse *var* gene family and has a central role in the *P. falciparum* malaria. It is expressed on the surface of infected red blood cells (iRBCs) and acts as adhesion molecule avoiding parasite destruction in the spleen. PfEMP1 binds CD36, present on macrophages and mediates phagocytosis of malarial infected erythrocytes by an opsonin-independent way (Miller L. *et al.*, 2002). PfEMP1 also binds CD36 on dendritic cells inhibiting their maturation and reducing their capacity of stimulating T cells (Urban B. *et al.*, 1999).

Recent publications contradict this role of PfEMP1 and argue that although *Plasmodium* affects the maturation of DCs, this mechanism is independent of PfEMP1 (Vichchathorn P. *et al.*, 2006; Elliott S. *et al.*, 2007). The contradictory results can be explained by the use of different *Plasmodium* strains (lethal or non-lethal) in mice with a different genetic background (Wykes M. *et al.*, 2008).

It has been demonstrated that during the blood stage, CD4⁺ T cells contribute to the acquired immunity (Hafalla J. *et al.*, 2003). Indeed the Th1 response, characterized by production of IFN- γ and IL-2 is necessary not only to mediate the cellular immune response, but also to promote the antibody response during the chronic stage of the infection.

1.2.4 Pathogenesis of malaria disease

Among the four species of *Plasmodium*, only *P. falciparum* provokes severe malaria, a complication of the malaria infection with symptoms like anaemia, respiratory distress or the most severe manifestation, cerebral malaria. This illness causes around 1 million deaths every year (Miller L. *et al.*, 2002; Stevenson M. *et al.*, 2004).

Cerebral malaria affects mainly children living in endemic areas who have already established some antimalarial immunity or travellers from non-endemic areas. The disease is characterised by a reversible encephalopathy with seizures and loss of consciousness.

There are two mainly hypothesis about the pathogenesis of cerebral malaria. Both are still controversially discussed. The “sequestration hypothesis“ suggests that the adherence of the pRBCs to the cerebral vascular endothelium would produce an obstruction of the blood circulation causing hypoxia in several parts of the central nervous system, compromising its normal function.

Indeed the phenomenon of infected erythrocytes adhering to the vascular endothelium in humans is exclusively found in *P. falciparum* malaria (Clark I. *et al.*, 2004).

In contrast, the “cytokine” hypothesis postulates that the mediators produced as result of an immune response against the malaria infection would have an adverse effect to the cerebral function (Rae C. *et al.*, 2004).

Cerebral malaria has been correlated with high circulating levels of IFN- γ , TNF- α , lymphotoxin alpha (LT- α), IL-1 and IL-6 (Wenisch C. *et al.*, 1999; Lyke K., 2004). The most common idea is that cerebral malaria is an immune-mediated disease

where the innate immunity of the host would play a central role in the appearance of the complications associated with the *P. falciparum* malaria infection (Stevenson M. *et al.*, 2004).

There are several techniques, which have been used to elucidate the importance of both theories. Among them, the study of post-mortem cerebral and retina tissues of patients who succumbed to cerebral malaria, genetic studies of susceptibility or resistance in some human populations and several studies in malaria mouse models were used (Clark I. *et al.*, 2003; Rae C. *et al.*, 2004;). Histopathological examinations of brain samples showed the sequestration of monocytes, destruction of microvasculature and activation of microglial cells (Rae C. *et al.*, 2004). However in a large study of brains of African children diagnosed as having cerebral malaria, the sequestration of pRBCs in the brain was negligible (Clark I. *et al.*, 2003).

Concerning the cytokine importance in the affection of the brain, it has been demonstrated in several studies that TNF- α can stimulate glycolysis and lactate production in a variety of cell types including astrocytes in mice (Clark I. *et al.*, 2004; Rae C. *et al.*, 2004; Hanum S. *et al.*, 2003). IFN- γ can also induce the production of lactate in murine astrocytes (Rae C. *et al.*, 2004). Elevated levels of lactate have been found in cerebrospinal liquid of patients with cerebral malaria (Clark I. *et al.*, 2004). This lactate production and its effects have been named as “cytopathic hypoxia” and would explain the fact that patients suffering of cerebral malaria show normal cerebral venous pO₂, an unexpected consequence if there was a substantial vascular obstruction (Clark I. *et al.*, 2004).

1.2.5 Co-stimulation and pathology

The presence of CD4⁺ T cells expressing CTLA-4 is induced during the blood stage of malaria infection in humans as well as mice (Schlotmann T. *et al.*, 2000; Jacobs T. *et al.*, 2002; Jacobs T. *et al.*, 2004). *In vivo* blockade of CTLA-4, using a monoclonal antibody in C57BL/6 mice infected with *P. berghei* leads to an exacerbation of the course of cerebral malaria and also liver pathology occurs much earlier than in untreated mice.

Moreover, the expression of CTLA-4 prevents liver pathology during the liver stage of malaria infection since it restricts the T cell response, avoiding the secretion of pro-inflammatory cytokines (Jacobs T. *et al.*, 2004).

The role of CTLA-4 has also been studied with *P. yoelii*, another mouse model of malaria that in contrast to the infection caused by *P. berghei* is characterised by a balance between Th1 and Th2 responses. In this model, CTLA-4 blockade markedly increases the frequency of CD4⁺ T cells leading to a rapid clearance of the parasites and a lower peak parasitemia. Although mice show high amounts of IFN- γ in serum, high levels in IL-4 and IL-10 are also observed, suggesting that the CTLA-4 blockade does not influence the balance between Th1 and Th2 response (Lepenies B. *et al.*, 2007).

In conclusion, CTLA-4 plays an important role in the control of the immune response preventing peripheral tissue damage.

1.2.6 Co-stimulation and protection

The function of CTLA-4 has also been used in enhancing the effectiveness of vaccines (Chambers C. *et al.*, 2001; Keler T. *et al.*, 2003).

This is also the case of vaccines against *Plasmodium*. The detoxified adenylate cyclase toxoid (ACT) of *Bordetella pertussis* delivers its N-terminal catalytic domain into the cytosol of CD11b-expressing APCs and it is used to introduce *P. berghei* antigen CSP into the MHC class I presentation pathway generating a specific CD8⁺ T cell population specific for CSP (Simsova M. *et al.*, 2004). Although the immunization of mice with this construction ACT-CSP, leads to an increase in the frequency of CSP-specific CD8⁺ T cells, this does not result in protection against *P. berghei* malaria infection (Tartz S. *et al.*, 2006). In contrast, the administration of monoclonal antibody against CTLA-4 during the immunization with ACT-CSP between priming and boost induces an even higher number of CSP-specific CD8⁺ T cells that confer protection in 60 % of treated animals (Tartz S. *et al.*, 2006).

BTLA is a newly discovered member of the B7 family and shares not only structural similarities with CTLA-4 and PD-1, but also function (Watanabe N. *et al.*, 2003). Recently, herpes virus entry mediator (HVEM) has been described as a ligand for BTLA (Sedy J. *et al.*, 2005). The role of BTLA in the pathology of cerebral malaria has been analyzed using the murine model *P. berghei* ANKA (Lepenies B. *et al.*, 2007). BTLA is expressed on naïve T cells and is induced during infection. An agonistic antibody against BTLA could reduce the incidence of cerebral malaria in infected mice with a diminished sequestration of T cells in the brain and decreased

levels of pro-inflammatory cytokines in serum of treated mice (Lepeniev B. *et al.*, 2007).

Taken together, the importance of different members of the B7/CD28 family in the pathology of malaria has been demonstrated in several studies, clearly indicating that the modulation of co-stimulatory signals influences the outcome and degree of the immune response.

1.2.7 Animal models of malaria

There are several murine models that allow researchers to examine the pathological processes of malaria in the laboratory.

The infection of C57BL/6 mice with the ANKA strain of *P. berghei* reproduces the symptoms of human cerebral malaria although it fails to provoke that infected erythrocytes adherence to the vascular endothelium in the brain as seen in humans, therefore the raised doubts about the relevance of this model (Hanum S. *et al.*, 2003). C57BL/6 mice, that are susceptible to the disease, develop cerebral symptoms as ataxia, paralysis, deviation of the head and convulsions at day 10 after infection and finally die with a parasitemia around 15–20 %. On the other hand the infection of BALB/c mice with the same strain does not induce cerebral malaria and the mice survive longer than 3 weeks dying of anaemia caused by a high parasitemia of around 80 %. A comparative study with cerebral malaria susceptible and resistant mouse strains was done by Hanum and Hayano in order to elucidate the differences in the cytokine production pattern at different time points during a *P. berghei* infection. Although both strains showed a Th1 skewed response at day 4 after infection, BALB/c mice had significantly higher levels of IFN- γ , TNF- α and NO in spleen cells suggesting that Th1 responses are involved in the resistance observed in these mice against the disease. During the course of infection the production of NO was higher in BALB/c mice than in C57BL/6 mice suggesting a higher activation of macrophages in the cerebral malaria resistant strain compared to the susceptible. Additionally, a strong expression of TNF- α was observed in the brain of infected BALB/c animals on day 6 after infection. Interestingly, the infection in both mouse strains could increase the expression of chemokine genes in the brain as well as in the liver and spleen as early as 24 hours post-infection (Hanum S. *et al.*, 2003). Astrocytes were discussed to be the source of chemokine expression in the brain and this seems to be a common phenomenon in response to LPS, injury, viral infection,

etc. Thus, it is not clear yet what provokes cerebral malaria in mice and which are the differences between murine and human cerebral malaria.

While the *P. berghei* mouse model has been used to investigate pathogenesis and cerebral malaria, the infection with *P. yoelii* permits researchers a model with a more balanced immune response between pro-inflammatory and anti-inflammatory cytokines that allows the better study of the immunity during the erythrocytic stage of *Plasmodium* infection. *P. yoelii* infections are characterized by high peaks of parasitemia followed by clearance of the parasite in around three weeks (Ching L. *et al.*, 2001). *P. yoelii* infected mice show production of not only IFN- γ , and tumor growth factor β (TGF- β) but also IL-4 and IL-10 indicating that both Th1 and Th2 cells contribute to the elimination of the parasite. This balance between Th1 and Th2 immune responses seems to be critical for the development of the disease as it has been observed from the analysis using two different virulent strains of *P. yoelii*, *P. yoelii* 17XL (lethal) and *P. yoelii* 17NL (non-lethal) (Li C. *et al.*, 2001). High levels of both IFN- γ and IL-10 have been found in the case of the lethal infection whereas only increased IFN- γ was found in the non-lethal infection. This early imbalance between Th2 and Th1 responses in the spleen of *P. yoelii* 17XL infected mice would result in lower elimination of the parasite, subsequent higher parasitemia and death (Li C. *et al.*, 2001).

Although mouse models are being very useful in the elucidation of the immune response against malaria, several authors have criticised the methodology. First, the parasite is not a natural mouse pathogen. Second, the infections routes are not usual (intravenous injection with sporozoites or intraperitoneal injection of infected blood cells) instead of intradermal inoculation by the mosquito. And third, the large number of injected parasites provokes an unnatural high stimulation of the innate immune system (Langhorne J. *et al.*, 2008).

1.3 Aims of this study

PD-1 and its ligands have been involved in the necessary regulation of the immune response that is important not only to maintain tolerance to self structures in the body but also to avoid possible tissue damage in the host during infection. An important mechanism implicated in this control is the exerted by the suppressive capacity of Tregs to inhibit Teffs.

INTRODUCTION

The aim of this study is to elucidate the role of the interaction between PD-1 and its ligand PD-L1 during malaria and how this interaction influences the host's immune response against the parasite.

To this purpose, first the expression of PD-1 and PD-L1 is analyzed on different cell types, including CD4⁺ and CD8⁺ T cells, BMDCs and Tregs.

Additionally, the role of PD-1 and PD-L1 in the modulation of the T cell response is analyzed *in vitro* using an antibody against PD-1 (anti-PD-1 8A7) and a newly generated antibody against PD-L1 (anti-PD-L1 6H6). Whether the PD-1/PD-L1 pathway is involved in the suppressive capacity of Tregs is also term of study.

The role of PD-1 and PD-L1 during malaria is analyzed using the mouse model with *P. berghei* ANKA. After immunization with the vaccine ACT-CSP, the number of CD8⁺ CSP-specific T cells increases without conferring protection. The expression of PD-1 on these liver stage specific CD8⁺ T cells during the disease is analyzed in this study. Additionally the expression of PD-L1 on hepatocytes as well as non-parenchymal liver cells (LSECs and KCs) is determined during both stages of the *Plasmodium* infection.

Finally, anti-PD-1 8A7 is also used *in vivo* to blockade the interaction between PD-1 and its ligand PD-L1 during malaria. The effect of this blockade is determined by the amount and functionality of CD8⁺ CSP-specific T cells as well as changes in the outcome of the disease.

2. MATERIALS

2.1. Instruments

Centrifuge 5415C	<i>Eppendorf, Hamburg</i>
CO ₂ incubator	<i>Heraeus Instruments, Hanau</i>
Cryostat	<i>Microm HM 560</i>
Digital scales	<i>Kern&Söhne, Alberstadt</i>
ELISA reader Lamda E	<i>MWG Biotech, Ebersberg</i>
ELISPOT reader	<i>Byo-Sys, Karben-Frankfurt</i>
FACSCalibur	<i>Becton Dickinson, Mountain View, USA</i>
FACS Software CELLQuestPro 3.0	<i>Becton Dickinson, Mountain View, USA</i>
Fluorescent Microscope	<i>Zeiss, Oberkochen</i>
Irradiation system (γ -source)	<i>STS, Braunschweig</i>
Inverse Microscope	<i>Nikon, Japan</i>
Light Microscope	<i>Zeiss, Oberkochen</i>
Liquid scintillation-meter	<i>Wallac, Turku, Finland</i>
Magnets	<i>Jahnke&Kunkel, IKA Labortechnik, Staufen</i>
Megafuge 1.0 R	<i>Heraeus Instruments, Hanau</i>
Micropipettes (1000 μ l, 200 μ l, 100 μ l, 10 μ l)	<i>Eppendorf, Hamburg</i>
Microwave	<i>Panasonic, Wiesbaden</i>
PanasonicMinishaker	<i>IKA @Labortechnik, Staufen</i>
pH meter MP225	<i>Labortec, Wiesbaden</i>
Photometer	<i>Brandt, Wertheim</i>
Pipetus Akku	<i>Hirschmann Laborgeräte</i>
Sigma 3-16 K	<i>Sigma, Deisenhofen</i>
Spectrophotometer	<i>Hitachi, Japan</i>
Sterile cabin (Lamin Air HB 2448)	<i>Heraeus Instruments, Hanau</i>
Thermomix MM	<i>B Braun Biotech International, Melsungen</i>
Thermomixer 5436	<i>Eppendorf, Hamburg</i>
Water purification system MilliQ	<i>Millipore, Bedford, USA</i>

MATERIALS

2.2 Plastic and glass material

All material used for cell culture was sterile.

5 mL polystyrene round-bottom tubes (FACS tubes)	<i>Falcon, Beckton Dickinson, Heidelberg</i>
6-well culture plates	<i>Greiner, Frieckenhausen</i>
48-well culture plates	<i>Greiner, Frieckenhausen</i>
96-well round-bottom culture plates	<i>Greiner, Frieckenhausen</i>
96-well ELISA plates	<i>Greiner, Frieckenhausen</i>
96-well MultiScreen HTS TM HA	<i>Millipore, Bedford, USA</i>
15-mL tubes	<i>Falcon/BD, Heidelberg</i>
50-mL tubes	<i>Falcon/BD, Heidelberg</i>
Cryotubes	<i>Brand, Wertheim</i>
0.5 mL Eppendorf tubes	<i>Eppendorf, Hamburg</i>
1.5 mL Eppendorf tubes	<i>Eppendorf, Hamburg</i>
CellStrainer 70µm Nylon	<i>BD Bioscience, Heidelberg</i>
Cover glasses	<i>Marienfeld,</i>
Culture flasks	<i>Nunc, Roskilde, Denmark</i>
Glass pipettes	<i>Brand, Wertheim</i>
Hypodermic needle 0.40x20mm	<i>B Braun, Melsungen</i>
Insulin syringe	<i>B Braun, Melsungen</i>
Microscope slides	<i>Resy,</i>
Neubauer chamber 0.0025mm ²	<i>Brandt, Melsungen</i>
Single-use syringe 5 mL	<i>B Braun, Melsungen</i>
Stericup™ Presterized Vacuum filtration system	<i>Millipore, Bedford, USA</i>
Tissue culture dish 100x20mm	<i>Sarstedt, Nümbrecht</i>

2.3 Mouse, rat and *P. berghei* strains

2.3.1 Mouse strains

All mice used for experiments were between 8 and 10 weeks old.

BALB/c mice (H2-K ^d)	<i>UKE, Hamburg</i>
C57BL/6 mice (H2-K ^b)	<i>UKE, Hamburg</i>
DO.11.10tg mice (H2-K ^d)	<i>UKE, Hamburg</i>

2.3.2 Rat strain

Rat Lewis *BNI, Hamburg*

2.3.3 Plasmodium strain

Stabilate *P. berghei* ANKA *BNI, Hamburg*
(iRBCs)

Sporozoites *Plasmodium berghei* ANKA *Dr. Volker Heussler (BNI, Hamburg)*

2.4 Antibodies and fusion molecules

Anti-FITC–Oregon Green *Molecular Probes, Eugene, USA*
 Chicken anti–rat IgG–Alexa Fluor®594 *Invitrogen, Karlsruhe*
 CromePure Rat IgG whole molecule *Jackson Immunoresearch, Soham, UK*
 Goat anti–human IgG–PE *Jackson Immunoresearch, Soham, UK*
 Hamster anti–mouse CD11c–APC *BD Bioscience Pharmingen, Heidelberg*
 Hamster anti–mouse PD–1–PE (J43) *BD Bioscience Pharmingen, Heidelberg*
 Hamster anti–mouse PD–1–bio (J43) *BD Bioscience Pharmingen, Heidelberg*
 Hamster IgG1 isotype control–PE *BD Bioscience Pharmingen, Heidelberg*
 Rat anti–mouse CD3–PE–Cy5 *BD Bioscience Pharmingen, Heidelberg*
 Rat anti–mouse CD4–APC *Caltag, Burlingame, USA*
 Rat anti–mouse CD4–PE *Caltag, Burlingame, USA*
 Rat anti–mouse CD8–APC *Caltag, Burlingame, USA*
 Rat anti–mouse CD8–PE (CT–CD8) *Caltag, Burlingame, USA*
 Rat anti–mouse CD11b–PerCP–Cy5.5 *BD Bioscience Pharmingen, Heidelberg*
 Rat anti–mouse CD62L–PE *BD Bioscience Pharmingen, Heidelberg*
 Rat anti–mouse CD25–FITC *BD Bioscience Pharmingen, Heidelberg*
 Rat anti–mouse CD26–FITC *BD Bioscience Pharmingen, Heidelberg*
 Rat anti–mouse Foxp3–PE *BD Bioscience Pharmingen, Heidelberg*
 Rat anti–mouse ICAM–1–FITC *BD Bioscience Pharmingen, Heidelberg*
 Rat anti–mouse PD–L1–PE *BD Bioscience Pharmingen, Heidelberg*
 Rat anti–mouse PD–L1–biotin *BD Bioscience Pharmingen, Heidelberg*
 Rat anti–mouse PD–1 8A7 *Dr. A. von Bonin, BNI, Hamburg*
 Rat anti–mouse PD–L1 16B8 *BNI, Hamburg*
 Rat IgG2a isotype control–Alexa Fluor®488 *Caltag, Burlingame, USA*
 Rat IgG2a isotype control–PE *Caltag, Burlingame, USA*
 Rat IgG2a isotype control–biotin *BD Bioscience Pharmingen, Heidelberg*

Peroxidase-labelled goat anti rat-IgG	<i>Jackson Immunoresearch, Soham, UK</i>
Streptavidin-APC	<i>BD Bioscience Pharmingen, Heidelberg</i>
PD-1Ig	<i>Dr. A. von Bonin, BNI, Hamburg</i>
PD-L1Ig	<i>Dr. A. von Bonin, BNI, Hamburg</i>
PD-L2Ig	<i>Dr. A. von Bonin, BNI, Hamburg</i>

2.5 Chemicals

All chemicals were purchased from Sigma (Deisenhofen), Merck (Darmstadt), Roth (Karlsruhe) or Fluka (Neu Ulm).

2.6 Materials for cell culture, animal immunization and histology

2.6.1 Reagents

Acetone	<i>Fluka, Neu Ulm</i>
ACT-CSP	<i>Dr. Peter Sebo, Czech Academy of Sciences, Prague, Czech Republic</i>
Alexa Fluor [®] 488 Protein Labelling Kit	<i>Molecular Probes, Eugene, USA</i>
Anti-CD3	<i>BD Bioscience Pharmingen, Heidelberg</i>
APC-labelled CSP-loaded pentamer	<i>Proimmune, Oxford, UK</i>
Avidin-HRP	<i>BD Bioscience Pharmingen, Heidelberg</i>
BDM ELISPOT Mouse IFN- γ Pair	<i>BD Bioscience Pharmingen, Heidelberg</i>
BD TM ELISPOT AEC Substrate Set	<i>BD Bioscience Pharmingen, Heidelberg</i>
BSA (Bovine serum albumin)	<i>Serva, Heidelberg</i>
CD4 ⁺ CD25 ⁺ T Regulatory T cell Isolation Kit	<i>Miltenyi Biotec, Bergisch Gladbach</i>
Cohn II (fraction solution human γ -globulin)	<i>Sigma, Deisenhofen</i>
CSP ₂₄₅₋₂₅₃ SYIPSAEKI	<i>MWG Biotech AG, Ebersberg</i>
Complete Freund's adjuvant (CFA)	<i>Sigma, Deisenhofen</i>
CpG ODN1826	<i>Invitrogen, Karlsruhe</i>
DAPI (4', 6-diamidin-2'phenylindol)	<i>Sigma, Deisenhofen</i>
Dimethylsulphoxid (DMSO)	<i>Sigma, Deisenhofen</i>
DuoSet Economy Pack ELISA mouse IL-2	<i>R&D Systems, Abingdon, UK</i>
DuoSet Economy Pack ELISA mouse IFN- γ	<i>R&D Systems, Abingdon, UK</i>

MATERIALS

Fc-block 2.4G2 (supernatant Rat anti-mouse CD16/32 cell line)	<i>BNI, Hamburg</i>
Foetal calf serum (FCS)	<i>Invitrogen, Karlsruhe</i>
Foxp3-PE staining kit	<i>eBioscience, San Diego, USA</i>
Gentamicin	<i>PAA Laboratories, Linz, Austria</i>
[³ H] thymidine	<i>Amersham Pharmacia, Uppsala, Sweden</i>
Hi Trap Protein G Column	<i>Amersham Pharmacia, Uppsala, Sweden</i>
Incomplete Freund's adjuvant (CFA)	<i>Sigma, Deisenhofen</i>
LD-separation column	<i>Miltenyi Biotec, Bergisch Gladbach</i>
L-glutamine (200mM)	<i>Gibco BRL, Eggenstein</i>
Limulus Amebocyte lysate-test (LAL)	<i>Cambrex, Walkersville, USA</i>
LPS	<i>BD Bioscience Pharmingen, Heidelberg</i>
MS-separation column	<i>Miltenyi Biotec, Bergisch Gladbach</i>
Murine GM-CSF	<i>BNI, Hamburg</i>
NycoPrep™ Universal	<i>Axis-Shield PoC, Oslo, Norway</i>
OVA ₃₂₃₋₃₃₉	<i>MWG Biotech AG, Ebersberg</i>
Pan T cell kit	<i>Miltenyi Biotec, Bergisch Gladbach</i>
Phalloidin	<i>Molecular Probes, Eugene, USA</i>
Rat monoclonal Isotyping Kit	<i>Serotec, Düsseldorf</i>
RPMI 1640 medium without glutamine	<i>Gibco BRL, Eggenstein</i>
3, 3', 5, 5' Tetramethyl benzidin (TMB)	<i>Roth, Karlsruhe</i>
Tissue freezing medium Jung	<i>Leica Instruments, Nussloch</i>
Trypan Blue	<i>Serva Feinbiochemika, Hamburg</i>
Tween-20	<i>Sigma, Deisenhofen</i>
Wright's stain	<i>Sigma, Deisenhofen</i>

2.6.2 Culture media and buffers

Foetal calf serum (FCS) was inactivated at 56 °C for 45 minutes to eliminate the factors of the complement system. It was stored at -20 °C.

MATERIALS

RPMI-culture medium with 10 % FCS (complete medium)

500 mL RPMI 1640 (Roswell Park Memorial Institute medium) without L-glutamine

50 mL FCS

2.5 mL gentamicin

5 mL L-glutamine

Freezing medium

20 mL complete medium

25 mL FCS

5 mL DMSO (Dimethylsulphoxid)

Culture medium for dendritic cells

8.5 mL complete medium

1.5 mL GM-CSF

Digestion medium for liver cell preparation

500 mL RPMI 1640

25 mL FCS (5 %)

250 mg Collagenase IV(0.05 %)

10 mg DNase I (0.002 %)

Freeze solution for malaria infected erythrocyte stock (stabilate)

0.9 g NaCl

4.2 g sorbitol

in 100 mL sterile H₂O

All the following buffers were prepared with distilled water and sterilized by temperature or filtration.

Buffers for antibody purification:

Phosphate buffer

20 mM Na₂HPO₄

20 mM NaH₂PO₄

mixed together and adjusted at pH 7, filtered and degassed

MATERIALS

Glycin buffer

0.1 M Glycin pH 2.7, filtered and degassed

Tris/HCl

1 M pH 8

Erythrocyte-lysis-buffer

0.83 % NH₄Cl adjusted at pH 7.5 with Tris-HCl

FACS buffer

1 % FCS

0.1 % NaN₃

in 1 x PBS

Fixation buffer for FACS

4 % PFA in 1 x PBS

MACS buffer (magnetic cell sorting buffer)

2 mM EDTA

0.5 % BSA

in 1 x PBS

Coating buffer for ELISA and ELISPOT

Solution A: 1.24 g Na₂CO₃·x H₂O

in 100 mL H₂O

Solution B: 1.68 g NaHCO₃

in 200 mL H₂O

70 mL of dilution A and addition of solution B till pH 9.6.

Final solution is filtered and degassed.

Block Buffer for ELISA and ELISPOT

1 % BSA in 1 x PBS

Substrate buffer for ELISA

15.6 g NaH₂PO₄·2H₂O

in 500 mL H₂O, pH 4–5.5

MATERIALS

Substrate buffer for ELISPOT

0.1 M NaHCO₃ pH 9.2–9.5

Trypan Blue stain

2 mg in 100 mL PBS

3, 3', 5, 5' Tetramethyl benzin (TMB) for ELISA

30 mg TMB in 5 mL DMSO

DMEM–10/HEPES/pyruvate

DMEM medium

10 mM HEPES

1 mM pyruvate

DMEM–10/HEPES/pyruvate/HAT

DMEM-10/HEPES/pyruvate

100 x HAT (final 1x)

3. METHODS

3.1 Blockade of the binding of the fusion molecules PD-L1Ig and PD-L2Ig to endogenous PD-1 by anti-PD-1 8A7 antibody

In order to characterize the binding specificity of anti-PD-1 8A7 antibody, cells from a DO11.10 T cell hybridoma expressing PD-1 were incubated with unlabeled anti-mouse PD-1 8A7 (IgG2a, 2 µg/mL) for 30 minutes on ice. Either PD-L1Ig or PD-L2Ig fusion molecule (2 µg/mL) were added and incubated for 30 minutes on ice. Cells were washed and incubated with PE-labelled anti-human IgG (1:50) for 30 minutes for detection of the binding of the fusion molecules by flow cytometry.

3.2 Labelling of anti-PD-1 8A7 with Alexa Fluor[®]488

Rat monoclonal anti-mouse PD-1 (IgG2a, clone 8A7) was labelled with Alexa[®]488 using *Alexa Fluor[®]488 Protein Labelling Kit (Molecular Probes)*. Total amount 0.5 ml at 2 mg/mL of antibody was used for the labelling. 50 µL 1 M bicarbonate was added. The protein solution was transferred to a vial of reactive dye and incubated for 1 hour at room temperature. The resin provided with the kit was stir and applied into the column. The mixture of antibody and dye was applied into the column. After the mixture entered completely into the resin, elution buffer (0.1 M potassium phosphate, 1.5 M NaCl, pH 7.2 with 2 mM sodium azide) was added for 30 minutes till the antibody was eluted. Labelled antibody and free dye were optically distinguished. First band appearing representing the labelled antibody was collected. The concentration of the labelled antibody was determined following the protocol instructions.

3.3 Generation of a monoclonal antibody anti-PD-L1 6H6

3.3.1 Immunization

A total amount of 50 µg of fusion protein PD-L1Ig was mixed with the same volume of complete Freund's adjuvant. After emulsifying the mixture by pipetting up and down several times, the volume was collected in an insulin syringe. The emulsion was injected i.p. into a Lewis rat (1 ml total emulsion). After 14 days the animal was boost with the same amount of fusion protein dissolved in incomplete Freund's adjuvant.

3.3.2 Selection of hybridomas and fusion

The boosted animal was sacrificed. The spleen and lymph nodes were removed, placed on a Petri dish and squeezed till obtaining a single cell suspension. Cells were transferred into a tube and DMEM (Dulbecco's Modified Eagle's Medium) was added. The cells were centrifuged for 5 minutes at 1,500 rpm at room temperature. The supernatant was discarded and red blood cells were eliminated by pipetting 5 mL of erythrocyte-lysis buffer and incubating it for 2 minutes at room temperature. A volume of 45 mL DMEM were added and cells were centrifuged at 1,500 rpm for 5 minutes at room temperature.

The mouse P3/X63-Ag 8.658 B cell myeloma line was used for the fusion. It was expanded one week before the fusion in DMEM-10/HEPES (N-[2-hydroxyethyl] piperazine-N'-[2-ethansulfonic] acid)/pyruvate medium.

The mixture of spleen-lymph node cells and the myeloma cells were counted and diluted till a cell suspension of 2.5×10^6 cells/mL. To perform the fusion the ratio between lymphocytes and myeloma cells was 1:1. Cells were mixed into a 50 mL conical tube and DMEM was added. Cell mixture was centrifuged 5 minutes at 1,500 rpm at room temperature. The supernatant was aspirated and discarded.

The cell fusion was performed at 37 °C placing the tube with the cell suspension inside a water bath. 1 mL of pre-warmed 50 % phosphoethylenglicol (PEG) was added drop-by-drop over 1 minute into the cell suspension. A volume of 1 mL of pre-warmed DMEM was added in the same way. Additional 7 mL of pre-warmed DMEM were added drop-by-drop over 3 minutes. Cell suspension was centrifuged at 1,500 rpm for 5 minutes at room temperature. Supernatant was discarded and 10 mL of the pre-warmed DMEM-20/HEPES/pyruvate medium was discharged to cell pellet. The total required amount of DMEM-20/HEPES/pyruvate medium was calculated depending on the total amount of spleen-lymph node cell suspension.

Cell suspension was plated into a 96-well flat-bottom plate (100 µl/well).

DMEM-20/HEPES/pyruvate/hypoxanthine aminopterin thymidine (HAT) medium was added (100 µl/well) and plates were incubated in a humidified 37 °C, 5 % CO₂ incubator.

Medium was aspirated, discarded and replaced by fresh one every 3-4 days.

3.3.3 Screening of positive clones

Screening of the producing antibodies hybridomas was performed 14 days after the fusion of the cells and using a PD-L1 Ig ELISA. A 96-well flat-bottom plate was coated with 0.5 µg/mL of PD-L1 fusion protein (50 µl/well). The fusion molecule was diluted in ELISA coating buffer. As negative control plates were coated with the same amount of BTLA fusion molecule. Plates were incubated overnight at 4 °C. After discarding the fusion protein, plates were washed three times with 0.05 % Tween[®]20 in 1 x PBS solution and flush out as described for the cytokine ELISA assays. 200 µl of the ELISA blocking buffer were added and plates were incubated overnight at 4 °C. The buffer was aspirated and 50 µl of the supernatant from the antibody producing hybridomas culture were incubated for 24 hours at 4 °C. Plates were washed three times with 0.05 % Tween[®]20 in 1 x PBS solution and flush out as described before.

The peroxidase-labelled goat anti-rat IgG was diluted 1:50 and added in a volume of 50 µl and the plates were incubated at room temperature for 2 hours. 100 µl/well of substrate solution were added and after the change of colour the reaction was stopped with 25 µl/well of Stop Solution. After incubation at room temperature for 10 minutes the optical density of each well at 450 nm was determined using a spectrophotometer.

The positive clones were maintained in culture, placing them in 24-well plate, whereas the negative clones were discarded. All the tested clones were negative for BTLA and positive for PD-L1.

3.3.4 Cloning by limiting dilution

Four clones were selected depending on their specificity and affinity checked by ELISA. To achieve a monoclonal antibody producing hybridoma, cloning of these positive hybridomas was performed.

The number of viable cells of each of the 5 selected hybridomas was counted. Cell suspensions were diluted to achieve a statistically concentration of 3.1 and 0.3 cells per well of each clone. Cells were plated into a 96-well plate (100 µl/well) and 100 µl of feeder cells suspension were added.

Feeder cells were prepared from a spleen cell suspension. Cells were γ -irradiated for 360 seconds (2,000 rad). The amount of added cells were between 10^5 - 10^6 cells per well.

3.3.5 Obtaining a stable monoclonal antibody producing hybridoma

Positive clones for antibody production were incubated in a humidified 37 °C, 5 % CO₂ incubator. Cells were tested for evidence of monoclonal hybridoma growing and as well as for antibody production. Positive clones for detection of PD-L1 and negative for BTLA were frozen in liquid nitrogen. Best specific ones (6H6 and 16B8) were expanded in PFHM-II medium (Protein free hybridoma medium-II). Clones were first cultured in a 24-well plate till grown confluent. Cells were expanded first in 25 mL medium in 50 mL culture bottles, later in 200 mL culture bottles, and finally in 500 mL culture bottles with fresh medium and incubated at 37 °C and 5 % CO₂ for 2–3 days in every step. Lastly, culture bottles were placed in an incubator with rolling system for bottles. After one week, 500 mL fresh PFHM-II medium was added. After two weeks supernatant of both expanded clones were collected (cell culture centrifuged at 10,000 x g, 30 minutes, 4 °C) and antibodies were purified using a *HiTrap Protein G column (Amersham Pharmacia Biotech)* because of the capacity of its specific binding to the Fc-region of IgG antibody.

3.3.6 Purification of anti-PD-L1 6H6 and anti-PD-L1 16B8

The *HiTrap Protein column* was first pre-equilibrated with 100 mL phosphate buffer. Then, the filtered supernatant from expanded antibody producing hybridomas was passed through the column at room temperature. The column was washed with 100–200 mL phosphate buffer and eluted with 50 mL glycine buffer. Fractions were collected in 1 mL *Eppendorf* tubes and 1 mL Tris/HCl pH 8 was added to neutralize the solution. The amount of antibody was measured by 280 nm using a photometer. The extinction coefficient for IgG isotype was 0.7 mL/mL.

3.3.7 LPS contamination test

The possible contamination of the antibody charge with LPS during the purification procedure was detected using the *Limulus Amebocyte lysate-test (Cambrex)* following the manufacturer's instructions.

3.3.8 Determination of isotypes for anti-PD-1 8A7, anti-PD-L1 6H6 and anti-PD-L1 16B8 antibodies

The determination of isotypes for anti-PD-1 8A7, anti-PD-L1 6H6 and anti PD-L1 16B8 was performed using the *Rat monoclonal Isotyping Kit (Serotec)* following manufacturer's instructions.

3.3.9 Blockade of the binding of the fusion molecule PD-L1Ig to endogenous PD-1 by anti-PD-L1 6H6 antibody

In order to characterize the binding specificity of anti-PD-L1 6H6 antibody, cells from a DO.11.10 T cell hybridoma were incubated with anti-mouse PD-L1 6H6 (IgG1 κ , 2 μ g/mL) and PD-L1Ig fusion molecule (2 μ g/mL) simultaneously for 30 minutes on ice. As negative control cells were incubated with 2 μ g/mL rat IgG (*CromePure rat IgG*, whole molecule). Subsequently, for the detection of the fusion molecule, cells were washed and incubated with PE-labelled anti-human IgG (1:50) for 30 minutes. Finally, cells were analyzed by flow cytometry.

3.4 Methods in cell biology

3.4.1 General culture conditions

Cells were cultured in RPMI 1640 medium supplemented with 10 % FCS, glutamine and 0.5 % gentamicin in a humidified 37 °C 5 % CO₂ incubator.

3.4.2 Count of viable cells

The number of viable cells was determined by staining the cell suspension 1:1 with Trypan Blue solution. Cells were counted using a *Neubauer* chamber and inverse microscope at a 100 X magnification.

3.4.3 Staining of blood smears to determine parasitemia

Every day after injection of the iRBCs, a blood film was prepared for each mouse to determine the percentage of parasitemia.

The tip of the tail of every mouse was cut with a scissors. The tail was squeezed in order to form a small drop, which was placed on a microscope slide. A second grasped slide was placed at a 45 ° angle onto the drop of blood, which was spread by pushing the slide forward the other with a rapid movement. The slides were dried at room temperature and over-laid with eight drops of *Wright* stain for 2 minutes. Eight

drops of water were added for 3 minutes. The slides were washed with water, dried at room temperature and examined under oil immersion at the microscope. The amount of parasitized and non-infected erythrocytes was counted in a total of 6 microscope fields.

3.4.4 Determination of cell proliferation

T cell proliferation responses were assessed by determining the incorporation of [³H] thymidine into cellular DNA added during the last 6 hours of the cell culture. A harvesting apparatus was used to lyse the cells with water and precipitate the radioactive labelled DNA on filters, which after drying were counted by a liquid scintillation counter.

A [³H] thymidine solution was prepared diluting 145 µl of [³H] thymidine in 50 mL RPMI 1460 medium. 25 µl of the [³H] thymidine solution was added per well to the cell culture which was placed into a humidified 37 °C, 5 % CO₂ incubator overnight. Cultures were harvested with the semi-automated cell harvesting apparatus and the amount of radioactivity was determined following manufacturers instructions.

3.4.5 Preparation of spleen cells

Spleen was removed from the abdominal cavity of the mouse and plated in a Petri dish. A volume of 5 mL of an erythrocyte lysis buffer was used to flush out the spleen cells using a 5 mL-syringe and a hypodermic needle. The obtained cell suspension was incubated for 2 minutes at room temperature to lyse the erythrocytes. Spleen cells were transferred into a tube and centrifuged at 1,200 rpm 4 °C for 5 minutes. The supernatant was removed and cells were washed once with RPMI 1640 medium. Viable cells were counted as described. Finally cells were diluted with RPMI 1640 medium and cultured at 37 °C in a 5 % CO₂ incubator.

3.4.6 Preparation of bone marrow-derived dendritic cells (BMDCs)

After removing the muscles from tibias and femurs of the mouse, bones were placed in a Petri dish with 70 % ethanol for 2 minutes. Bones were dried in a new Petri dish for 2 minutes. Ends of the bones were cut with scissors and the marrow was obtained by flushing out the shafts with 5 mL RPMI 1640 medium using a 5 mL-syringe and a hypodermic needle. Tissue was resuspended and passed through a nylon mesh to remove small pieces of debris or clumps. The viable cells were counted and

centrifuged at 1,200 rpm for 10 minutes at 4 °C. The supernatant was removed and the cells were resuspended in an appropriate volume of RPMI 1640 medium to adjust a cell concentration of 1×10^6 cells/mL. 1 mL of the cell suspension was plated into a dish plate with 8 mL RPMI 1640 medium and 2 mL of culture from granulocyte-macrophage colony-stimulating factor (GM-CSF) producing cells. Plates were incubated for 3 days at 37 °C and supplemented again with 2 mL of GM-CSF solution and 10 mL RPMI 1640 medium. At day 6, 10 mL medium from the plate were removed, centrifuged at 1,200 rpm for 10 minutes and the pellet was resuspended in 9 mL of RPMI 1640 plus 1 mL GM-CSF solution. The mixture was plated in the same dish. Again at day 7, the plates were gently washed and the not adherent cells were collected, centrifuged, counted and diluted in RPMI 1640 medium till a final concentration of 1×10^6 cells/mL. In a 24-well plate, 1 mL of the cell suspension was plated per well and cells were stimulated with 500 ng/mL of LPS for 24 hours in the case of the experiment of co-culture with T cells. In the case of analyzing the expression of PD-1 and PD-L1 on dendritic cells after activation, cells were incubated in 24-well plate for 24 and 72 hours in the presence of LPS (500 ng/mL) or CpG ODN1826 (1 µg/mL).

3.4.7 Isolation of infiltrated lymphocytes in the liver

Mice livers were injected with 5 mL PBS/10 %FCS through the portal vein. Livers were homogenized with 10 mL PBS/10 %FCS in a Petri dish using the plunger of a syringe. The suspension was then filtered through a *CellStrainer* and centrifuged at 1,400 rpm, 4 °C for 10 minutes. The cell pellet was resuspended in 1 mL RPMI 1640 medium. A volume of 5.5 mL (30 % diluted) of *NycoPrep™ Universal* density gradient was added and the suspension was pipetted into 2 mL RPMI 1640 medium. Centrifugation was performed at 2,500 rpm, for 20 minutes at 4 °C without brake. The lymphocyte ring was collected with a pipette, washed with RPMI 1640/10 %FCS and centrifuged at 1,200 rpm at 4 °C for 20 minutes.

3.4.8 Isolation of non-parenchymal liver cells

A volume of 3 mL of digestion medium was perfused via portal vein. Livers were collected in Petri dishes and homogenized with the plunger of a syringe. Suspension was pipetted into a glass Erlenmeyer and digestion medium was added up to 50 mL total volume. Mixture was incubated in a shaker at 250 rpm at 37 °C for 35 minutes.

The digested tissue was filtered through a *CellStrainer* and washed twice with 10 mL RPMI 1640/10 %FCS (centrifuged at 1,200 rpm, 10 minutes at 4 °C). Pellet was resuspended with 1 mL RPMI 1640 medium. 5.5 mL (30 % diluted) of *NycoPrep™ Universal* density gradient was added and the suspension was pipetted into 2 mL RPMI 1640 medium. Centrifugation was performed at 2,500 rpm, for 20 minutes at 4 °C without brake. Non-parenchymal liver cells was collected with a pipette and washed with RPMI 1640/10 %FCS and centrifuged at 1,200 rpm, 4 °C for 20 minutes.

3.4.9 Isolation of hepatocytes

Hepatocytes were prepared by Dr. Johannes Herkel, in *Universität Klinikum Eppendorf (UKE)*. Therefore, livers were perfused with 0.05 % NB8 collagenase (*Serva, Heidelberg*). After mechanical disruption, the liver cell suspension was centrifuged at 30 x g for 10 minutes. Non-hepatic cells were removed by incubation of liver suspension with a monoclonal antibody cocktail specific against non-hepatic cells. The incubation was performed for 20 minutes at 37 °C followed by washing with 1 x PBS. Hepatocytes show a typical nucleus form which is observed by fluorescent microscopy after staining with Dapi (1:1000) and phalloidin (1:1000).

3.4.10 Isolation of T cells by magnetic cell sorting (MACS)

The isolation of T cells was performed using the *Pan T cell isolation kit (Mittenyi Biotec)*. A single cell suspension was prepared from mouse spleen as previously described. The initial cell amount was 1×10^7 cells. They were spin down by centrifugation at 1,200 rpm for 10 minutes. The supernatant was removed completely and the cell pellet resuspended in 40 µl cold MACS buffer. 10 µl Biotin-Antibody Cocktail were added and mixed. The mixture was incubated for 10 minutes at 4 °C. A volume of 30 µl cold MACS buffer and 20 µl Anti-Biotin Microbeads were added followed by an additional incubation for 15 minutes at 4 °C.

Cells were washed with 1 mL cold MACS buffer and centrifuged at 1,200 rpm for 10 minutes. The supernatant was removed completely and the cell pellet was resuspended in 500 µl cold MACS buffer. A *MS MACS Column* and a *MACS Separator* were placed in the suitable magnetic field. The column was equilibrated with 500 µl cold MACS buffer and the cell suspension was added onto the column.

The effluent was collected as well as the following washes with cold MACS buffer (3 x 500µl). The effluent represents the enriched T cell fraction.

3.4.11 Isolation of CD4⁺/CD25⁺ Tregs cells by magnetic sorting

The isolation of CD4⁺/CD25⁺ T cells and CD4⁺/CD25⁻ T cells was performed using the *CD4⁺CD25⁺ T Regulatory T Cell Isolation Kit (Miltenyi)*. A single cell suspension was prepared from the mouse spleen as previously described. 1x10⁷ cells were resuspended in 40 µl cold MACS buffer and 10 µl Biotin–Antibody Cocktail. The mixture was incubated for 10 minutes at 4°C. 30 µl cold MACS buffer, 20 µl Antibody–Biotin Microbeads and 10 µl PE–labelled anti–CD25 were added. The suspension was mixed by pipetting and incubated for 15 minutes in the dark at 4 °C. The cells were washed with 2 mL cold MACS buffer, at 1,200 rpm for 10 minutes and the supernatant was removed completely. The cell pellet was resuspended in 500 µl cold MACS buffer and applied onto a pre–equilibrated *LD Column* (with 2 mL cold MACS buffer) placed in a suitable magnetic field with a MACS Separator. The column was washed twice with 1mL cold MACS buffer and the effluent was collected in a tube representing the CD4⁺ T cell fraction.

The isolated CD4⁺ T cells were centrifuged at 1,200 rpm for 10 minutes and the supernatant was removed completely. The cell pellet was resuspend in 90 µl cold MACS buffer and 10 µl Anti–PE Microbeads. The mixture was incubated in the dark for 10 minutes at 4 °C. The cells were washed with 2 mL cold MACS buffer, centrifuged at 1,200 rpm for 10 minutes and the supernatant was removed completely. The pellet was resuspended in 500 µl cold MACS buffer and applied onto a pre–equilibrated *MS Column* (with 500 µl cold MACS buffer) placed in a suitable magnetic field and a *MACS Separator*. The column was washed three times with 500 µl cold MACS buffer. Subsequently the column was removed and placed on a new clean 10 mL tube. 1 mL cold MACS buffer was added onto the column and immediately the CD4⁺/CD25⁺ T cells were flushed out by applying the plunger supplied with the column. The fraction was transferred onto a new *MS Column* and washed three times with 1 mL cold MACS buffer to achieve a higher CD4⁺/CD25⁺ T cell purity.

For the analysis of PD–1 and PD–L1 expression on Tregs and Teffs, cells were incubated in a 96–well plate for 24 and 48 hours with anti–CD3 (3 µg/mL). At each

time point, cells were stained with monoclonal antibodies and analyzed by flow cytometry.

3.4.12 Flow cytometry

The fluorescence-activated cell sorter (FACS) is an instrument that allows the identification of cellular subsets by the detection of cell surface molecules. These are detected by fluorescent dyes labelled to specific monoclonal antibodies against these surface molecules. “Stained” cells pass in a stream through a laser beam where the fluorescent is detected. Hence, each cell is represented as a point with a determined fluorescent level on the screen of the flow cytometer. FACS permits also the possibility of physically separating these identified cells populations for further experiments.

For flow cytometry analysis, (2×10^5 cells) were always first incubated on ice for 30 minutes with Fc-blocking solution (Fc-2.4G2) in order to avoid unspecific binding of the antibodies to Fc receptors present on cells to be analyzed. The incubation with the antibodies was performed for 30 minutes on ice and in the dark, following two washes with FACS buffer. Cells were then fixed with 200 μ l 4% paraformaldehyde and analyzed on *FACSCalibur* using the *CellQuestPro* program. To analyze PD-1 expression on T cells, spleen cells were stained with APC-labelled anti-CD4 (1:200) or APC-labelled anti-CD8 (1:400) and Alexa Fluor[®]488-labelled anti-PD-1 (1:100) or Alexa Fluor[®]488-labelled isotype control (1:100) at different time points and under different stimuli.

Spleen cells from *P. berghei* infected mice were also analyzed concerning their PD-1 and PD-L1 expression. Cells were stained with PE-Cy5-labelled anti-CD3 (1:200) and either PE-labelled anti-CD4 (1:200) or PE-labelled anti-CD8 (1:200). PE-labelled anti-PD-1 (1:100) or PE-labelled anti-PD-L1 (1:100) as well as the respective isotype controls (PE-labelled hamster IgG, or PE-labelled rat IgG) were also used.

Spleen cells as well as isolated liver lymphocytes (7×10^5 cells per staining) from *P. berghei* infected mice were stained first with a APC-labelled CSP-loaded MHC class I pentamer (4 μ l) for 10 minutes on ice following an incubation with FITC-labelled anti-CD8 (1:200), and PE-labelled anti-CD62L (1:200) for 30 minutes on ice. After washing with FACS buffer, cells were fixed with 200 μ l 4 %PFA in PBS.

For staining of non-parenchymal liver cells (LSECs and KCs), cells isolated from the digested livers were incubated with PerCP-Cy5.5-labelled anti-CD11b (1:400), FITC-labelled anti-ICAM-1 (1:200) and PE-labelled anti-PD-L1 (1:100).

BMDCs were stained with APC-labelled anti-CD11c (1:200) and PE-labelled anti-PD-1 (1:100) and PE-labelled anti-PD-L1 (1:200). Samples were also stained in parallel with the respective isotype controls.

The PD-1 and PD-L1 expression on Tregs and Teffs was analyzed using CD4-FITC (1:200) and either biotinylated anti-PD-1 or biotinylated anti-PD-L1 (1:100). After washing once with FACS buffer cells were incubated with APC-labelled streptavidin (1:400) for 30 minutes on ice. The use of an anti-CD25 was not necessary because of the characteristics of the Tregs isolation kit that already involved an incubation step with PE-labelled anti-CD25 for the isolation of Tregs which allows the posterior detection of this population by flow cytometry.

In the *in vivo* mouse experiments with *P. berghei* infection the Treg population was determined using the PE-labelled anti-Foxp3 staining kit. A total amount of 2×10^5 cells were first incubated with Fc-blocking solution (100 μ l) for 30 minutes. APC-labelled anti-CD4 (1:200) and FITC-labelled anti-CD25 were added for 30 minutes on ice. Cells were permeabilised overnight with 2 mL of 1x Fixation/Permeabilisation buffer. After washing with 1x Permeabilisation buffer, cells were stained with PE-labelled anti-Foxp3 (0.3 μ g/mL) or the respective isotype control for 30 minutes. Finally, cells were washed twice with 1x Permeabilisation buffer (1 mL) and analyzed by flow cytometry.

3.4.13 Histology

To perform histological analysis livers from mice were removed, frozen in tissue freezing medium Jung (*Leica Instruments*) and stored at -20 °C till sectioning. Section about 8 μ m were cut with the *Cryostat Microm*[®] *HM 560*, disposed on microscope glass slides, dried overnight at room temperature and fixed in ice-cold acetone for 1 minute. Slides were then frozen at -20 °C till staining. Samples were blocked with Cohn II fraction solution (human γ -globulin, 10mg/mL) for 30 minutes at room temperature to avoid unspecific binding of the antibodies. After that PE-labelled anti-PD-L1 16B8 and FITC-labelled anti-CD26 were incubated for 30 minutes in the dark. Dapi (4', 6-diamidin-2'-phenylindol) was also used to stain cellular nuclei. Samples were washed twice with PBS. For the PD-L1 staining, an

Alexa Fluor[®]594-labelled chicken anti-rat IgG (H+L) was used for 30 minutes as well as an Oregon Green labelled anti-FITC to increase the signal of CD26 staining. Slides were again washed with 1 x PBS. A drop mounting medium and a cover-glass were disposed on each preparation and stored at 4 °C till examination with the fluorescence microscope.

3.4.14 ELISA (Enzyme linked immunosorbent assay)

ELISA was used to measure the cytokine concentration in cell culture supernatants. Coating antibodies, standards and detection antibodies for the cytokine measurement of IFN- γ and IL-2 were obtained from *R&D*.

A flat bottom 96-well plate for ELISA was coated overnight at 4 °C with 50 μ l/well of a diluted capture antibody (4 μ g/mL) in coating buffer. The plate was washed three times with 0.05 % Tween[®]20 in 1x PBS solution. Any rest of solution was removed by inverting the plate and blotting it against clean paper towels. The plate was blocked with 100 μ l/well of blocking buffer overnight at 4 °C. The blocking buffer was then aspirated and the standards and cell culture supernatants (in triplicates) were added in a volume of 50 μ l/well and incubated at 4°C overnight. The IFN- γ or IL-2 standard was diluted in 1 x PBS/0.1 % BSA till a working concentration of 2,000 pg/mL. Two fold serial dilutions of that initial concentration in 1 x PBS/0.1 % BSA were performed. The plate was washed three times with 0.05 % Tween[®]20 in 1 x PBS solution and dried following the procedure as mentioned above. A volume of 50 μ l/well of the detection antibody diluted in 1 xPBS/0.1 %BSA were added at a concentration 400 ng/mL and incubated at room temperature for 2 hours. A volume of 50 μ l/well of a diluted (1:200) Streptavidin labelled to horseradish-peroxidase was added and incubated at room temperature for 30 minutes. The plate was washed three times with 0.05 % Tween[®]20 in 1 x PBS solution and dried as described before. 100 μ l/well of Substrate solution were added and depending on the colorimetric reaction, this was stopped with 25 μ l/well of Stop Solution. After incubation at room temperature for 10 minutes the optical density of each well at 450 nm was determined using a spectrophotometer.

3.4.15 IFN- γ -ELISPOT (Enzyme linked immunospot assay)

The IFN- γ -ELISPOT permits the detection of IFN- γ producing cells in a qualitative manner. Anti-mouse IFN- γ (5 μ g/mL, 50 μ l/well) was coated on the membrane of a *MultiScreen MHA S4510 ELISPOT* plate overnight at 4 °C. After washing the plate three times with 200 μ l/well sterile 1 x PBS, plates were blocked with 200 μ l/well of blocking buffer overnight. Blocking buffer was removed and 2×10^5 cells/well were added either with medium, anti-CD3 (3 μ g/mL) or CSP₂₄₅₋₂₅₃ peptide (1 μ g/mL) for 18 hours at 37 °C. After cell incubation, plates were washed three times with 200 μ l/well 1 x PBS and biotinylated detection antibody (2 μ g/mL, 50 μ l/pro well) in PBS was added for 1 hour at room temperature. Plates were washed three times with 1 x PBS (200 μ l/well) and incubated 30 minutes with avidin-HRP (1:500 in PBS, 50 μ g/mL) at room temperature. Finally plates were incubated for 2 minutes with *BD TM ELISPOT AEC Substrate Solution* until spots were visible. Reaction was blocked by washing the plates with dH₂O. After drying the plates, the number of spots per well were determined using an *ELISPOT Reader* and the result is expressed as “spot forming units” (sfu) per total 1×10^6 cells.

3.5 In vivo experiments

3.5.1 Induction of malaria disease with *P. berghei* ANKA

Liver stage infection:

Liver stage malaria was induced by intravenously injection of 2,000 sporozoites in sterile PBS per mouse.

In experiments with γ -irradiated sporozoites (γ -irradiation, 10,000 rad), mice were infected with 5,000 γ -irradiated sporozoites per mouse in sterile PBS. Sporozoites were kindly provided by Dr.V. Heussler (*BNI, Hamburg*).

Blood stage infection:

The asexual blood stage parasites were maintained in liquid nitrogen as cryopreserved stabilates. Therefore blood from infected mice with a parasitemia between 10–20 %, blood was collected by cardiac puncture into heparinized tubes. A volume of 9 mL PBS was added and the number of infected erythrocytes was determined. Blood was centrifuged at 1,200 rpm, 4 °C. The supernatant was discarded and the erythrocytes were resuspended in 1 x PBS till a concentration of 1×10^8 iRBCs/mL. The same volume of freeze solution was added. The mixture was

homogenized and the volume was dispensed in 0.2 mL aliquots per cryovial. The aliquots were frozen overnight at -70°C and transferred to liquid nitrogen the next day.

Mice were i.p. infected with 0.2 mL of the (1:10) diluted stabilate in sterile 1 x PBS representing a total number of 2×10^6 iRBCs per mouse.

3.5.2 Immunization with ACT–CSP

Mice were intraperitoneally immunized with 20 μg of *B. pertussis* adenylate cyclase toxoid fused to CSP (ACT–CSP; Dr. Peter Sebo) per mouse in a total volume of 0.2 mL in 1 x PBS. The administration was performed seven days before infection with *P. berghei* ANKA (day –7).

3.5.3 Administration of anti–PD–1 8A7 antibody

Rat anti–mouse PD–1 8A7 (200 μg per mouse) was intraperitoneally injected in a total volume of 0.2 mL in 1 x PBS at the same day as the infection with *P. berghei* ANKA.

3.6 Statistical analysis

All statistical analysis was performed using the Prism 4.00 software (*GraphPad Software, San Diego*). To evaluate differences between two groups a t–test (two tailed, unpaired) was used. In all cases a value of $p < 0.05$ was considered to be significant.

4. RESULTS

The aim of this study was to evaluate the role of the interaction between PD-1 and its ligand PD-L1 during infection in a malaria mouse model with *P. berghei* ANKA.

For this purpose, two monoclonal antibodies against mouse PD-1 and PD-L1 were used.

The anti-PD-1 8A7 antibody was generated in our department by Dr. Arne von Bonin (*BNI*) and anti-PD-L1 was newly generated during this study. Anti-PD-1 8A7 was labelled with a fluorescent dye and its specificity was compared to a commercially available antibody by flow cytometry. Anti-PD-1 8A7 was used to analyze the PD-1 expression on different cell types. After testing its blocking capacity, anti-PD-1 8A7 was also used in several *in vitro* experiments to determine the role of the interaction between PD-1 and its ligands after T cell activation.

Anti-PD-L1 6H6 was generated by immunization of a rat with PD-L1Ig. Similarly as in the case of anti-PD-1 8A7 antibody, the capacity of anti-PD-L1 6H6 to block the interaction between PD-L1 and PD-1 was tested *in vitro*. The *in vitro* effect of anti-PD-L1 was analyzed on spleen cells and BMDCs. Lastly, the role of the PD-1/PD-L1 pathway during infection was analyzed by the *in vivo* blockade of PD-1 using anti-PD-1 8A7 antibody in a malaria mouse model with *P. berghei* ANKA.

4.1 Antibody evaluation

4.1.1 Comparison of anti-PD-1 8A7 antibody with the commercially available anti-PD-1 J43

In order to determine whether Alexa Fluor[®]488-labelled anti-mouse PD-1 8A7 can be used in flow cytometry to detect mouse PD-1, a comparison with a commercially available PE-labelled anti-PD-1 J43 (*Becton Dickinson*) was performed. Spleen cells from a C57BL/6 mouse were isolated and stimulated for 48 hours with anti-CD3. Cells were stained with PerCP-labelled anti-CD45 and either Alexa Fluor[®]488-labelled anti-PD-1 8A7 or PE-anti-PD-1 J43 simultaneously. CD45 is a marker for hematopoietic cells. Cells were analyzed by flow cytometry. Fig. 4.1.1 shows the expression of PD-1 on gated CD45⁺ cells by using Alexa Fluor[®]488-labelled anti-PD-1 8A7 (A) or PE-labelled anti-PD-1 J43 (B). In

RESULTS

both cases a similar staining pattern compared to the respective isotype control was observed, demonstrating that Alexa Fluor[®]488-labelled anti-PD-1 8A7 can be used in flow cytometry to detect PD-1.

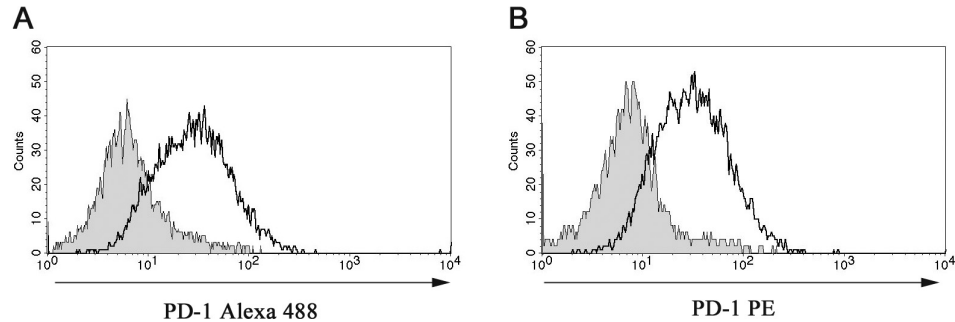


Fig. 4.1.1: Comparison between the anti-PD-1 8A7 antibody and the commercially available anti-PD-1 J43. Spleen cells from a C57BL/6 mouse stimulated with anti-CD3 for 48 hours were incubated with PerCP-labelled anti-CD45 and either Alexa Fluor[®]488-labelled anti-PD-1 8A7 or PE-labelled anti-PD-1 J43. Staining was analyzed by flow cytometry. A. PD-1 expression on CD45⁺ spleen cells by using Alexa Fluor[®]488-anti-PD-1 8A7 (grey shadow: isotype control; bold line: anti-PD-1). B. PD-1 expression on CD45⁺ spleen cells by using PE-anti-PD-1 J43 (grey shadow: isotype control; bold line: anti-PD-1). Representative data of three experiments are shown

4.1.2 Evaluation of the blocking capacity of anti-PD-1 8A7 antibody

DO.11.10 T cell hybridoma constitutively expressing PD-1, were used to analyze the blocking capacity of the anti-mouse PD-1 8A7 antibody by inhibiting the binding of fusion molecules PD-L1Ig and PD-L2Ig to the endogenous PD-1 molecule. Fusion molecules were constructed with the sequence of PD-L1 and PD-L2. The transmembrane and cytoplasmic domain, were substituted by the constant fragment of the human IgG immunoglobulin. Fusion molecules are usually used as soluble ligands to study the function of receptors they bind to. The constant fragment of the fusion molecule facilitates its dimerisation via the formation of disulfide bonds. This increases the binding affinity of the fusion molecule compared to the normal monomeric ligand. Fusion molecules can also be used to analyze the binding of a monoclonal antibody by a competition assay, where the fusion molecule and the antibody compete for the binding of the endogenous molecule they are specific for.

To this end, cells were incubated with purified anti-mouse PD-1 8A7. Subsequently, either PD-L1Ig or PD-L2Ig was added and their binding to the endogenous PD-1 was analyzed by flow cytometry via the detection of the human IgG fragment of the fusion molecules using a PE-labelled anti-human IgG antibody. Incubation of cells with anti-PD-1 8A7 diminishes the binding of the fusion molecules PD-L1Ig and

RESULTS

PD-L2Ig to the endogenous PD-1 as shown in the decreased detection of both fusion molecules in the histograms represented in Fig. 4.1.2. These results confirm that anti-PD-1 8A7 blocks the interaction between endogenous PD-1 and fusion molecules PD-L1Ig and PD-L2Ig. For this reason anti-PD-1 8A7 is an appropriate tool to study the role of the interaction between PD-1 and its ligands.

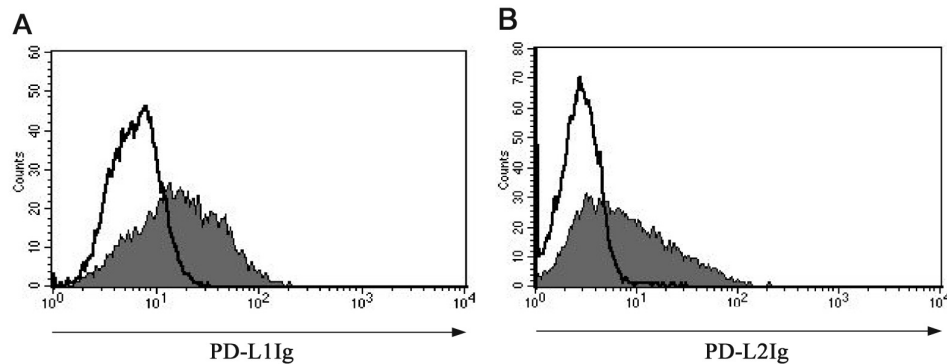


Fig. 4.1.2: Blockade of the binding of the fusion molecules PD-L1Ig and PD-L2Ig to endogenous PD-1 by anti PD-1 8A7 antibody. D.O.11.10 T cell hybridoma cells were incubated with anti-PD-1 8A7 for 30 minutes. PD-L1Ig (A) or PD-L2Ig (B) was added. After washing, fusion molecules were detected using PE-labelled anti-human IgG. Cells incubated only with fusion molecules and anti-human IgG were used as control (grey shadow: fusion molecule; bold line: fusion molecule with anti-PD-1 8A7 pre-incubation). Representative data of three experiments are shown.

4.1.3 Evaluation of the blocking capacity of anti-PD-L1 6H6 antibody

The capacity of anti-PD-L1 6H6 to bind to the endogenous PD-L1 molecule was demonstrated using the specific blockade of the ligation of the PD-L1Ig fusion molecule to endogenous PD-1 by this antibody. DO.11.10 T hybridoma cells were incubated with anti-mouse PD-L1 6H6 antibody and PD-L1Ig fusion molecule simultaneously. As negative control the fusion molecule was also incubated with rat IgG (*CromePure*, whole molecule). The binding of the fusion molecule was detected using a PE-labelled antibody against the human IgG fragment. Cells were analyzed by flow cytometry and results are shown in Fig. 4.1.3. Anti-PD-L1 6H6 binds specifically the fusion molecule PD-L1Ig avoiding its binding to the endogenous PD-1 (bold line). Incubating the cells with a rat IgG as control antibody, fusion molecule PD-L1Ig can bind endogenous PD-1 (grey shadow).

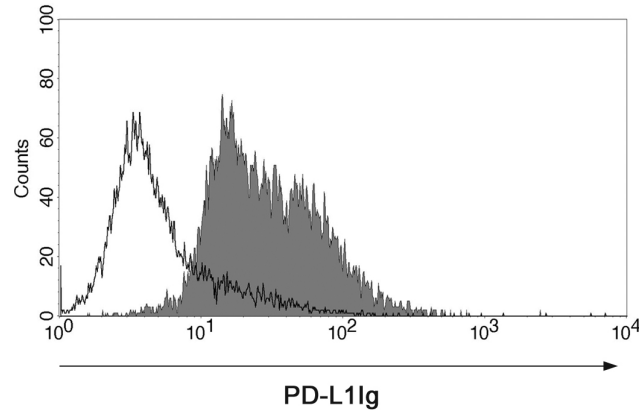


Fig. 4.1.3: Blockade of the binding of the fusion molecule PD-L1Ig to endogenous PD-1 by anti PD-L1 6H6 antibody. DO.11.10 T cell hybridoma cells were incubated with anti-PD-L1 6H6 and PD-L1Ig simultaneously for 30 minutes. After washing, the fusion molecule on the cell surface was detected using PE-labelled anti-human IgG. Cells incubated with fusion molecule and rat IgG were used as control (grey shadow: fusion molecule with rat IgG; bold line: fusion molecule with anti-PD-L1 6H6). Representative data of three experiments are shown.

4.1.4 Determination of the isotypes of anti-PD-1 8A7, anti-PD-L1 6H6 and anti-PD-L1 16B8 antibodies

The determination of the isotypes of each antibody was part of their evaluation. This approach was important in the case of the new generated antibodies anti-PD-L1 6H6 and anti-PD-L1 16B8 because to be able to use them for immunohistology. The use of a secondary antibody that recognizes the constant region of the anti-PD-L1 antibodies results in an amplification of the specific detection of the primary anti-PD-L1 antibody.

Isotypes were determined for each antibody using the *Rat monoclonal Isotyping Kit* (Serotec). Anti-PD-1 8A7 is an IgG2a. Anti PD-L1 6H6 is an IgG1 κ and anti-PD-L1 16B8 an IgG1 κ (data not shown).

4.2 PD-1 and PD-L1 expression on different cell types

4.2.1 Induction of PD-1 expression on T cells upon *in vitro* stimulation of spleen cells with anti-CD3

Spleen cells from a C57BL/6 mouse were stimulated with anti-CD3 for 72 hours. PD-1 expression was analyzed on different T cell subsets by flow cytometry using fluorescence directly labelled antibodies against CD4, CD8 and PD-1. PE-labelled monoclonal antibodies were used to determine the CD4⁺ and CD8⁺ T cell populations whereas the PD-1 expression was detected using the Alexa Fluor[®] 488-labelled anti-PD-1 8A7. Fig. 4.2.1 shows the representing

RESULTS

histograms of the PD-1 expression on CD4⁺ (A and C) and CD8⁺ T cell populations (B and D).

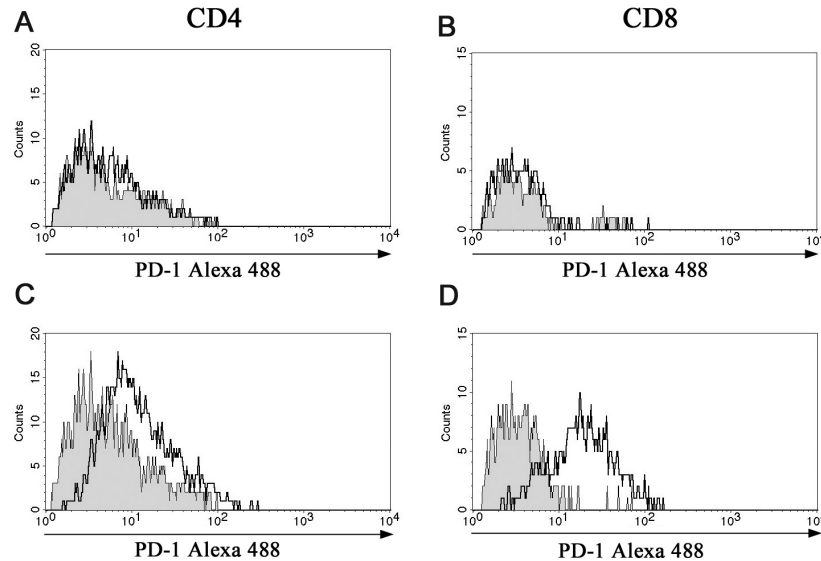


Fig. 4.2.1: PD-1 expression on naïve and activated CD4⁺ (A and C) and CD8⁺ T cells (B and D). Spleen cells were isolated from a C57BL/6 mouse and PD-1 expression on CD4⁺ and CD8⁺ T cells was determined by flow cytometry (grey shadow: isotype control; black line: PD-1). Spleen cells were incubated with anti-CD3 for 72 hours and PD-1 expression was also analyzed on CD4⁺ (C) and CD8⁺ T (D) cells (grey shadow: PD-1 expression on naïve cells; black line: PD-1 expression on stimulated cells). Representative data of three experiments are shown.

Naïve CD4⁺ and CD8⁺ T cells exhibit only marginal PD-1 expression (Fig. 4.2.1A and B) compared to the isotype control (grey shadow). Individual differences in PD-1 expression were observed by analyzing different mice (data not shown). Older mice showed a little induction of PD-1 expression on naïve spleen cells. This could be explained by the existence of autoreactive T lymphocytes that would already have an activated status expressing PD-1 (data not shown).

Upon activation with anti-CD3 for 72 hours, CD4⁺ T cells induce PD-1 expression (Fig. 4.2.1C, bold line). In the case of CD8⁺ T cells, the PD-1 expression (Fig. 4.2.1D, bold line) is more pronounced compared to CD4⁺ T cells.

In conclusion, T cell activation through CD3 molecule cross-linking leads to an induction of PD-1 expression on CD4⁺ and CD8⁺ T cells after 72 hours of stimulation. Stimulated CD8⁺ T cells show a higher PD-1 expression compared to CD4⁺ T cells.

4.2.2 Induction of PD-1 and PD-L1 expression on BMDCs upon *in vitro* stimulation with LPS and CpG ODN1826

To further analyze the PD-1 expression on other cell types, BMDCs were prepared by culturing bone marrow cells from a C57BL/6 mouse in the presence of GM-CSF. To determine the influence of the engagement of different pattern recognition receptors on the PD-1 expression, cells were stimulated either with LPS (TLR4) or CpG ODN1826 (TLR9) for 24 and 72 hours. The PD-1 and PD-L1 expression was analyzed at each time point by flow cytometry using fluorescence directly labelled antibodies. BMDCs were stained using a PerCP-labelled anti-CD11c antibody and PD-1 expression was determined by using the commercially available PE-labelled anti-PD-1 J43 antibody (*Becton Dickinson, Pharmingen*). For PD-L1 detection on these cells a PE-labelled anti-PD-L1 antibody (*Becton Dickinson, Pharmingen*) was used.

Fig. 4.2.2A represents the analysis of the PD-1 expression on CD11c⁺ naïve BMDCs. The data clearly show that PD-1 was not expressed on naïve BMDCs.

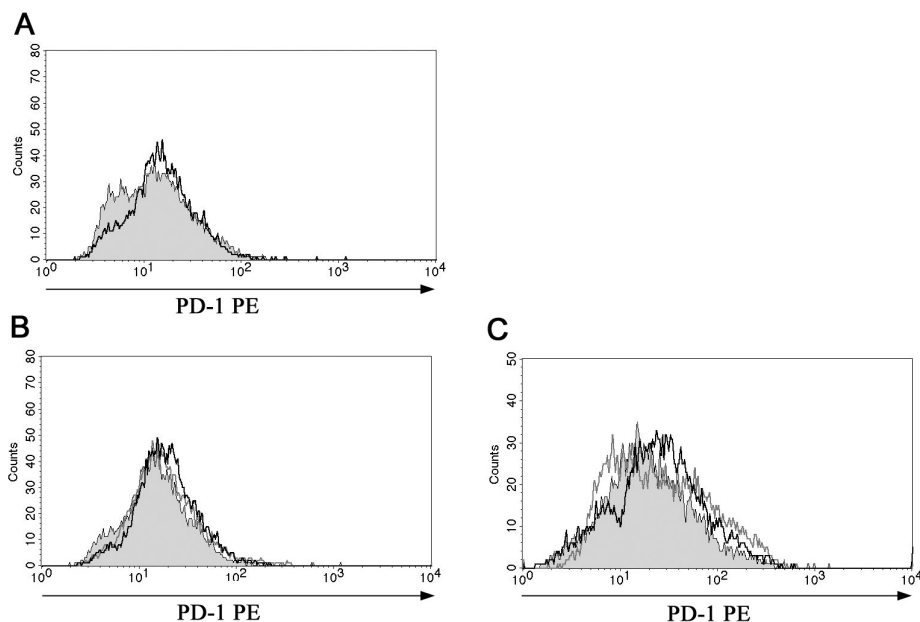


Fig. 4.2.2: PD-1 expression on CD11c⁺ BMDCs upon stimulation with LPS or CpG ODN1826. A. Naïve BMDCs were prepared from a C57BL/6 mouse and the expression of PD-1 was analyzed by flow cytometry using fluorescence directly labelled antibodies (grey shadow: isotype control; black line: PD-1 expression). B. Cells were stimulated either with 500 ng/mL LPS (grey line) or 1 µg/mL CpG ODN1826 (bold line) for 24 hours (grey shadow: medium). C. Stimulation after 72 hours (grey shadow: medium; grey line: LPS; bold line: CpG ODN1826). Representative data of three experiments are shown.

RESULTS

PD-1 expression on BMDCs after 24 hours of stimulation either with LPS or CpG ODN1826 is represented in Fig. 4.2.2C. Neither LPS nor CpG ODN1826 induced the expression of PD-1 on these cells. After 72 hours of stimulation, there was a slight increase of PD-1 expression on BMDCs upon stimulation with LPS or CpG ODN1826 compared to cells that did not receive any stimulus.

Simultaneously, PD-L1 expression was analyzed under the same stimulation conditions (Fig. 4.2.3). PD-L1 was expressed constitutively on CD11c⁺ BMDCs (Fig. 4.2.3A) compared to the isotype control. After 24 hours of stimulation with LPS or CpG ODN1826 (Fig. 4.2.3B), the PD-L1 expression on these cells increased. A further induction of PD-L1 expression was observed after 72 hours of incubation with both stimuli (Fig. 4.2.3C).

The activation of BMDCs via TLR 4 or 9 using LPS or CpG ODN1826 led to an increase of PD-L1 but not PD-1 expression on CD11c⁺ BMDCs at 24 and 72 hours of stimulation.

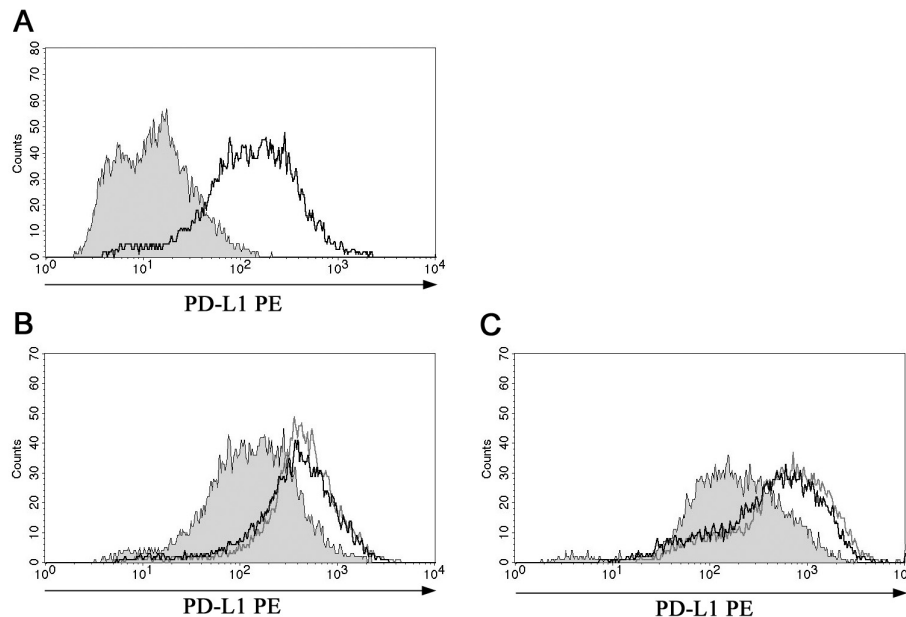


Fig. 4.2.3: PD-L1 expression on CD11c⁺ BMDCs upon stimulation with LPS or CpG ODN1826. A. Naive BMDCs were prepared from a C57BL/6 mouse and the expression of PD-L1 was analyzed by flow cytometry using fluorescence directly labelled antibodies (grey shadow: isotype control; bold line: PD-L1 expression). B. Cells were stimulated either with 500 ng/mL LPS (grey line) or 1 µg/mL CpG ODN1826 (bold line) for 24 hours (grey shadow: medium). C. Stimulation after 72 hours (grey shadow: medium; grey line: LPS; bold line: CpG ODN1826). Representative data of three experiments are shown.

4.2.3 Induction of PD-1 and PD-L1 expression on Teffs and Tregs upon *in vitro* stimulation with anti-CD3

PD-1 and PD-L1 expression was analyzed by flow cytometry on Teffs and Tregs upon *in vitro* stimulation with anti-CD3. Cells were prepared using the *CD4⁺CD25⁺ T Regulatory Isolation Kit*. Teffs and Tregs were incubated for 24 and 48 hours in the presence or absence of anti-CD3. PD-1 and PD-L1 expression was analyzed using commercially available biotinylated antibodies as well as a biotinylated isotype control. Cells were subsequently incubated with APC-labelled streptavidin. Fig. 4.2.4 shows the PD-1 and PD-L1 expression on Teffs (Fig. 4.2.4A and C) and Tregs (Fig. 4.2.4B and D).

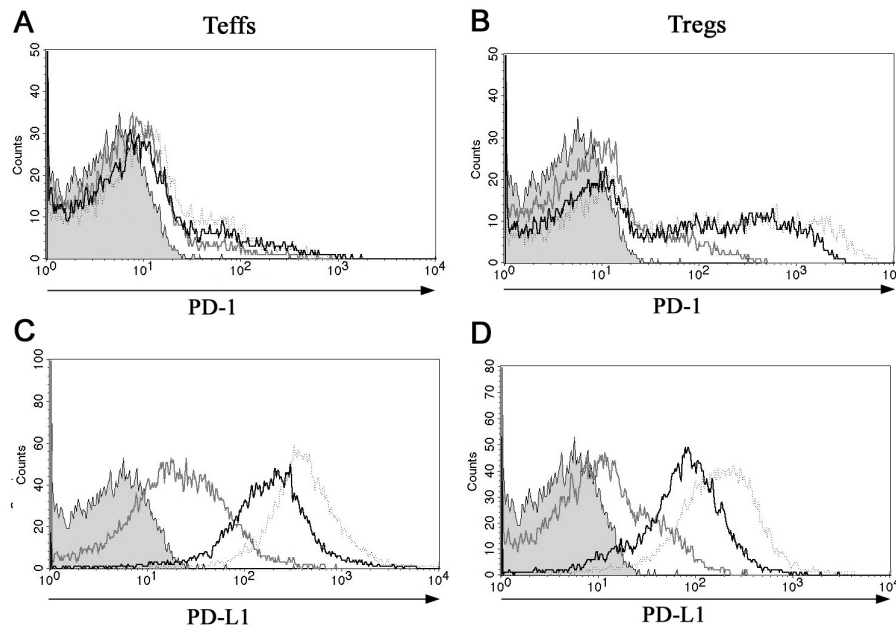


Fig. 4.2.4: PD-1 and PD-L1 expression on Teffs and Tregs upon stimulation with anti-CD3. Teffs and Tregs were isolated from spleen of a C57BL/6 mouse and using the *CD4⁺CD25⁺ T Regulatory T Cell Isolation Kit*. Cells were incubated with anti-CD3 for 24 and 48 hours. A. PD-1 expression on Teffs (grey shadow: isotype control; grey line: naïve cells; bold line: 24 hours stimulation; pointed line: 48 hours). B. PD-1 expression on Tregs (grey shadow: isotype control; grey line: naïve cells; black line: 24 hours stimulation; dotted line: 48 hours). C. PD-L1 expression on Teffs (grey shadow: isotype control; grey line: naïve cells; bold line: 24 hours stimulation; dotted line: 48 hours). D. PD-L1 expression on Tregs (grey shadow: isotype control; grey line: naïve cells; bold line: 24 hours stimulation; dotted line: 48 hours). Representative data of three experiments are shown.

Both, Teffs and Tregs expressed PD-1 constitutively to a low extent, although this expression was higher on Tregs. In contrast to previous experiments where naïve

CD4⁺ and CD8⁺ T cells marginally expressed PD-1, in this experiment Tregs isolated from spleen of a naïve mouse showed a slight expression of PD-1 by flow cytometry.

After 24 hours of stimulation with anti-CD3, PD-1 expression was induced on both T cell types although again, Tregs showed a higher expression of PD-1 compared to Tregs. After 48 hours of anti-CD3 stimulation, only Tregs induced PD-1 whereas the PD-1 expression on Tregs did not vary.

Although Tregs and Tregs expressed PD-L1 constitutively, Tregs showed a higher expression than Tregs. Upon stimulation with anti-CD3 for 24 or 48 hours, the expression of PD-L1 was higher on Tregs than Tregs.

4.3 *In vitro* effects of the blockade between PD-1 and its ligands

4.3.1 *In vitro* effect of anti-PD-1 8A7 antibody on spleen cells stimulated with anti-CD3

The *in vitro* effect of the anti-PD-1 8A7 antibody on spleen cells was tested by incubation of spleen cells from a C57BL/6 mouse in the presence or absence of anti-CD3 with different concentrations of anti-PD-1 8A7. IFN- γ and IL-2 levels in cell culture were measured by ELISA 48 hours later. Fig. 4.3.1A shows the amount of IFN- γ produced in relation to the concentration of anti-PD-1 8A7 antibody. The binding of anti-PD-1 8A7 to PD-1 led to a significantly increased production of IFN- γ ($p < 0.0001$) in a dose-dependent manner ($p = 0.0003$). It has already been published that PD-1 is a co-inhibitory molecule expressed on activated T cells and no PD-1 has been found in naïve T cells (Agata Y., *et al.*, 1996). Similar data are obtained in this study (Fig. 4.2.1). In this context, no IFN- γ production was found in cells incubated with an anti-PD-1 antibody without anti-CD3 stimulation whereas the inhibition of PD-1 signalling after CD3 engagement resulted in high production of IFN- γ . In a similar way, more IL-2 (Fig. 4.3.1B) was produced after blockade of the interaction between PD-1 and its ligands but only at a high concentration of 5 $\mu\text{g/mL}$. This increase was statistically significant ($p = 0.0370$) compared to non-stimulated cells.

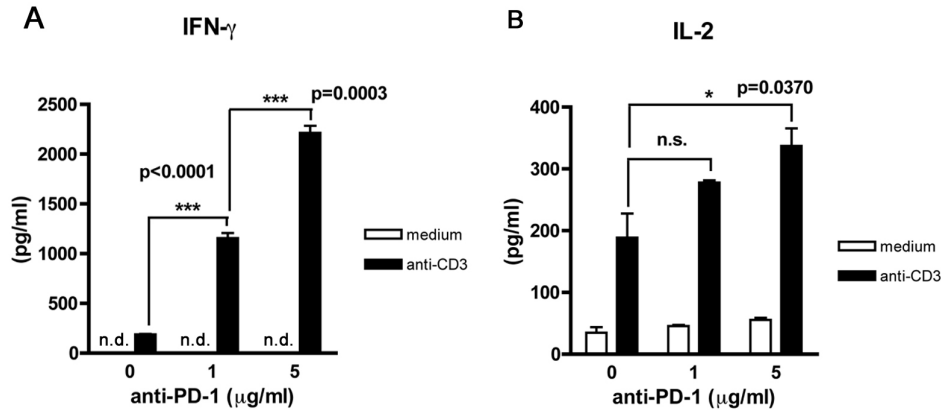


Fig. 4.3.1: *In vitro* effect of anti-PD-1 8A7 antibody on spleen cells in the presence or absence of anti-CD3. Spleen cells were incubated with anti-CD3 and different concentrations of anti-PD-1 8A7 for 48 hours. Supernatants were collected and amounts of IFN- γ (A) and IL-2 (B) were measured by ELISA. Data are expressed as the mean \pm the standard deviation of values from three wells within a representative experiment of three performed. n.d.: not detected. n.s.: no statistically significant differences.

4.3.2 *In vitro* effect of anti-PD-1 8A7 on antigen specific stimulation.

The effect of the blockade of PD-1 was analyzed in an antigen specific model where BMDCs, as APCs are incubated with antigen specific T cells in the presence of antigen, simulating an *in vivo* situation of antigen presentation. T cells were isolated from a transgenic DO.11.10 mouse in which all T cells are MHC-II restricted and recognize the C-terminal epitope from OVA₃₂₃₋₃₃₉ from ovalbumin. Cells were incubated with the anti-PD-1 8A7 antibody for 24 and 48 hours. IFN- γ and IL-2 were measured in cell culture supernatants by ELISA. Cell proliferation was determined by [³H]-thymidin incorporation. Results are shown in Fig. 4.3.2.

After 24 hours of incubation with the antibody a statistically significant increase of IFN- γ ($p=0.0041$) and IL-2 ($p=0.0007$) was found compared to cells incubated with the control antibody. Differences were more pronounced after 48 hours of incubation with anti-PD-1 8A7 (IFN- γ , $p=0.0084$; IL-2, $p=0.0037$). The blockade of PD-1 led to an increase of IFN- γ and IL-2 production upon OVA₃₂₃₋₃₃₉ recognition. In contrast, cell proliferation was partially affected by the blockade of the interaction between PD-1 and its ligands.

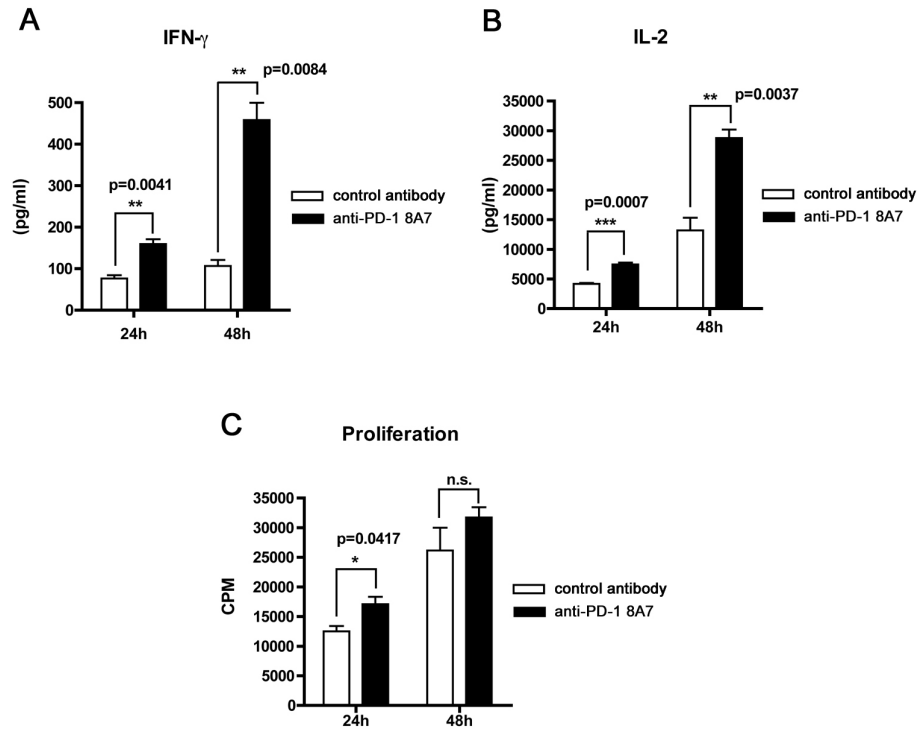


Fig. 4.3.2: *In vitro* effect of anti-PD-1 8A7 antibody on antigen specific stimulation. BMDCs and T cells were isolated from a DO.11.10 transgenic mouse. Cells were mixed (ratio BMDC: T cells; 1:100) and incubated with OVA₃₂₃₋₃₃₉ for 24 and 48 hours in the presence of anti-PD-1 8A7 or control antibody. Cytokines, IFN- γ (A) and IL-2 (B) were measured in the supernatants by ELISA and cell proliferation (C) was detected by [³H]-thymidin incorporation. Data are expressed as the mean \pm the standard deviation of values from three wells within a representative experiment of three performed. CPM: counts per minute; n.s.: no statistically significant differences.

4.3.3 *In vitro* effect of anti-PD-1 8A7 concerning the suppressive capacity of Tregs

Tregs are defined by their capacity of suppressing the activity of Teffs. This effect seems to be mediated not only by the secretion of inhibitory cytokines such as IL-10, but also by cell-cell contact dependent mechanisms leading to the inhibition of IL-2 gene transcription in effector T cells. IL-2 is an important cytokine being a growth factor for T cells produced after activation by T cells themselves. The suppression activity of Tregs can be measured by the decrease in IL-2 production by Teffs in the presence of Tregs and anti-CD3.

The induction of PD-1 and PD-L1 expression on Tregs and Teffs upon stimulation with anti-CD3 was already examined by flow cytometry (Fig. 4.2.4). To determine the effect of the blockade of the interaction between PD-1 and its ligands, Teffs and

Tregs were isolated using the *CD4⁺CD25⁺ T Regulatory Isolation Kit (Miltenyi)*, mixed in different ratios and incubated in the presence of anti-CD3 together with either anti-PD-1 8A7 or control rat IgG antibody for 48 hours. After this time, supernatants were collected and the amount of IL-2 was determined by ELISA. Fig. 4.3.3 shows the obtained results.

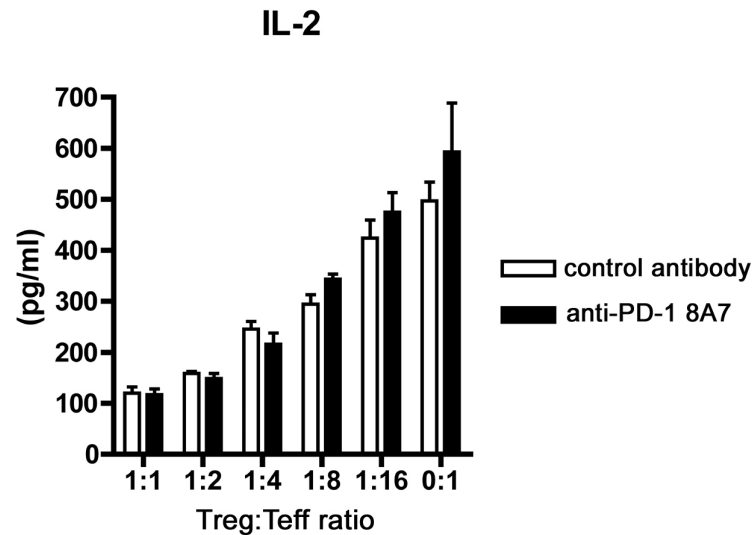


Fig. 4.3.3: *In vitro* effect of anti-PD-1 8A7 antibody concerning the suppressive capacity of Tregs. Teffs and Tregs were isolated from spleen of a C57BL/6 mouse using *CD4⁺CD25⁺ T Regulatory Isolation Kit (Miltenyi)*. Teffs and Tregs were mixed in different ratios and incubated in the presence of anti-CD3 with anti-PD-1 or control antibody for 48 hours. After incubation, IL-2 amount was determined in the supernatants by ELISA. Data are expressed as the mean \pm the standard deviation of values from three wells within a representative experiment of two performed.

In the control situation, in absence of Tregs (ratio 0:1), Teffs produced high amounts of IL-2 in response to stimulation with anti-CD3. The amount of IL-2 production diminished when the ratio between Tregs and Teffs was increased, meaning that more Tregs were able to suppress Teffs. In the case of addition of anti-PD-1 8A7 antibody no differences were seen compared to the control antibody. The blockade of the interaction of PD-1 with its ligands did not affect the suppressive capacity of Tregs.

4.3.4 *In vitro* effect of anti-PD-L1 6H6 antibody on spleen cells

In order to analyze the effect of the blockade of endogenous PD-L1, spleen cells from a C57BL/6 mouse were incubated with two different concentrations of

anti-PD-L1 6H6 antibody for 48 hours in the presence of anti-CD3. IFN- γ levels were measured in cell culture by ELISA. The results are shown in Fig. 4.3.4. The blockade of PD-L1 with the anti-PD-L1 6H6 antibody led to a significant increase of IFN- γ production ($p=0.0256$), although lower than in the case of the blockade using anti-PD-1 8A7 antibody. The effect did not increase when cells were incubated with higher amount of anti-PD-L1 6H6 (5 $\mu\text{g}/\text{mL}$).

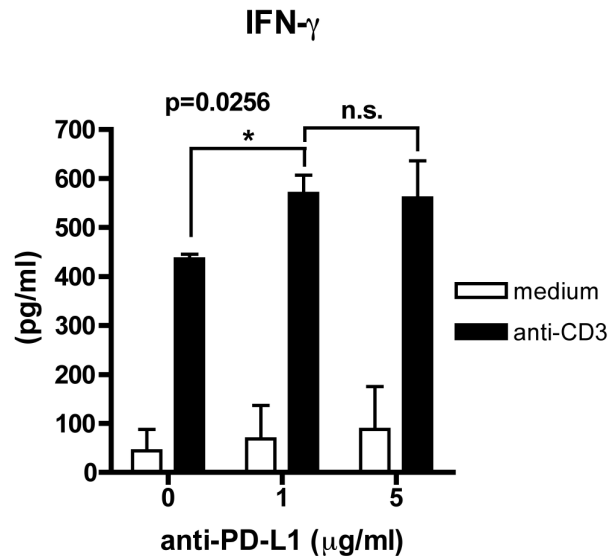


Fig. 4.3.4: *In vitro* effect of anti-PD-L1 6H6 antibody on spleen cells. Spleen cells were isolated from a BALB/c mouse and incubated in the presence or not of anti-CD3 (3 $\mu\text{g}/\text{mL}$) and different concentrations of anti-PD-L1 (1 and 5 $\mu\text{g}/\text{mL}$). After 48 hours IFN- γ amounts were determined in the cell culture by ELISA. Data are expressed as the mean \pm the standard deviation of values from three wells within a representative experiment of three performed. n.s.: no statistically significant differences.

4.4 Analysis of the interaction between PD-1 and its ligands during *P. berghei* ANKA infection

4.4.1 Regulation of the CSP-specific CD8⁺ T cell response during *P. berghei* ANKA infection

In mice as well as in humans a sterile protection against a *Plasmodium* infection has been achieved by the vaccination with γ -irradiated sporozoites (Clyde D.F. *et al.*, 1973; Hoffman S. *et al.*, 2002; Morrot A. *et al.*, 2004). Mice and humans infected with γ -irradiated sporozoites only show arrested liver stage of the infection. The so modified sporozoites are not able to proceed with the blood stage and therefore the symptoms and complications derived from the blood stage malaria do not manifest. It has also been demonstrated that the sterile protection achieved by the immunization

with γ -irradiated sporozoites is consequence of the presence of a CSP-specific CD8⁺ T cell population that is able to eliminate the sporozoite infected hepatocytes in case of re-infections (Hoffman S. *et al.*, 2002; Morrot A. *et al.*, 2004). Why natural infections do not induce a protective CSP-specific CD8⁺ T cell response despite of the constant contact of the host with the parasite in endemic areas, remains unclear. One explanation is the inhibitory effects on T cell activation that DCs exert during blood stage malaria (Ocaña-Mogner C. *et al.*, 2003).

Another possibility is that the interaction between PD-1 and its ligands modulates the CSP-specific CD8⁺ T cell population. The role of PD-1 and its ligands is important in the control of the immune response at the site of infection in order to avoid tissue damage but can eventually influence the CSP-specific CD8⁺ T cell population.

It was interesting to analyze the dynamic of this CSP-specific CD8⁺ T cell population induced during the course of malaria and moreover if this specific population could be somehow differentially regulated during the blood stage.

The limited number of this CSP-specific CD8⁺ T cell population makes its study difficult. The ACT of *Bordetella pertussis* has been used as antigen delivery system for several vaccination strategies because of its capacity of delivering its N-terminal catalytic domain into the cytosol of CD11b-expressing APCs (Simsova M. *et al.*, 2004). This characteristic allows the introduction of peptides into the MHC class I presentation pathway generating a specific CD8⁺ T cell response. Detoxified ACT can be combined with the epitope CSP of *P. berghei* and used to immunize mice. This leads to an increase in the frequency of CSP-specific CD8⁺ T cells but does not result in protection against a *P. berghei* infection (Tartz S. *et al.*, 2006).

To study the role of the interaction between PD-1 and its ligands in the dynamic of the CSP-specific CD8⁺ T cell population during *Plasmodium* infection, BALB/c mice were immunized with ACT-CSP one week before infection with either γ -irradiated or non-irradiated *P. berghei* ANKA sporozoites. The CSP-specific CD8⁺/CD62L^{low} T cell population was analyzed by flow cytometry in spleen and liver at days 2, 7 and 10 p.i. using fluorescence directly labelled antibodies. CSP-specific CD8⁺ T cell population was detected using an APC-labelled CSP-loaded pentamer (*Proimmune, Oxford*) and FITC-labelled anti-CD8. The CD62L expression was also analyzed since low expression of CD62L is indicative of T cell activation. Results are shown in Fig. 4.4.1 as percentage of

RESULTS

pentamer⁺ (CSP-specific)/CD62L^{low} of total CD8⁺ T cells found in spleen (Fig. 4.4.1A) and liver (Fig. 4.4.1B). The parasitemia was also determined (Fig. 4.4.1C).

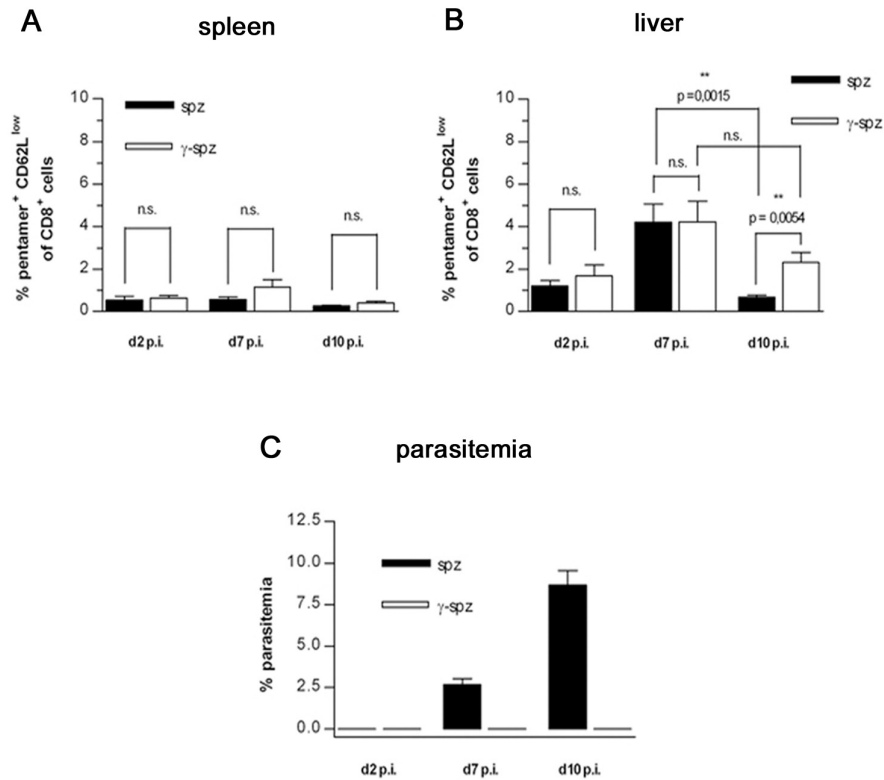


Fig. 4.4.1: Regulation of the CSP-specific CD8⁺ T cell response during *P. berghei* ANKA infection. Lymphocytes were isolated from spleen (A) and liver (B) from mice that were immunized with ACT-CSP one week before infection with either non-irradiated or γ -irradiated sporozoites. Samples were collected at days 2, 7 and 10 p.i. The CSP-specific CD62L^{low} CD8⁺ T cell population was detected using APC-labelled CSP-loaded pentamer and fluorescence directly labelled antibodies. Cells were analyzed by flow cytometry. Percentages of positive cells within the CD8⁺ T cell population are shown. The parasitemia at days 2, 7 and 10 p.i. was also determined (C). Data are expressed as mean \pm the standard deviation of values from three mice within a representative experiment of two performed. n.s.: no statistically significant differences; p.i.: post-infection; spz: sporozoites; γ -spz: γ -irradiated sporozoites.

In spleen, no differences in the frequency of CSP-specific CD62L^{low} CD8⁺ T cells during the infection were found. However, in liver, an increase of this cell population on day 7 p.i. was observed, although no differences between mice receiving γ -irradiated or non-irradiated sporozoites were found. In contrast, significant differences were observed at day 10 p.i. ($p=0.0054$). Mice receiving non-irradiated sporozoites, and therefore having a normal blood stage infection indicated by presence of parasites in blood (Fig. 4.4.1C, parasitemia), showed a lower number of

RESULTS

CSP-specific CD62L^{low} CD8⁺ T cells compared to those receiving γ -irradiated sporozoites.

In conclusion, there was an increase of the CSP-specific CD62L^{low} CD8⁺ T cell population during liver stage in this organ and early blood stage (day 7 p.i.). In mice suffering from a normal infection, this population decreased at day 10 p.i. ($p=0.0015$) whereas mice that had been infected with γ -irradiated sporozoites, showed a statistically not significant change in the number of these cells.

4.4.2 Regulation of Tregs during infection with γ -irradiated *P. berghei* ANKA sporozoites

Tregs exert a regulatory function over the immune response (O'Garra A. *et al.*, 2004). For this reason it was interesting to analyze whether Tregs were induced during malaria. The amount of Tregs during the *Plasmodium* infection was analyzed comparing mice infected with γ -irradiated sporozoites and mice receiving non-irradiated sporozoites. The population of Tregs was determined by the detection of CD4⁺, CD25⁺ and Foxp3⁺ T cells by flow cytometry. The presence of the transcription factor Foxp3 has been described as specific marker for Tregs (O'Garra A. *et al.*, 2004). Fig. 4.4.2 shows the results obtained as percentage of Foxp3⁺CD25⁺ T cells of CD4⁺ T cells.

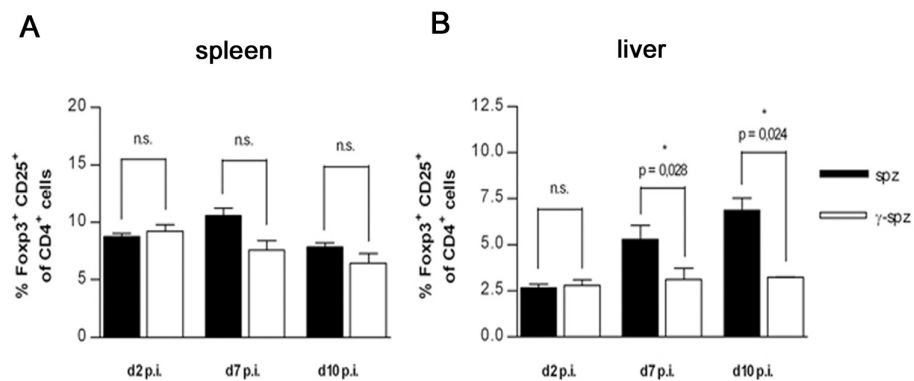


Fig. 4.4.2: Analysis of the Treg population in mice during *P. berghei* ANKA malaria. Lymphocytes were isolated from spleen (A) and liver (B) of mice that were immunized with ACT-CSP one week before the infection with either non-irradiated or γ -irradiated sporozoites. Samples were collected at days 2, 7 and 10 p.i. Tregs were detected by flow cytometry using antibodies against CD4, CD25 and the transcription factor Foxp3. Percentages of Foxp3⁺, CD25⁺ positive cells within the CD4⁺ positive population are shown. Data are expressed as the mean \pm the standard deviation of values from three mice within a representative experiment of two performed. n.s.: no statistically significant differences; p.i.: post-infection; spz: sporozoites; γ -spz: γ -irradiated sporozoites.

RESULTS

No differences were found in the spleen (Fig. 4.4.2A) whereas in the liver a statistically higher percentage of Tregs was detected at day 7 ($p=0.028$) and 10 p.i. ($p=0.024$) in mice infected with non-irradiated sporozoites.

There were no changes along the infection in mice that received γ -irradiated sporozoites. In conclusion, the blood stage malaria induced an increase of Tregs in the liver.

4.4.3 PD-1 expression on CSP-specific CD8⁺ T cells

The PD-1 expression on CSP-specific CD8⁺ T cells in spleen and liver during liver stage malaria was examined. Mice were immunized with ACT-CSP one week before infection with γ -irradiated sporozoites. At day 7 p.i. spleens and livers from mice were isolated and the PD-1 expression on CSP-specific CD8⁺ T cells was determined by flow cytometry using APC-labelled CSP-loaded pentamer, FITC-labelled anti-CD8 and Alexa Fluor[®]488-labelled anti-PD-1 8A7. Fig. 4.4.3 shows the PD-1 expression and CSP-specificity of CD8⁺ T cells.

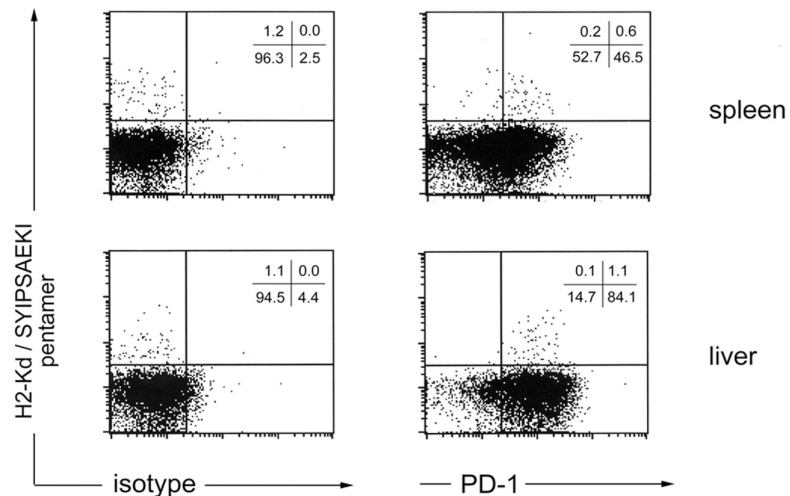


Fig. 4.4.3: PD-1 expression on CSP-specific CD8⁺ T cells in the liver. Lymphocytes were isolated from spleen (upper panels) and liver (lower panels) of mice that had been immunized with ACT-CSP one week before the infection with γ -irradiated sporozoites. CSP-specific CD8⁺ T cells were detected using APC-labelled CSP-loaded pentamer and fluorescence directly labelled antibodies against CD8 (FITC-labelled anti-CD8) and PD-1 (Alexa Fluor[®]488-labelled anti-PD-1 8A7). Cells were analyzed by flow cytometry and gated on CD8⁺ T cells. Numbers in the corners represent the percentage of cells in the respective quadrant. Representative data of three experiments are shown.

All CSP-specific T cells expressed PD-1. Only 0.6% CSP-specific T cells expressing PD-1 were found in the spleen whereas in the liver this percentage rose up to 1.1 %. It is important to indicate that in contrast to the spleen where a high number of CD8+ T cells did not express PD-1 (52.9 %), almost all CD8+ T cells in the liver showed expression of PD-1 (85.2 %).

4.4.4 PD-L1 expression on non-parenchymal liver cells during liver stage of *P. berghei* ANKA infection

The liver is an important organ inducing tolerance. LSECs and KCs have already been described as responsible for such tolerance (Crispe N., 2003). As already published, the induction of PD-L1 expression on liver epithelium during chronic viral infections leads to the inhibition of virus specific CD8⁺ T cells (Dong H. *et al.*, 2004; Rodig N. *et al.*, 2003). In the case of malaria, the expression of PD-L1 on these cells could be responsible for the loss of CSP-specific CD8⁺ T cells in the liver during blood stage malaria. For this reason PD-L1 expression was analyzed on liver sinusoidal endothelial cells (LSECs) and Kupffer cells (KCs) as non-parenchymal liver cells. These cells were isolated from livers of non-infected and *P. berghei* ANKA sporozoites infected mice (day 3 p.i.). Afterwards *in vivo* PD-L1 expression was analyzed by flow cytometry on KCs (Fig. 4.4.4A) and LSECs (Fig. 4.4.4B) Results are represented in Fig. 4.4.4.

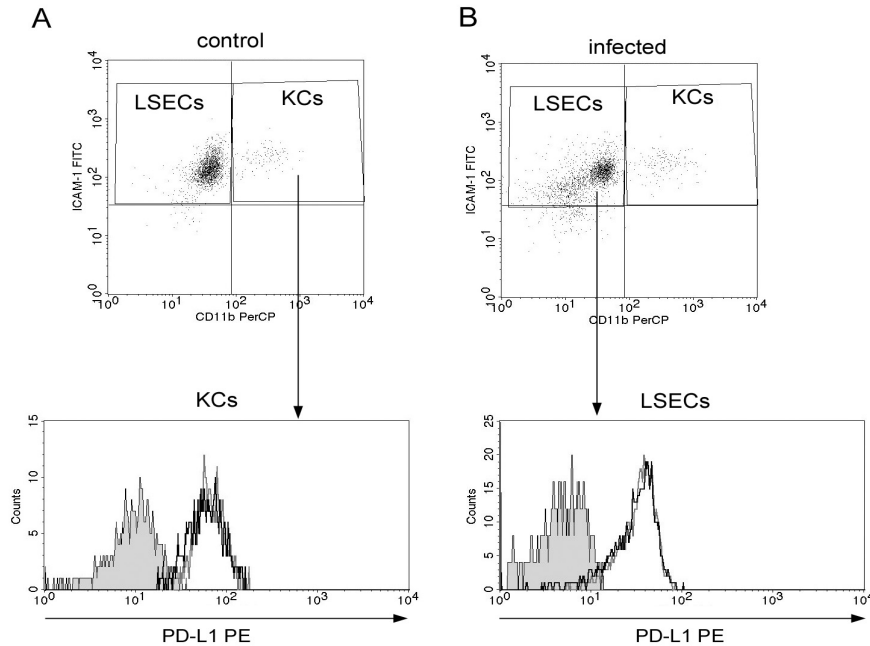


Fig. 4.4.4: PD-L1 expression on non-parenchymal liver cells during liver stage *P. berghei* ANKA infection. KCs were identified by expression of ICAM-1 and high expression of CD11b (A). PD-L1 expression on KCs was determined of a non-infected control and infected mice (3 p.i.) in ICAM-1⁺ CD11b^{high} gate using a PE-anti-PD-L1 antibody and analyzed by flow cytometry (grey shadow: isotype control; grey line: control non-infected mouse; bold line: infected mouse day 3 p.i.). (B) PD-L1 expression in LSECs was determined in control non-infected and infected mice (3 p.i.) in ICAM-1⁺ CD11b^{low} gate (grey shadow: isotype control; grey line: control non-infected mouse; bold line: infected mouse day 3 p.i.). Representative data of three experiments are shown.

LSECs and KCs express the molecule ICAM-1 (CD154) and differ in the expression of CD11b, which is a classical marker for macrophages. Hence, using monoclonal antibodies and flow cytometry analysis, KCs are generally described as CD11b^{high} and LSECs as CD11b^{low}, respectively (Iwai Y. *et al.*, 2003).

Both, LSECs and KCs constitutively expressed PD-L1 as shown in the histograms. However, during liver stage *P. berghei* ANKA malaria, PD-L1 was not up-regulated neither on LSECs nor KCs.

4.4.5 PD-1 and PD-L1 expression on CD4⁺ and CD8⁺ T cells during blood stage of *P. berghei* ANKA infection

The *in vivo* expression of PD-1 on T cells in the spleen during blood stage malaria infection was determined using the malaria mouse model with *P. berghei* ANKA. Spleen cells were isolated from non-infected control and infected mice at day 7 p.i. (blood stage malaria). Cells were stained for CD3, CD4, CD8, PD-1 and PD-L1

RESULTS

using fluorescence directly labelled monoclonal antibodies. Results are shown in Fig. 4.4.5.

Fig. 4.4.5A shows the expression of PD-1 on CD3⁺/CD4⁺ T cells in a non-infected and infected mouse. Activated CD4⁺ T cells from *P. berghei* infected mouse expressed higher amounts of PD-1 compared to a non-infected mouse used as control.

Concerning CD3⁺/CD8⁺ T cells, PD-1 was expressed on these cells but expression did not increase upon infection with *P. berghei* (Fig. 4.4.5B).

There was a minimal expression of PD-L1 on CD3⁺/CD4⁺T cells in spleens of non-infected mice (Fig. 4.4.5C, grey line) but in *P. berghei* ANKA infected mice, PD-L1 was clearly induced (Fig. 4.4.5C, bold line). A high expression of PD-L1 was found on CD3⁺/CD8⁺ T cells (Fig. 4.4.5D, grey line). Infection with *P. berghei* substantially increased the PD-L1 expression on these cells (Fig. 4.4.5D, bold line).

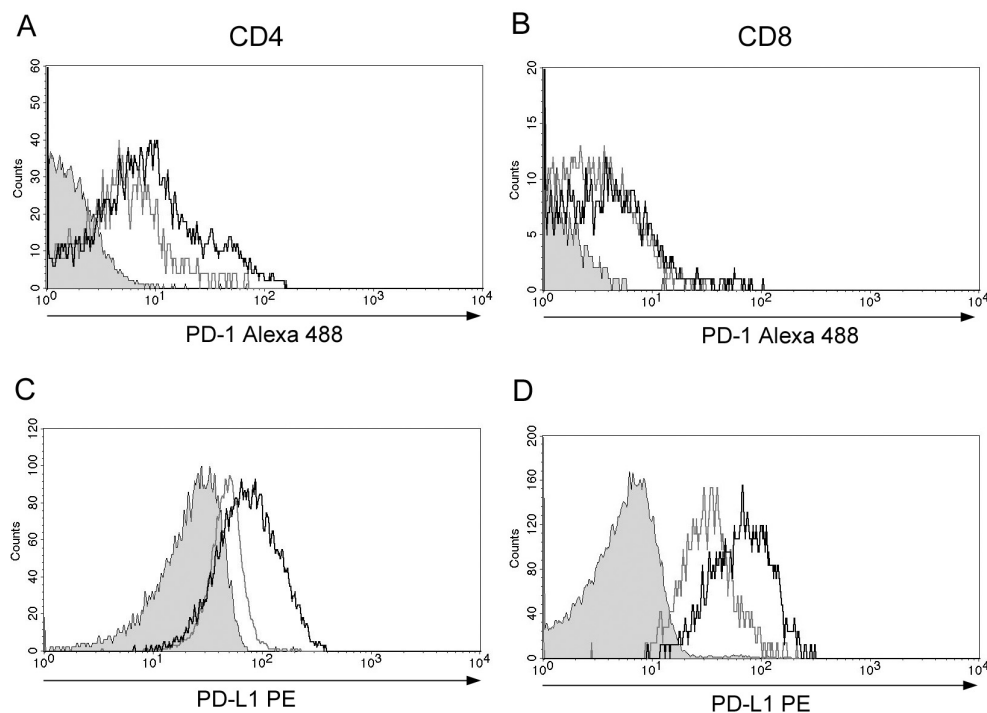


Fig. 4.4.5: PD-1 and PD-L1 expression on CD4⁺ and CD8⁺ T cells during blood stage *P. berghei* ANKA infection. Lymphocytes were isolated from spleen of infected and non-infected control mice during blood stage malaria (day 7 p.i.) and the PD-1 and PD-L1 expression on CD4⁺ and CD8⁺ T cells were analyzed by flow cytometry using fluorescence directly labelled antibodies. The histograms show PD-1 expression on gated CD3⁺/CD4⁺ (A) and CD3⁺/CD8⁺ T cells (B). PD-L1 expression on these cells was also determined for CD3⁺/CD4⁺(C) and CD3⁺/CD8⁺ T cells (D). Grey shadow: isotype control; grey line: non-infected control mouse; bold line: infected mouse. Representative data of three experiments are shown.

In conclusion, the blood stage of malaria caused by *P. berghei* ANKA induced the expression of PD-1 as well as PD-L1 on activated CD4⁺ T cells in the spleen but only the expression of PD-L1 on activated CD8⁺ T cells.

4.4.6 PD-L1 is induced on non-parenchymal liver cells and hepatocytes during the blood stage of *P. berghei* ANKA malaria

In order to determine whether the blood stage of *Plasmodium* infection influences the expression of PD-L1 in the liver, the PD-L1 expression was analyzed on LSECs and KCs by flow cytometry using fluorescence directly labelled antibodies. BALB/c mice were infected with *P. berghei* ANKA iRBCs to induce the blood stage of the disease. Livers were digested and non-parenchymal cells were isolated and stained with fluorescence directly labelled antibodies against ICAM-1, CD11b and PD-1. During the blood stage the liver suffers from a high cell infiltration resulting in tissue damage. For this reason the differentiation of LSECs and KCs was not possible. Fig. 4.4.6 shows a histogram of the PD-L1 expression on non-parenchymal liver cells observed from a non-infected and infected mouse considering the whole ICAM-1⁺ population without distinguishing between LSECs and KCs.

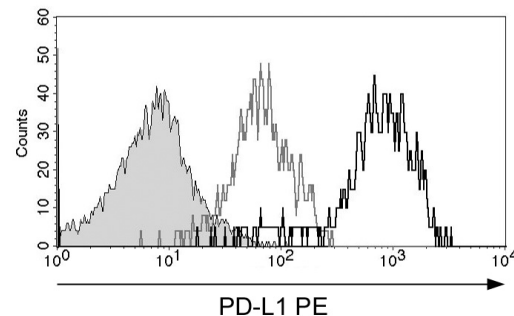


Fig. 4.4.6: PD-L1 expression on non-parenchymal liver cells during blood stage *P. berghei* ANKA malaria. Non-parenchymal liver cells were isolated from a non-infected control and infected mouse (blood stage day 7p.i.) from digested livers and a gradient centrifugation step. The histogram shows PD-L1 expression on non-parenchymal liver cells gated on ICAM-1⁺. Grey shadow: isotype control; grey line: non-infected mouse; bold line: infected mouse). Representative data of three experiments are shown.

In order to analyze whether liver cells up-regulate PD-L1 during the blood stage malaria, the PD-L1 expression was also analyzed on hepatocytes by immunohistology and flow cytometry (Fig. 4.4.7). Cryosections of liver specimens

RESULTS

were prepared from non-infected and infected mice with *P. berghei* ANKA (blood stage, day 6 p.i.). PD-L1 was detected using anti-PD-L1 16B8 antibody. Samples were also stained with an antibody against CD26, a surface marker expressed on hepatocytes. Dapi was used in order to stain cellular nuclei (Fig. 4.4.7A).

Hepatocytes isolated from non-infected and *P. berghei* ANKA infected mice were purified and detected by the typical form of the nucleus (Fig. 4.4.7B). The PD-L1 expression on these cells was analyzed by flow cytometry (Fig. 4.4.7C).

Hepatocytes did not exhibit a constitutive expression of PD-L1. In contrast during blood stage malaria hepatocytes showed an increase in PD-L1 expression.

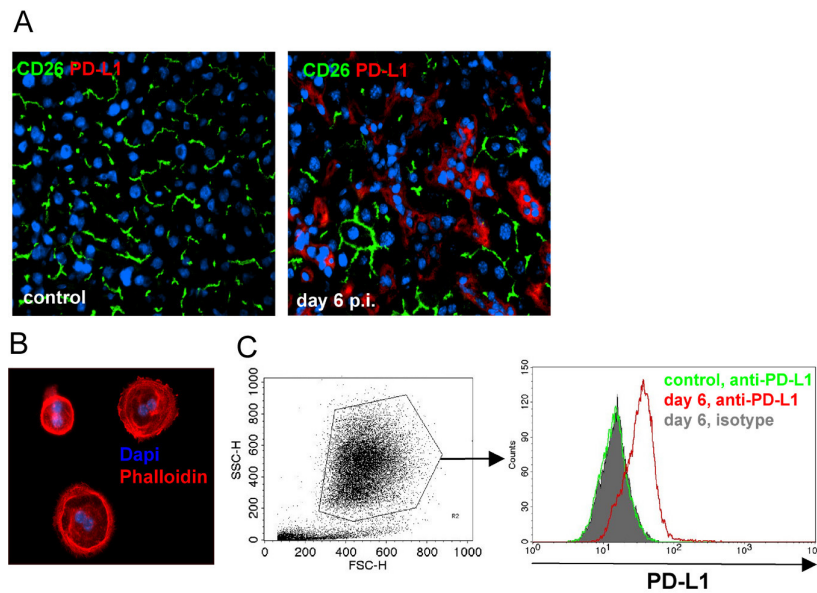


Fig. 4.4.7: PD-L1 expression during the blood stage malaria. A: Livers from a non-infected and infected mouse (blood stage) were frozen in medium (*Jung medium*, *Leica Instruments*). Cryosections (8 μ m) were dried, fixed in acetone and blocked with human γ -globulin (Cohn II fraction). Cells were stained using anti-PD-L1 16B8 and a secondary antibody Alexa Fluor[®]594 anti-rat IgG. Hepatocytes were detected by staining with FITC-labelled anti-CD26 followed by Oregon Green-labelled anti-FITC as secondary antibody. Nuclei were stained with Dapi. B: Hepatocytes were detected by their typical nucleus form after staining with Dapi and Phalloidin. C: PD-L1 expression on hepatocytes was analyzed from a non-infected and an infected mouse (blood stage) by flow cytometry using PE-labelled anti-PD-L1 (*Becton Dickinson*). Representative data of two experiments are shown.

4.4.7 *In vivo* blockade of the interaction between PD-1 and its ligand PD-L1 with anti-PD-1 8A7 during *P. berghei* ANKA infection

In order to examine the role of the interaction between PD-1 and PD-L1 during *P. berghei* ANKA malaria infection, an *in vivo* blockade with the anti-PD-1 8A7 antibody was performed. Mice were infected with *P. berghei* ANKA sporozoites. At

RESULTS

the day of infection, anti-PD-1 8A7 antibody was also administered. The CSP-specific CD8⁺ T population in spleen and liver was determined at day 7 p.i. by flow cytometry. Fig. 4.4.8 shows the percentage of CSP-specific CD62L^{low} T cells in the CD8⁺ gate found in the spleen (A) and liver (D). There was no difference in the amount of CSP-specific CD8⁺/CD62L^{low} T cells in the spleen of mice that received anti-PD-1 8A7 antibody compared to mice that received a control antibody (rat IgG). This indicates that the PD-1 pathway does not play an important role in the priming of CD8⁺T cells. In the case of the liver, there is a statistically significant ($p=0.0016$) increase in the amount of that population in mice that received anti-PD-1 8A7 (Fig. 4.4.8D). However the administration of anti-PD-1 8A7 did not alter the course of the disease in mice or produced changes in parasitemia (Fig. 4.4.8C).

The IFN- γ production of the CSP-specific T cell population after re-stimulation with peptide was analyzed by IFN- γ ELISPOT. To this end cells collected from spleen and liver from *P. berghei* ANKA infected mice (day 7 p.i.) treated with anti-PD-1 8A7 or control antibody (rat IgG) were re-stimulated *in vitro* with CSP₂₄₅₋₂₅₃ peptide overnight. Fig. 4.4.8 shows the results obtained in the spleen (Fig. 4.4.8B) and liver (Fig. 4.4.8E). No significant changes were found in both organs, although in the liver, a tendency of a higher amount of IFN- γ -producing CSP-specific T cells in anti-PD-1 8A7 treated mice was observed. The blockade of PD-1 with a monoclonal antibody against PD-1 during the infection with *P. berghei* ANKA led to an increase in the CSP-specific CD8⁺ T cell population in the liver although this blockade did not result in a significant increase of IFN- γ producing specific cells nor altered the outcome of the disease.

The immunization of mice with ACT-CSP induced a CSP-specific CD8⁺ T cell population in the liver that expressed PD-1. During the blood stage, hepatocytes, KCs and LSECs showed a high expression of PD-L1. The interaction between PD-1 and PD-L1 in the liver could negatively regulate this CSP-specific T cell population. In order to elucidate whether the blockade of PD-1 could increase the amount of these sporozoite specific CD8⁺ T cells, mice were immunized with ACT-CSP one week before the infection with *P. berghei* ANKA. One group of mice was treated with anti-PD-1 8A7 whereas the control group received control antibody (rat IgG) at the day of infection. CSP-specific CD62L^{low}/CD8⁺ T cells were detected by flow

RESULTS

cytometry at day 7 p.i. in spleen and liver. Fig. 4.4.9 shows the results in spleen (A) and liver (D).

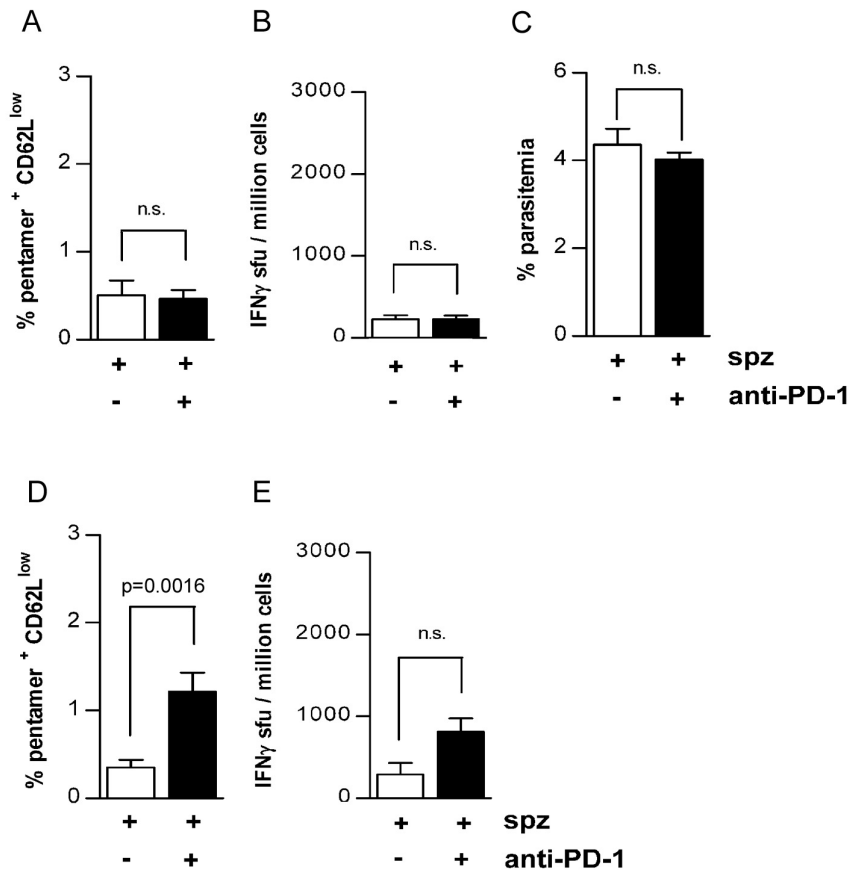


Fig. 4.4.8: *In vivo* blockade of PD-1 during *P. berghei* ANKA infection. Anti-PD-1 8A7 was injected the same day mice were infected with *P. berghei* ANKA sporozoites. Lymphocytes were isolated from spleen and liver at day 7 p.i. and the CSP-specific CD8⁺/CD62L^{low} T cell population was analyzed by flow cytometry. The results are shown as percentage of positive CSP-specific CD62L^{low} T cells in the CD8⁺ T cell gate (A: spleen; D: liver). IFN- γ production after *in vitro* re-stimulation with CSP₂₄₅₋₂₅₃ peptide overnight was determined by ELISPOT and expressed as spots forming units (sfu) per million cells (B: spleen; E: liver). C. parasitemia of mice at day 7 p.i. Data are expressed as the mean \pm the standard deviation of values from three mice per group within a representative experiment of two performed. n.s.: no statistically significant differences; spz: sporozoites

Again, no differences were observed regarding the cells in the spleen. In the case of the liver, a statistically significant higher number of CSP-specific CD8⁺/CD62L^{low} T cells was found in mice treated with anti-PD-1 8A7 antibody ($p=0.0132$). Following the same procedure as in the previous experiment, the CSP-specific IFN- γ producing cells were also analyzed after CSP₂₄₅₋₂₅₃ peptide re-stimulation from spleen (Fig. 4.4.9B) and liver (Fig. 4.4.9E). Although no

RESULTS

differences in the spleen are observed, a significant increase ($p=0.0047$) in the IFN- γ -producing CSP-specific T cells in the liver was found. Importantly, mice treated with the anti-PD-1 8A7 antibody also showed a statistically significant decrease ($p=0.039$) in parasitemia (Fig. 4.4.9C).

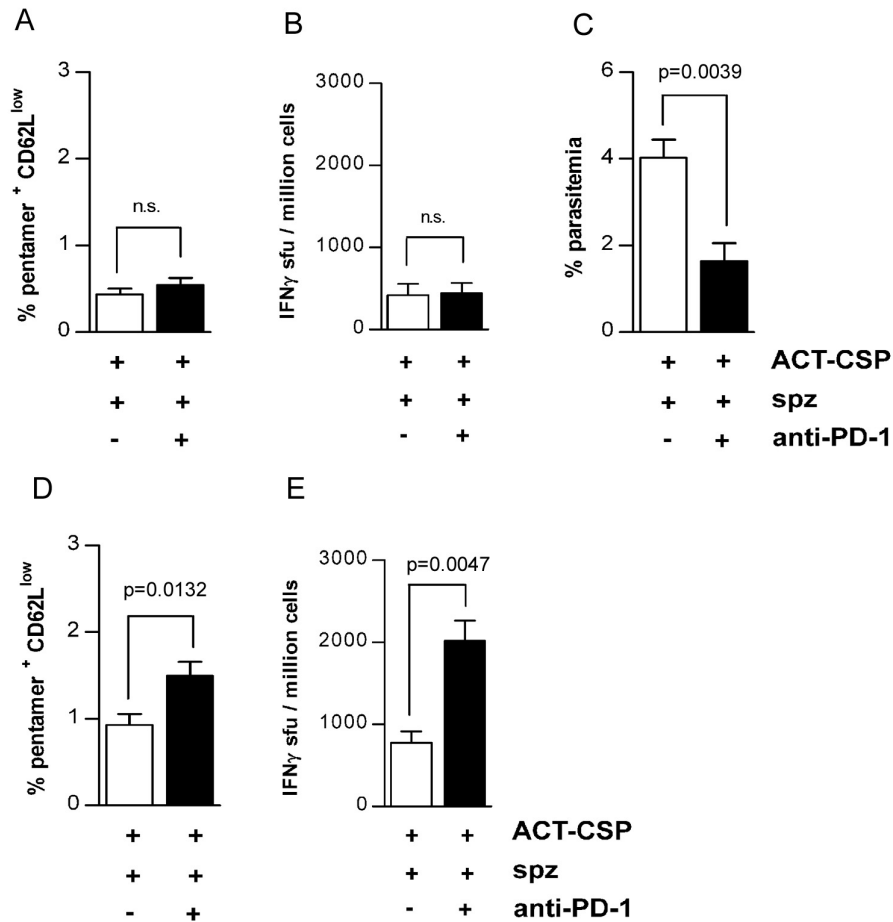


Fig. 4.4.9: *In vivo* blockade of PD-1 during *P. berghei* ANKA infection after immunization with ACT-CSP. Mice were immunized with ACT-CSP one week before administration of anti-PD-1 8A7 or control antibody (rat IgG). Mice were also infected the same day with *P. berghei* ANKA sporozoites. Lymphocytes were isolated from spleen and liver at day 7 p.i. and the CSP-specific CD8⁺/CD62L^{low} T cell population was analyzed by flow cytometry. The results are shown as percentage of positive CSP-specific CD62L^{low} T cells in the CD8⁺ T cell gate (A: spleen; D: liver). IFN- γ production after *in vitro* re-stimulation with CSP₂₄₅₋₂₅₃ peptide overnight was determined by ELISPOT and expressed as spots forming units (sfu) per million cells (B: spleen; E: liver). C shows parasitemia of mice at day 7 p.i. Data are expressed as the mean \pm the standard deviation of values from three mice per group within a representative experiment of two performed. n.s.: no statistically significant differences; spz: sporozoites

To conclude, the immunization with ACT-CSP conferred a liver-stage specific IFN- γ -producing CD8⁺ T cell population that remained in the liver after the

RESULTS

blockade of PD-1 with anti-PD-1 8A7 antibody. Additionally, this blockade affects the outcome of the disease as shown in the decreased parasitemia observed in mice that received anti-PD-1 8A7 antibody compared to mice that received control antibody (Fig. 4.4.9C).

5. DISCUSSION

5.1 *In vitro* PD-1 and PD-L1 expression on T cells and BMDCs

The induction of PD-1 expression on T cells upon TCR activation has been described in several publications (Chen L. *et al.*, 2004; Liang S. *et al.*, 2003). In this study a mouse monoclonal anti-PD-1 8A7 antibody (previously generated by A. von Bonin, *BNI*) was used to analyze the PD-1 expression on several immunological cell types under various conditions.

Anti-PD-1 8A7 antibody was compared to the commercially available anti-PD-1 J43 antibody by flow cytometry using spleen cells stimulated with anti-CD3. The results showed the same staining pattern indicating that both antibodies stained the same cell population.

Similar to the results obtained by other research groups (Carter L. *et al.*, 2002; Yamazaki T. *et al.*, 2002; Iwai Y. *et al.*, 2003) a marginal PD-1 expression on resting CD4⁺ and CD8⁺ T cells was found in this study. Upon TCR activation with anti-CD3, both cell types showed an induction of PD-1 expression 72 hours after stimulation. Differences between CD4⁺ and CD8⁺ T cells were found, showing CD8⁺ T cells with a higher PD-1 expression. It has been published that CD4⁺ and CD8⁺ T cells have different requirements for activation (Szabo S.J. *et al.*, 2002). According to these publications, naïve CD4⁺ T cells need at least six hours of *in vitro* antigenic stimulation by APCs to be able to proliferate (Iezzi, G. *et al.*, 1998) whereas CD8⁺ T cells started to proliferate after only two hours (van Stipdonk M. J. *et al.*, 2001). MHC class I molecules are expressed on every cell type and MHC class II molecules are only found on APCs. This different location could explain that CD8⁺ T cells achieve a threshold of activation faster than CD4⁺ T cells. CD8⁺ T cells would then have a higher possibility to encounter antigen via MHC class I molecules (Kaech S. *et al.* 2002). In this context, activated CD8⁺ T cells can also be very dangerous if not under control as they can mediate tissue damage. The fact that they express a higher level of the co-inhibitor PD-1 compared to CD4⁺ T cells as found in this study may suggest that the existence of negative regulatory mechanisms in these cells is of major importance. Activated cytotoxic CD8⁺ T cells expressing high amounts of PD-1 could be more effectively inhibited by cells expressing the ligands of PD-1.

The expression of PD-1 and PD-L1 on BMDCs was also analyzed by flow cytometry. Cells were stimulated with both LPS and CpG ODN1826. It was found

that BMDCs did not express PD-1 constitutively. Additionally only a little induction of PD-1 expression on these cells was found after 72 hours of incubation under both stimuli. Therefore PD-1 does not seem to be an important regulatory molecule on BMDCs. In contrast, naïve BMDCs clearly expressed PD-L1 and the stimulation of BMDCs via TLR 4 and 9 through LPS and CpG, respectively, provokes an induction of PD-L1 expression after 24 hours, with a continuous increase after 72 hours of stimulation. According to these results certain danger signals for the immune system, like LPS and CpG oligodeoxynucleotides involved in the maturation of BMDCs, also induce the expression of PD-L1. This suggests that these cells could inhibit the function of activated T cells expressing PD-1.

5.2 *In vitro* effect of the blockade of PD-1 on spleen cells by anti-PD-1 8A7 antibody

In this study a monoclonal antibody against mouse PD-1 (anti-PD-1 8A7) was used in order to block the interaction of PD-1 with its ligands and thus, delineate the function of PD-1 during an ongoing immune response. The blocking capacity of anti-PD-1 8A7 was determined by the decreased binding of fusion molecules PD-L1Ig and PD-L2Ig to endogenous PD-1 on a DO.11.10 T cell hybridoma in the presence of the antibody. According to these results, anti PD-1 8A7 can block the binding of endogenous PD-1 to both ligands PD-L1 and PD-L2 (Fig. 4.1.2).

The PD-1 blockade on spleen cells by anti-PD-1 8A7 led to a significant increase of IFN- γ production after stimulation with anti-CD3 (Fig. 4.3.1). Given that T cells are the main source of IFN- γ , this result confirms that PD-1 is expressed after TCR activation. A significant increase in IL-2 production as a result of PD-1 blockade was also observed but only at the highest concentration of anti-PD-1 8A7. No big difference was observed concerning IL-2 production and cell proliferation (data not shown). This can be explained by the fact that both events require co-stimulatory signals through CD28 (Janeway, C. A. *et al.*, 2001). These results indicate a co-inhibitory role for PD-1 inhibiting IFN- γ and in a lesser extent IL-2 production by activated T cells.

A more physiological method to activate T cells can be achieved by using an antigen specific model. T cells of a TCR-transgenic mouse recognizing OVA₃₂₃₋₃₃₉ from ovalbumin (DO.11.10) were incubated with BMDCs in the presence or absence of anti-PD-1 8A7 and antigen. The incubation with anti-PD-1 8A7 resulted in a higher

increase of IFN- γ and IL-2 at 24 hours after antigen stimulation than those cells incubated with control antibody. Even greater differences were observed after 48 hours of incubation. In contrast with these results, the PD-1 blockade produced only a little effect in cell proliferation at 24 hours after stimulation and no significant differences were observed after 48 hours. The ligation of PD-1 by its ligands impairs TCR signalling. After PD-1 engagement, PD-1 is phosphorylated on two intracellular tyrosines. This phosphorylation induces the recruitment of Src homology 2-domain-containing tyrosine phosphatase-2 (SHP-2), preventing the phosphorylation of crucial intermediate molecules that are involved in TCR signalling (Yamazaki T. *et al.* 2002; Liang S. *et al.* 2003; Keir *et al.*, 2007). Taken together, the function of PD-1 required TCR engagement and seemed to mainly mediate the inhibition of IFN- γ and IL-2 production having only a slight effect on cell proliferation. These effects of PD-1 were inhibited using the blocking antibody anti-PD-1 8A7.

5.3 *In vitro* effect of the blockade of PD-L1 on spleen cells by anti-PD-L1 6H6 antibody

In order to elucidate the function of the interaction between PD-1 and PD-L1, specific monoclonal antibodies against PD-1 and PD-L1 were used. During this study a new antibody against mouse PD-L1 (anti-PD-L1 6H6) was generated by immunization of a Lewis rat with the mouse fusion molecule PD-L1Ig. The blocking capacity of the antibody was demonstrated by the blockade of the binding of fusion molecule PD-1Ig to endogenous PD-L1 expressing T cell hybridoma in the presence of the antibody. This showed that anti-PD-L1 6H6 could block the interaction between PD-1 and PD-L1.

The *in vitro* effect of anti-PD-L1 6H6 on spleen cells was analyzed by incubation of spleen cells with several concentrations of anti-PD-L1 in the presence of anti-CD3. Subsequently the production of IFN- γ was measured. Thereby PD-L1 blockade induced a significant increase in IFN- γ concentration already at 1 $\mu\text{g}/\text{mL}$ of anti-PD-L1 6H6. Interestingly no further increase was found at higher concentration of antibody. In contrast to anti-PD-1 8A7 that blocks the engagement of PD-1 with both ligands PD-L1 and PD-L2, anti-PD-L1 6H6 blocks only the interaction between PD-L1 and PD-1 but not between PD-1 and PD-L2. This could explain the differences observed using either anti-PD-1 8A7 or anti-PD-L1 6H6.

5.4 *In vivo* PD-1 and PD-L1 expression during *P. berghei* ANKA infection

The control of the T cell response during an infection is very important. To avoid tissue damage through uncontrolled inflammatory processes, the existence of negative pathways to inhibit T cell proliferation and activation are crucial. To delineate the function of PD-1 and PD-L1 during malaria infection the mouse model *P. berghei* ANKA was used.

After the immunization of mice with γ -irradiated *P. berghei* ANKA sporozoites, an induction of a MHC-I-restricted CD8⁺ T cell population specific for the circumsporozoite protein was found (Morrot A. *et al.*, 2004). These cells produce large amounts of IFN- γ and TNF- α when stimulated *in vitro* with the antigen and can inhibit the development of the parasite but only during the liver stage, when this protein is present. This liver stage specific IFN- γ producing cells have been also described in humans after the immunization with γ -irradiated *P. falciparum* sporozoites (Clyde D.F. *et al.*, 1973; Hoffman S. *et al.*, 2002). Why natural infections in malaria endemic areas only induce little specific CD8⁺ T cell responses even after continuous exposition to sporozoites is still unknown. It is already accepted that the blood stage malaria modulates the liver stage and it has also been shown that dendritic cells induced during the blood stage suppress CD8⁺ T cell responses *in vitro* and *in vivo* (Ocaña-Mogner C. *et al.*, 2003).

A CSP-specific CD8⁺ T cell population could also be induced in mice after immunization with the CSP epitope of *P. berghei* ANKA fused to the detoxified ACT of *Bordetella pertussis* (Simsova M. *et al.*, 2004; Tartz S. *et al.*, 2006). ACT delivers the CSP epitope into the MHC class I presentation pathway of CD11b-expressing professional antigen presenting cells. This induces a CSP-specific CD8⁺ T cell population, although it does not protect against *P. berghei* ANKA malaria infection (Tartz S. *et al.*, 2006).

The limited numbers of CD8⁺ T cells and lack of specificity made it difficult to study their regulation. The immunization with ACT-CSP induced a specific CD8⁺ T cell population that allowed detecting them by flow cytometry.

In this study the influence of the blood stage on this CSP-specific CD8⁺ T cell population induced during the liver stage was examined in a mouse model of malaria. To this end, mice were first immunized with the ACT-CSP one week before they were infected with either non-irradiated *P. berghei* ANKA sporozoites or γ -irradiated sporozoites. These modified sporozoites are incapable to proceed to the

blood stage of the infection. Thus infected mice with γ -irradiated sporozoites suffer only from liver stage malaria. The presence of CSP-specific activated CD8⁺ T cells in the spleen and liver at days 2, 7 and 10 p.i. was detected by flow cytometry. Although no changes were observed in the spleen, differences were found in the liver at day 10 p.i. In the natural infection, there was a statistically significant decrease of CSP-specific CD8⁺ T cells in the liver at day 10 p.i. (Fig. 4.4.1). In mice that received γ -irradiated sporozoites, there was only a slight decrease in this CSP-specific CD8⁺ T cell population, which was statistically not significant. There was a higher percentage of CSP-specific/CD62L^{low} cells in the CD8⁺ T cell population at day 10 p.i., in mice that received γ -irradiated sporozoites compared to those infected with non-irradiated sporozoites. This indicated that the blood stage malaria as shown by the increasing parasitemia seemed to mediate the decrease of the liver stage specific CD8⁺ T cell population in the liver.

In further experiments it was interesting to analyze the PD-1 expression on the CSP-specific CD8⁺ T cells induced by the immunization with ACT-CSP. PD-1 expression was analyzed by flow cytometry showing that all CSP-specific CD8⁺ T cells in the liver expressed PD-1 (Fig. 4.4.3). It is interesting to mention that almost all CD8⁺ T cells in the liver were positive for PD-1 (84.1 %) independent from their specificity for CSP, indicating that the liver is an accumulation site for activated PD-1⁺ T cells. In the spleen approximately only 50 % of all CD8⁺ T cells expressed PD-1. This high amount of activated T cells expressing PD-1 present in the liver could also indicate that the induction of PD-1 expression occurred in this organ rather than in the spleen.

The liver plays an important role in the regulation of the T cell homeostasis. Liver sinusoidal endothelial cells (LSECs) and Kupffer cells (KCs) are located in the hepatic sinusoids in close contact to the blood stream. They control the traffic of substances coming from the gastrointestinal tract and entering the liver. Both these cell types express molecules associated with antigen presentation, such as MHC class I and II, ICAM-1 (CD54), B7-1 and B7-2, allowing them to activate the immune system in response to an infection (Crispe N., 2003). But the existence of other regulatory mechanisms in the liver is important in order to avoid a continuous activation of the immune system by harmless food antigens or commensal organisms. Indeed, several publications have shown that the liver induces tolerance (Knolle P.A. *et al.*, 2000; Knolle P. A. *et al.*, 2001) and LSECs and KCs are involved

in this mechanism (Yoshiko I. *et al.*, 2003). Interestingly, the constitutive PD-L1 expression on these cells has already been reported (Yoshiko I. *et al.* 2003) and the interaction of PD-L1 with PD-1 expressing activated T cells could be essential to their inhibition. The role of the interaction between PD-1 on CD8⁺ T cells and PD-L1 on LSECs and KCs in the accumulation and deletion of CD8⁺ T cells has already been shown (Iwai Y. *et al.*, 2003). In this study the constitutive expression of PD-L1 by KCs and LSECs was found. A higher number of CD8⁺ T cells was present in livers from adenovirus-infected PD-1 K.O. mice compared to wild-type mice. Despite the elimination of the virus observed in the PD-1 K.O. mice, the appearance of autoimmunity processes such as hepatocellular injury and mononuclear infiltration indicates that the control of these CD8⁺ T cells is very important (Iwai Y. *et al.*, 2003).

To further investigate whether the interaction between PD-1 and its ligand PD-L1 were involved in the decrease of CSP-specific CD62L^{low}/CD8⁺ T cells observed in the liver during the blood stage of malaria disease, the PD-L1 expression on LSECs and KCs was examined. Constitutive PD-L1 expression on these cells was found and no PD-L1 induction was observed during the liver stage of malaria. In contrast PD-L1 was highly induced during blood stage of the disease (Fig. 4.4.6). Additional experiments indicated that the blood stage not only induced PD-L1 expression on LSECs and KCs but also on hepatocytes, suggesting that these cells can also be implicated in inducing tolerance in the liver. This is in accordance with the literature (Limmer A. *et al.*, 2000; Chen Y. *et al.*, 2002).

Several authors have described that interferons up-regulate surface expression of PD-L1 on macrophages and DCs (Yamazaki T. *et al.* 2002; Loke P. *et al.* 2003). During the blood stage of malaria a strong interferon production occurs as a consequence of the strong activation of the immune system. This could be responsible for the induction of PD-L1 expression observed on hepatocytes and liver non-parenchymal cells.

The PD-1 and PD-L1 expression on splenic T cells during blood stage of malaria was also investigated (Fig. 4.4.5). Upon infection PD-1 expression was induced on CD4⁺ T cells in the spleen, but not on CD8⁺ T cells.

The basal PD-1 expression observed on T cells isolated from naïve non-infected mice in some experiments can be explained by the existence of autoreactive T cells

in these animals. The presence of these cells with activated phenotype expressing PD-1 correlated with the age of the animals (data not shown).

Concerning PD-L1, non-infected mice showed only a weak PD-L1 expression on CD4⁺ and a robust expression on CD8⁺ T cells in the spleen. Upon infection with *P. berghei* ANKA, a clear induction of PD-L1 expression on both cell types was observed (Fig. 4.4.5). The up-regulation of PD-L1 on T cells after TCR activation has been demonstrated in other experimental settings (Latchman Y. *et al.*, 2004; Okazaki T. *et al.*, 2007). Studies with T cells deficient for PD-L1 showed that PD-L1 is involved in the down-regulation of cytokine production (Latchman Y. *et al.*, 2004). Since both PD-1 and PD-L1 are expressed on activated T cells, it is possible that bidirectional interactions between these cells represent another regulatory mechanism to control the T cell response. However, this theory remains to be demonstrated.

5.5 *In vivo* effect of PD-1 blockade during *P. berghei* ANKA infection

To analyze the role of the interaction between PD-1 and PD-L1 in the regulation of liver specific responses in the malaria mouse model used in this study, the monoclonal antibody anti-PD-1 8A7 was used.

For this purpose mice were injected with anti-PD-1 8A7 and on the same day infected with *P. berghei* ANKA sporozoites.

The amount of CSP-specific CD8⁺ T cells in the spleen during the blood stage (day 7 p.i.) did not change upon the administration of the antibody (Fig. 4.4.8). In contrast, a significantly higher percentage of these cells was found in the liver. These cells produced IFN- γ after stimulation with CSP peptide. The administration of anti-PD-1 8A7 did not change the course of infection as measured by parasitemia (Fig. 4.4.8) This indicated that either the increase of the CSP-specific CD8⁺ T cells in the liver did not result in a significant clearance of parasites or that the induction of these cells occurred too late to fight the parasite in this organ since the pathogen is already developing inside the erythrocytes.

In order to achieve a higher frequency of CSP-specific CD8⁺ T cells, mice were immunized with ACT-CSP one week before infection with sporozoites and PD-1 blockade (Fig. 4.4.9). A higher number of CSP-specific CD8⁺ T cells was found in the liver and again no significant differences between groups were found in the spleen. These cells produced high amounts of IFN- γ upon re-stimulation with CSP

peptide and interestingly, immunized mice that received anti-PD-1 8A7 antibody showed a significantly lower parasitemia compared to control mice.

The immunization with ACT-CSP induced an increase of IFN- γ -producing CSP-specific CD8⁺ T cells in the liver after a second encounter of memory cells with the antigen during sporozoite challenge. The blockade of the PD-1/PD-L1 pathway prevented the disappearance of these IFN- γ -producing CSP-specific CD8⁺ T cells in the liver. This increase in liver stage specific T cell response observed in mice treated with anti-PD-1 8A7 antibody correlated with a decreased percentage of parasitemia in these animals.

During blood stage malaria a strong infiltration of T cells in the liver has been found (Jacobs T. *et al.* 2004). The number of liver stage specific CD8⁺ T cells may be related to the absolute number of infiltrated cells found in the liver (data not shown). The absence of differences is in this case irrelevant, more important is the functionality of these cells. For this reason the capacity of these cells to produce IFN- γ was analyzed to allow a comparison.

Another possible approach in the study of the function of PD-1 *in vivo* is the use of PD-1 K.O. mice. Although very useful, the disruption of a gene at the early stages of the development can result in compensatory mechanisms in which related proteins take over the deficit associated with the loss of the not functional gene. Additionally, in some cases a biological process is regulated by more than one gene, mechanism known as gene redundancy (Barbaric I. *et al.*, 2007).

5.6 Control of peripheral T-cell tolerance and autoimmunity via PD-1 pathway

The immune system has evolved in order to detect pathogens in a self context. This means that pathogens have to be distinguished from host self structures to avoid their destruction during inflammatory responses. T cells play the central role in inflammation and are selected during their development in the thymus. During this selection process T cells recognizing self structures are eliminated. The existence of peripheral tolerance mechanisms in peripheral tissues is of major importance to control autoreactive T cells that have escaped central tolerance. The breakdown of this peripheral tolerance results in autoimmunity. In the last years, two molecules have been found to play a role in the control of peripheral T cell tolerance: CTLA-4 and PD-1 (Fife B.T. *et al.*, 2008).

CTLA-4 is highly expressed on T cells upon activation. The critical role of CTLA-4 has been evidenced with the phenotype of CTLA-4 K.O. mice. These develop lymphoproliferative disease with a rapid multi-organ tissue infiltration and die within 3-4 weeks of birth (Waterhouse P. *et al.*, 1995).

Similar to CTLA-4, PD-1 expression also occurs on T cells upon activation. Several publications have reported an inhibitory role for PD-1 in T cell responses (Ansari M. *et al.*, 2003; Zhu B. *et al.*, 2006). To date, two ligands for PD-1 have been described: PD-L1 and PD-L2 (Freeman G. *et al.*, 2000; Latchman Y. *et al.*, 2001). Whereas the expression of PD-L2 is restricted to dendritic cells and macrophages, PD-L1 has been found not only on DCs and macrophages but also on vascular endothelial cells and therefore in several tissues. The broadly PD-L1 expression suggests that PD-1/PD-L1 pathway could be important for the maintenance of peripheral tolerance in tissues. Indeed PD-1 deficient mice also show lymphoproliferative disorders depending on their genetic background. Nevertheless, the time of appearance and severity for these autoimmune diseases, differ from those observed in CTLA-4 deficient mice. Only 50 % of mice deficient for PD-1 develop tissue-specific autoimmunity which appears later in life compared to disorders resulting from CTLA-4 K.O. mice. Moreover, CTLA-4 deficiency is responsible for multi-organ disorders independent from the genetic background which indicates the dominance of CTLA-4 as negative regulator of the immune response. The fact that CTLA-4 ligands are expressed on lymphoid tissues whereas PD-L1 is mainly expressed on the vascular endothelium of many tissues may contribute to their differential function. Regulation through CTLA-4 could influence T cells directly after their activation, whereas PD-1 could be decisive in the periphery, controlling these infiltrating cells in tissues.

It has been demonstrated that the expression of CTLA-4 is induced on CD4⁺ T cells upon infection with *P. berghei* (Jacobs T. *et al.*, 2002; 2004). Infiltrating CTLA-4-expressing CD4⁺ T cells were found in livers of mice infected with *P. berghei* ANKA. The blockade of CTLA-4 using a monoclonal antibody increased the percentage of infiltrating IFN- γ -producing cells in the liver. These cells mediated an immune response by the secretion of pro-inflammatory cytokines that affected the liver negatively with destruction of parenchymal tissue.

In this study the role of PD-1 and PD-L1 during the mouse model of malaria with *P. berghei* ANKA was analyzed. The results obtained showed that the blood stage

malaria induced the expression of PD-L1 on non-parenchymal liver cells and hepatocytes. This was responsible for the decrease of activated liver stage-specific CD8⁺ T cells that expressed PD-1. The control of these cytotoxic CD8⁺ T cells would be essential to avoid tissue damage after posterior re-infections with sporozoites but hypothetically could be also the reason why in human malaria a protective specific CD8⁺ T cell response is not achieved despite the constant contact with sporozoites in endemic areas.

In contrast to the results obtained using anti-CTLA-4 (Jacobs T. *et al.*, 2002), no autoimmune processes in mice infected with *P. berghei* ANKA were observed upon administration of anti-PD-1 8A7. Neither significant changes of weight nor increased mortality were observed (data not shown) indicating that the PD-1 blockade did not induce any kind of autoimmunity in the animals.

5.7 Role of PD-1 pathway on Tregs

Tregs are known for their ability to suppress immune responses *in vitro* and *in vivo* (Maloy K. *et al.*, 2001). Until now two subsets Tregs have been described the naturally occurring Tregs (nTregs) and inducible Tregs (iTregs). The first group represents 5–10% of the peripheral CD4⁺ T cells in humans and mice and is involved in preventing immune pathologies e. g. autoimmune thyroiditis, gastritis and diabetes. The group of iTregs is induced *in vitro* and *in vivo* under certain conditions of antigenic stimulation and seems to be involved in the control of autoimmune diseases including experimental autoimmune encephalomyelitis (EAE) as well as in the modulation of responses against infectious pathogens (O'Garra A. *et al.*, 2004). nTregs and iTregs produce IL-10, an immunosuppressive cytokine that can inhibit colitis in mice (Asseman C. *et al.*, 1999). It has also been shown that IL-10 plays an important role in limiting immune responses in numerous pathologies. For example IL-10-deficient mice infected with *Plasmodium chabaudi* develop a very strong immune response that provokes damage to the host (Li C. *et al.*, 1999). On the other hand IL-10 also inhibits immune responses against the parasite. The effect of IL-10 seems to be mediated by its ability of suppressing TNF- α production (Levings M. *et al.*, 2002).

IL-10 can be also produced by dendritic cells, B cells and Th2 cells (Moore K. W. *et al.*, 2001). The ability of Th2 cells to produce IL-10 explains the capacity of Th2 responses to inhibit Th1 responses. This mechanism, together with the fact that Th1

responses also inhibit Th2 cells, would lead to a more polarized response against the pathogen. Surprisingly it has been demonstrated that Th1 cells can also produce IL-10 (O'Garra A. *et al.*, 2004).

In this study the expression of PD-1 and PD-L1 on Tregs in comparison to effector T cells (Teffs) was analyzed by flow cytometry. A higher PD-1 expression on naïve Tregs was observed compared to Teffs and a higher induction of this molecule was shown after *in vitro* stimulation of these cells with anti-CD3. A slight PD-1 expression on Teffs was observed. As explained previously, individual differences in mice were observed concerning the PD-1 expression on Teffs. These differences can be partly correlated to the age of the animals. In older mice the incidence of autoreactive T cells with an activation status might be higher than in younger animals. These autoreactive T cells would express PD-1. Another possibility is that the procedure to isolate the cells affects their stimulation status leading to the expression of PD-1. Concerning the PD-L1 expression, naïve Teffs showed a higher expression than Tregs. The stimulation of the TCR with anti-CD3 resulted in PD-L1 induction on both cell types, stronger on Teffs. The co-expression of PD-1 and PD-L1 on Tregs has already been documented but the significance of their function is still unknown (Greenwald. *et al.*, 2004).

The role of the interaction between PD-1 and its ligands in Tregs was also analyzed in this study. Additionally to the immunosuppressive role of IL-10 secreted by Tregs, there are also evidences that Tregs can inhibit Teffs in a cell-cell dependent manner (Thornton A. *et al.*, 2000). In order to investigate if the interaction between PD-1 and its ligands has an effect on this suppressive mechanism, Tregs were incubated with Teffs at different ratios in the presence or absence of anti-PD-1 8A7. The level of IL-2 in the supernatants produced by Teffs was then determined indicating the degree of suppression (Fig. 4.3.3). No differences were observed showing that in this system, PD-1 and its ligands are not involved in the suppressive capacity of Tregs.

The possible induction of Tregs during malaria infection was investigated using the mouse model with *P. berghei* ANKA (Fig. 4.4.2). To this end mice were first immunized with ACT-CSP one week before infection with either non-irradiated or γ -irradiated sporozoites. The amount of Tregs was determined in spleen and liver at days 2, 7 and 10 p.i. by flow cytometry. No differences were observed in the spleen along the infection but in the liver, significant differences were found. Mice infected

DISCUSSION

with non-irradiated sporozoites showed an increase in the amount of Tregs in the liver at day 7 and 10 p.i. compared to mice that had been injected with γ -irradiated sporozoites, suggesting that blood stage malaria induced Treg population in this organ. Moreover this induction coincided with the decrease of CSP-specific CD8⁺ T cells found in the livers of these mice, suggesting that Tregs could be responsible for the inhibitory control of these cells. The administration of anti-PD-1 8A7 could interfere with the suppressive function of Tregs by increasing the amount of CSP-specific CD8⁺ T cells in the livers of treated mice. However this possibility is unlikely, as the blockade of the interaction between PD-1 and PD-L1 by anti-PD-1 8A7 did not influence the suppressive capacity of Tregs *in vitro*. This suggests that they were not involved in the disappearance of CSP-specific CD8⁺ T cells during the blood stage of the malaria mouse model with *P. berghei* ANKA.

More experiments have to be performed in order to elucidate the significance of Tregs induction in the liver during blood stage malaria.

6. REFERENCES

- Agata Y., Kawasaki A., Nishimura H. *et al.* Expression of the PD-1 antigen on the surface of stimulated mouse T and B lymphocytes. *Int. Immunol.* 8; 765–770 (1996).
- Ansari M., Salama A., Chitnis T. *et al.* The programmed death-1 (PD-1) pathway regulates autoimmune diabetes in nonobese diabetic (NOD) mice. *J. Exp. Med.* 198; 63–69 (2003).
- Asseman C., Mauze S., Leach M. *et al.* An essential role for interleukin 10 in the function of regulatory T cells that inhibit intestinal inflammation. *J. Exp. Med.* 190; 995–1004 (1999).
- Baecher-Allan C., Brown J., Freeman G. *et al.* CD4⁺ CD25^{high} regulatory cells in human peripheral blood. *J. Immunol.* 167: 1245–1253 (2001).
- Barbaric I., Miller G. and Dear N. Appearance can be deceiving: phenotypes of knockout mice. *Briefings in Functional Genomics and Proteomics.* 6(2):91–103 (2007)
- Barber D., Wherry E., Masopust D. *et al.* Restoring function in exhausted CD8 T cells during chronic viral infection. *Nature.* 439: 682–687 (2006).
- Butte M., Keir M., Phamduy T. *et al.* Programmed death-1 ligand 1 interacts specifically with the B7-1 co-stimulatory molecule to inhibit T cell responses. *Immunity.* 27; 111–122 (2007).
- Carswell E., Old L., Kassel S. *et al.* An endotoxin-induced serum factor that causes necrosis of tumors. *Proc. Natl. Acad. Sci. USA.* 72; 3666–3670 (1975).
- Carter L., Fouser L., Jussif J. *et al.* PD-1: PD-L1 inhibitory pathway affects both CD4⁺ and CD8⁺ T cells and is overcome by IL-2. *Eur. J. Immunol.* 32: 634–643 (2002).

REFERENCES

- Chambers C., Kuhns S., Egen J. *et al.* CTLA-4-mediated inhibition in regulation of T cell responses: mechanisms and manipulation in tumor immunotherapy. *Annual Review Immunol.* 19; 565–594 (2001).
- Chen L. Co-inhibitory molecules of the B7-CD28 family in the control of T-cell immunity. *Nature reviews.* 4; 336–347 (2004).
- Chen Y., McKenna G. J., Ong C. *et al.* Liver non-parenchymal cells involved in hyporesponsiveness induced by portal vein injection of alloantigen. *Immunol. Lett.* 81; 1–11 (2002).
- Chikuma S., Imboden J. and Bluestone J. Negative regulation of cell receptor-lipid raft interaction by cytotoxic T lymphocyte-associated antigen 4. *J. Exp. Med.* 197; 129–135 (2003).
- Ching L., Seixas E. and Langhorne J. Rodent malarial: the mouse as a model for understanding immune responses and pathology induced by the erythrocytic stages of the parasite. *Medical Microbiol. Immunol.* 189; 115–126 (2001).
- Clark I., Virelizier J., Carswell E. *et al.* Possible importance of macrophage-derived mediators in acute malaria. *Infect. Immun.* 32; 1058–1066 (1981).
- Clark I., Rockett K. and Burgner D. Genes, nitric oxide and malaria in African children. *Trends Parasitol.* 19: 335–337 (2003).
- Clark I., Alleva L., Mills A. *et al.* Pathogenesis of malaria and clinically similar conditions. *Clin. Microbiol. Reviews.* 7; 509–539 (2004).
- Clyde D., Most H., McCarthy V. *et al.* Immunization of man against sporozoite-induced falciparum malaria. *Am. J. Med. Sci.* 266: 169–177 (1973).
- Crispe N. Hepatic T cells and liver tolerance. *Nat. Rev. Immunol.* 3 (1):51–62 (2003).

REFERENCES

- De Souza M., Fontenot A., Mack D. *et al.* Programmed death 1 expression on HIV-specific CD4⁺ T cells is driven by viral replication and associated with T cell dysfunction. *The Journal of Immunology*. 1979–1987 (2007).
- Dong H., Zhu G., Tamada K. *et al.* B7–H1, a third member of the B7 family, co-stimulates T-cell proliferation and interleukin–10 secretion. *Nature Medicine*. 5; 1365–1369 (1999).
- Dong H., Zhu G., Tamada K. *et al.* B7–H1 determines accumulation and deletion of intrahepatic CD8⁺ T lymphocytes. *Immunity*. 20; 327–336 (2004).
- Elliott S. R. *et al.* Inhibition of dendritic cell maturation by malaria is dose dependent and does not require Plasmodium falciparum erythrocyte membrane protein 1. *Infect. Immun.* 75; 3621–3632 (2007).
- Elrefaei M., Baker C., Jones N. *et al.* Presence of suppressor HIV-specific CD8⁺ T cells is associated with increased PD–1 expression on effector CD8⁺ T cells. *The Journal of Immunology*. 7757–7763 (2008).
- Freeman G., Long A., Iwai Y. *et al.* Engagement of the PD–1 immunoinhibitory receptor by a novel B7 family member leads to negative regulation of lymphocyte activation. *J. Exp. Med.* 192; 1027–1032 (2000).
- Golden–Mason L., Klarquist J., Wahed A. *et al.* Cutting edge: Programmed death–1 expression is increased on immunocytes in chronic hepatitis C virus and predicts failure of response to antiviral therapy: race-dependent differences. *The Journal of Immunology*. 3637–3641 (2008).
- Greenwald R., Freeman G. and Sharpe, A. The B7 family revisited. *Ann. Rev. Immunol.* 23:515–548 (2005).

REFERENCES

- Hafalla J., Morrot A., Sano G. *et al.* Early self-regulatory mechanisms control the magnitude of CD8⁺ T cell responses against liver stages of murine malaria. *J. Immunol.* 171; 964–970 (2003).
- Hanum S., Hayano M. and Kojima S. Cytokines and chemokine responses in a cerebral malaria-susceptible or resistant strain of mice to *Plasmodium berghei* ANKA infection: early chemokine expression in the brain. *International Immunology.* 15; 633–640 (2003).
- Harty J. and Badovinac V. Shaping and reshaping CD8⁺ T-cell memory. *Nature Reviews Immunology.* 8; 107–119 (2008).
- Hoffman S., Goh L., Luke T. *et al.* Protection of humans against malaria by immunization with radiation-attenuated *Plasmodium falciparum* sporozoites. *J. Infect. Dis.* 185: 1155–1164 (2002).
- Ishida Y., Agata Y., Shibahara K. *et al.* Induced expression of PD-1, a novel member of the immunoglobulin gene superfamily, upon programmed cell death. *EMBO J.* 11:3887 (1999).
- Iwai Y., Terawaki S., Ikegawa M. *et al.* PD-1 inhibits antiviral immunity at the effector phase in the liver. *J. Exp. Med.* 198; 39–50 (2003).
- Jacobs T., Graefe S., Niknafs S. *et al.* Murine malaria is exacerbated by CTLA-4 blockade. *J. Immunol.* 169: 2323–2329 (2002).
- Jacobs T., Plate T., Gaworski I. *et al.* CTLA-4-dependent mechanisms prevent T cell induced-liver pathology during the erythrocyte stage of *Plasmodium berghei* malaria. *Eur. J. Immunol.* 34: 972–980 (2004).
- Janeway C. A. and Travers P. Immunology 5. The Immune system in the health and disease. *Garland Publishing Inc* (2001).

REFERENCES

- Kaech S., Wherry E. and Ahmed R. Effector and memory T-cell differentiation: implications for vaccine development. *Nature Reviews Immunology*. 2; 251–262 (2002).
- Keir M., Butte M., Freeman G. *et al.* PD-1 and its ligands in tolerance and immunity. *Annual Reviews Immunology*. 12; 677–704 (2007).
- Keler T., Halk L., Vitale T. *et al.* Activity and safety of CTLA-4 blockade combined with vaccines in cynomolgus macaques. *J. Immunol*. 171; 6251–6259 (2003).
- Khoury S. and Sayegh M. The roles of the new negative T cell costimulatory pathways in regulating autoimmunity. *Immunity*. 20; 529–538 (2004).
- Langhorne J., Ndungu F., Sponaas A. *et al.* Immunity to malaria: more questions than answers. *Nature Immunology*. 9; 725–732 (2008).
- Latchman Y., Liang S., Wu Y. *et al.* PD-L1-deficient mice show that PD-L1 on T cells, antigen presenting cells and host tissues negatively regulates T cells. *Proc. Natl. Acad. Sci. USA*. 101; 10691–10696 (2004).
- Lee K., Chuang E., Griffin M. *et al.* Molecular basis of T cell inactivation by CTLA-4. *Science*. 282; 2263–2266 (1998).
- Lepeniev B., Gaworski I., Tartz S. *et al.* CTLA-4 blockade differentially influences the outcome of non-lethal and lethal *Plasmodium yoelii* infections. *Microbes and infection*. 9; 687–694 (2007).
- Levings M. K., Sangregorio R., Sartirana C. *et al.* Human CD4 CD25 T suppressor cell clones produce transforming growth factor beta, but not interleukin 10, and are distinct from type 1 regulatory cells. *J. Exp. Med*. 196; 1335–1346 (2002).

REFERENCES

- Liang S., Latchman Y., Buhlmann J. *et al.* Regulation of PD-1, PD-L1 and PD-L2 expression during normal and autoimmune responses. *Eur. J. Immunol.* 33; 2706–2716 (2003).
- Li C., Corraliza I. and Langhorn J. A defect in interleukin 10 leads to enhanced malarial disease in *Plasmodium Chabaudi chabaudi* infection in mice. *Infect. Immun.* 67; 4435–4442 (1999).
- Limmer A., Ohl J., Kurts H.G. *et al.* Efficient presentation of exogenous antigen by liver endothelial cells to CD8⁺ T cells results in antigen-specific T-cell tolerance. *Nat Med* 6; 1348–1353 (2000).
- Loke P. and Allison J. PD-L1 and PD-L2 are differentially regulated by Th2 and Th2 cells. *Proc. Natl. Acad. Sci. USA*; 100; 5336–5341 (2003).
- Lyke K., Burges R., Cissoko Y. *et al.* Serum levels of the proinflammatory cytokines interleukin-1 beta (IL-1 β), IL-6, IL-8, IL-10, tumor necrosis factor alpha, and IL-12 (p70) in Malian children with severe *Plasmodium falciparum* malaria and matched uncomplicated malaria or healthy controls. *Infection and Immunity.* 10; 5630–5637 (2004).
- Maloy K., and Powrie F. Regulatory T cells in the control of immune pathology. *Nat. Immunol.* 2; 816–822 (2001).
- Maneerat Y., Viriyavejakul P., Punpoowong B. *et al.* Inducible nitric oxide synthase expression is increased in the brain fatal cerebral malaria. *Histopathology.* 37; 269–277 (2000).
- Miller L., Baruch D., Marsh K. *et al.* The pathogenic basis of malaria. *Nature.* 415; 673–679 (2002).
- Moore, K.W., de Waal Malefyt, R. *et al.* Interleukine-10 and the interleukin-10 receptor. *Annu. Rev. Immunol.* 19; 683–765 (2001).

REFERENCES

- Nebi T., De Veer M. and Schofield L. Stimulation of innate immune responses by malarial glycosylphosphatidylinositol via pattern recognition receptors. *Parasitology*. 130; 45–62 (2005).
- Ocaña–Morgner C., Mota M. and Rodriguez A. Malaria Blood stage suppression of liver stage immunity by dendritic cells. *J. Exp. Med.* 197; 143–151 (2003).
- O’Garra A. and Robinson D. Development and function of T helper 1 cells. *Adv. Immunol.* 83; 133–162. (2004).
- O’Garra A., Vieira P., Vieira P. *et al.* IL–10–producing and naturally occurring CD4⁺ Tregs: limiting collateral damage. *J. clin. Inv.* 114; 1372–1378 (2004).
- Okazaki T., Maeda A., Nishimura H. *et al.* PD–1 immunoreceptor inhibits B cell receptor–mediated signalling by recruiting src homology 2–domain–containing tyrosine phosphatase 2 to phosphotyrosine. *Proc. Natl. Acad. Sci. USA.* 98; 13866–13871 (2001).
- Okazaki T. and Tasuko H. PD–1 and PD–L1 ligands: from discovery to clinical application. *International Immunology*. 2007; 1–12 (2007).
- Rae C., McQuillan J., Parekhi S. *et al.* Brain expression, metabolism, and bioenergetics: interrelationships in murine models of cerebral and noncerebral malaria. *FASEB J.* 18; 499–510 (2004).
- Rodig N., Ryan T., Allen J. *et al.* Endothelial expression of PD–L1 and PD–L2 down–regulates CD8⁺ T cell activation and cytotoxicity. *Eur. J. Immunol.* 33; 3117–3126 (2003).
- Rowe J., Johanns T., Ertelt J. *et al.* PD–L1 blockade impedes T cell expansion and protective immunity primed by attenuated *Listeria monocytogenes*. *The Journal of Immunology*. 7553–7557 (2008).

REFERENCES

- Sakaguchi S. Regulatory T cells: mediating compromises between host and parasite. *Nat. Immunol.* 4; 10–11 (2003).
- Schlotmann T., Waase I., Julch C. *et al.* CD4 $\alpha\beta$ T lymphocytes express high levels of the T lymphocyte antigen CTLA-4 (CD152) in acute malaria. *J. Inf.Dis.* 182; 367–370 (2000).
- Schofield L. and Hackett F. Signal transduction in host cells by a glycosylphosphatidylinositol toxin of malaria parasites. *J. Exp. Med.* 177; 145–153 (2000).
- Sedy J., Gavrieli K., Poter K. *et al.* B and T lymphocyte attenuator regulates T cell activation through interaction with herpesvirus entry mediator. *Nat. Immunol.* 6; 90–98 (2005).
- Seo S., Jeong H., Park S. *et al.* Blockade of endogenous B7–H1 suppresses antibacterial protection after primary *Listeria monocytogenes* infection. *Immunology.* 123; 90–99 (2007).
- Shin T., Kennedy G., Girski K. *et al.* Cooperative B7–1/2 (CD80/CD86) and B7–DC costimulation of CD4⁺ T cells independent of the PD–1 receptor. *J. Exp. Med.* 198; 31–38 (2003).
- Simsova M., Sebo P. Leclerc C. *et al.* The adenylate cyclase toxin from *Bordetella pertussis*—a novel promising vehicle for antigen delivery to dendritic cells. *Int. J. Med. Microbiol.* 293; 571–576 (2004).
- Stevenson M. and Riley E. Innate immunity to malaria. *Nature reviews.* 4; 169–180 (2004).
- Sturm A., Amino R., van de Sand C. *et al.* Manipulation of host hepatocytes by the malaria parasite for delivery into liver sinusoids. *Science.* 313; 1287–1290 (2006).

REFERENCES

- Subudhi S., Zhou P., Yerian L. *et al.* Local expression of B7–H1 promotes organ specific autoimmunity and transplant rejection. *The Journal of clinical investigation.* 113; 694–700 (2004).
- Tamura H., Dong H., Zhu G. *et al.* B7–H1 costimulation preferentially enhances CD28–independent T–helper cell function. *Blood.* 97; 1809–1816 (2001).
- Tartz S., Kamanova J., Simsova M. *et al.* Immunization with a circumsporozoite epitome fused to *Bordetella pertussis* adenylate cyclase in conjunction with cytotoxic T–lymphocyte–associated antigen–4 blockade confers protection against *Plasmodium berghei* liver–stage malaria. *Infection and Immunity.* 74; 2277–2285 (2006).
- Thornton A. and Shevach E. Suppressor effector function of CD4 CD25 immunoregulatory T cells is antigen specific. *J. immunol.* 164: 183–190 (2000).
- Tivol E. Borriello F., Schweitzer A. *et al.* Loss of CTLA–4 leads to massive lymphoproliferation and fatal multiorgan tissue destruction, revealing a critical negative regulatory role of CTLA–4. *Immunity.* 3; 541–547 (1995).
- Urban B., Ferguson D., Pain A. *et al.* *Plasmodium falciparum* infected erythrocytes modulate the maturation of dendritic cells. *Nature.* 400; 73–77 (1999).
- Urban B., Willcox N. and Roberts D. A role for CD36 in the regulation of dendritic cell function. *Proc. Natl. Acad. Sci. USA.* 98; 8750–8755 (2001).
- Vichchathorn P., Jenwithisuk R., Leelaudomlapi S. *et al.* Induction of specific immune responses against the *Plasmodium vivax* liver–stage via *in vitro* activation by dendritic cells. *Parasitol. Int.* 55; 187–193 (2006).

REFERENCES

- Wahl C., Bochtler P., Chen L. *et al.* B7–H1 on hepatocytes facilitates priming of specific CD8 T cells but limits the specific recall of primed responses. *Gastroenterology*. 135; 980–988 (2008).
- Watanabe N. BTLA is a lymphocyte inhibitory receptor with similarities to CTLA–4 and PD–1. *Nature Immunol.* 4; 670–679 (2003).
- Waterhouse P., Penniger J., Timms E. *et al.* Lymphoproliferative disorders with early lethality in mice deficient in CtlA–4. *Science*. 270; 985–988 (1995).
- Wykes M. and Good M. What really happens to dendritic cells during malaria? *Nature Reviews Microbiology*. 8; 1–6 (2008).
- Yamazaki T., Akiba H., Iwai H. *et al.* Expression of programmed death 1 ligands by murine T cells and APC. *J. Microbiol.* 169; 5538–5545 (2002).
- Zhang X., Schwartz J., Guo X. *et al.* Structural and functional analysis of the costimulatory receptor programmed death 1. *Immunity*. 20; 337–347 (2004).
- Zhu B., Guleria I., Khosroshabi A. *et al.* Differential role of programmed death ligand 1 and programmed death ligand 2 in regulating the susceptibility and chronic progression of experimental autoimmune encephalomyelitis. *The Journal of Immunology*. 3480–3489 (2006).
- Zozulya A. and Wiendl H. The role of regulatory T cells in multiple sclerosis. *Nature Clinical Practice*. 4; 384–398 (2008).